

**ASSESSMENT OF THE EFFECTS OF DUMP SITE ON GROUNDWATER
QUALITY IN BARIKIN-SALE, MINNA NORTH-CENTRAL, NIGERIA**

By

**HARUNA, Mohammed Sabiu
MTech/SPS/2017/7157**

**DEPARTMENT OF GEOLOGY
FEDERAL UNIVERSITY OF TECHNOLOGY, MINNA**

JULY, 2021

**ASSESSMENT OF THE EFFECTS OF DUMP SITE ON GROUNDWATER
QUALITY IN BARIKIN-SALE, MINNA NORTH-CENTRAL, NIGERIA**

By

**HARUNA, Mohammed Sabiu
MTech/SPS/2017/7157**

**A THESIS SUBMITTED TO THE POSTGRADUATE SCHOOL
FEDERAL UNIVERSITY OF TECHNOLOGY MINNA, NIGERIA IN PARTIAL
FULFILLMENT OF THE REQUIREMENTS FOR THE AWARD OF THE
DEGREE OF MASTER OF TECHNOLOGY IN ENVIRONMENTAL GEOLOGY**

JULY, 2021

ABSTRACT

Discharge of leachate from refuse dumpsites is a source of groundwater pollution within its immediate environment of location. Geophysical investigation of an uncontrolled open solid waste dumpsite located at Barikin-Sale area of Minna was carried out for possible contamination of groundwater. The investigation was aimed at delineating groundwater contamination due to leachate percolation thereby assessing the quality of groundwater from hand dug wells and boreholes within the dumpsite and the surrounding environment. A total of ten (10) Vertical Electrical Sounding (VES) points with maximum current electrode spacing of 20 m and two (2) 2D Subsurface Electrical Imaging were investigated within and outside the dumpsite to assess leachate migration in the area. Schlumberger configuration was used for the VES while the Wenner configuration was used for the subsurface imaging. The VES data were analysed and a maximum of three (3) geoelectric sections were identified; the top soil, weathered basement and the fractured/fresh basement. The obtained apparent resistivity for those layers were between 19.4 Ωm and 122.6 Ωm for the first layer, 18.2 Ωm and 33.4 Ωm for the second layer and 93.5 Ωm and 166.4 Ωm for the third layer respectively. The range of thickness for the first layer is 0.9 m and 1.8 m and for the second layer are 4.0 m and 5.3 m respectively. The 2D resistivity data were processed and inverted using the RES2DINV software. The inverse resistivity models of the subsurface from the 2D subsurface electrical imaging revealed low resistivity value $<20 \Omega\text{m}$ which is taken to be leachate derived from decomposed waste while these wastes that cannot decompose are occurring as isolated parts with slightly higher resistivity value of $>20 \Omega\text{m}$. The areas with the highest resistivity value of $>100 \Omega\text{m}$ were further interpreted to be chemical weathering product of crystalline bedrock considered to be regolith. Sieve analysis of sixteen (16) soil samples from four (4) pits was carried out; the result shows that the soils are fine to medium sand and the hydraulic conductivity was computed from it using the HydrogeoSieveXL software. From the estimated hydraulic conductivity (K), the values range between 1.97×10^{-4} and 2.52×10^{-5} m/s. This further clarifies the geophysical investigation results. The physicochemical analyses of ten (10) water samples from hand dug wells and boreholes were carried out. The results show that the median and mean concentration of conductivity at 1290 $\mu\text{s/cm}$ and 1616 $\mu\text{s/cm}$, TDS at 864.5 mg/l and 1078.7 mg/l and nitrite at 0.039 mg/l and 0.4929 mg/l all exceed the permissible limits of 1000 $\mu\text{s/cm}$, 500 mg/l and 0.2 mg/l of NSDWQ (2007) and WHO (2010) indicating groundwater contamination. Although, at some locations the analysed parameters exceed the permissible limits but their median and mean concentrations are generally inside the permissible limits. From the results, it could be concluded that leachates are concentrated within the lower part of the dumpsite; therefore the surrounding environment groundwater sources are vulnerable to leachate contamination from the dumpsite.

TABLE OF CONTENTS

Content	Page
Title page	i
Declaration	ii
Certification	iii
Dedication	iv
Acknowledgement	v
Abstract	vi
Table of content	vii
List of tables	xi
List of figures	xii
List of plates	xiv

CHAPTER ONE

INTRODUCTION

1.1	Background to the Study	1
1.2	Statement of the Research Problem	5
1.3	Justification for the Study	6
1.4	Study Area	7
1.4.1	Relief and Drainage	9
1.4.2	Climate and Vegetation	10
1.4.3	Settlement and Land Use	11
1.5	Scope of Work	11
1.6	Aim and Objectives	11

1.7	Regional Geological Settings	12
1.7.1	The Basement Complex	12
1.7.1.1	The Older Granites	14
1.7.1.2	The Migmatite/Gneiss Complex	15
1.7.1.3	The Low Grade Schist Belt	15
1.7.1.4	Undeformed Acidic and Basic Dykes	16

CHAPTER TWO

LITERATURE REVIEW

2.1	Review of Related Literatures	20
2.1.1	Review of Geological and Hydrogeological related Literatures	20
2.1.2	Review of Geotechnical Related Literatures	24
2.1.3	Review of Geophysical Related Literatures	26
2.2	Principle of Electrical Resistivity Survey	31
2.2.1	The General Four Electrodes Theory	32

CHAPTER THREE

MATERIALS AND METHODS

3.1	Materials	36
3.2	Methods	36
3.2.1	Preliminary Desk Study and Reconnaissance	36
3.2.2	Geological Mapping	36
3.2.3	Geophysical Mapping	37
3.2.3.1	Vertical Electrical Sounding (VES)	37
3.2.3.2	Two dimensional (2D) electrical subsurface imaging	39

3.2.4	Hydrogeological Mapping	41
3.2.4.1	Groundwater flow direction	42
3.2.5	Grading analysis	42
3.2.5.1	Laboratory analysis of soil	43
3.2.6	Petrographic analysis	44
3.2.7	Laboratory analysis of groundwater samples	46

CHAPTER FOUR

RESULTS AND DISCUSSION

4.1	Study area observations	48
4.2	Geological mapping and petrography	48
4.3	Well parameters	53
4.4	Geophysical analysis	55
4.4.1	Vertical electrical sounding (VES)	55
4.4.2	Two dimensional (2D) resistivity subsurface imaging	59
4.5	Grain size distribution	61
4.5.1	Sieve analysis	61
4.5.2	Hydraulic conductivity	63
4.6	Laboratory analyses of groundwater	65
4.6.1	Physical parameters	67
4.6.2	Chemical parameters	70
4.6.2.1	Anions in the water	70
4.6.2.2	Cations in the water	74
4.6.2.3	Heavy metals	78

CHAPTER FOUR

CONCLUSION AND RECOMMENDATIONS

4.1 Conclusion 84

4.2 Recommendations 85

REFERENCES 86

Appendices 94

LIST OF TABLES

Table		Page
1.1	Stratigraphic Succession of the Nigerian Basement Complex (McCurry, 1976)	14
2.1	Relative Vulnerability to Pollution by Hydrologic Setting (Montgomery, 2000)	20
4.1	Well Parameters for the Study Area	53
4.2	VES Parameters and Lithologic Delineation of the Study Area	56
4.3	Grain Size Distribution Parameters for Sample L1 at 0.0 m	61
4.4	Hydraulic Conductivity (K) from the Sieve Analysis	63
4.5	Physico-Chemical and Heavy Metals Parameters Analyzed in the Water Sample from the Study Area	64
4.6	Statistical Summary of Groundwater Samples from the Study Area	65

LIST OF FIGURES

Figure	Page
1.1 Topography of Minna showing the study area	8
1.2 Drainage Pattern of Minna Metropolis	10
1.3 General Geology of Nigeria	12
1.4 Schist Belts of Nigeria	16
2.1 Water Tables Intersects Landfill	18
2.2 Leachate Infiltrates to Water Table through Permeable Materials under Landfill Site	19
2.3 General Four Electrodes Array	31
2.4 Equipotential Surface and Field Lines	32
2.5 Wenner Array	33
2.6 Schlumberger Array	34
2.7 Approximate Range of Resistivity Values of Some Rock Types	35
3.1 Diverse Configuration of Wenner	39
3.2 Sequence of 2D Wenner Resistivity Measurement to Build a Pseudosection	41
4.1 Locations of Rock Samples, Trial Pits and Dumpsite	49
4.2 Geological Map of the Study Area	50
4.3 Rose Diagram of Joint Directions from the Study Area	50
4.4 Hydraulic Head Distribution Map	54
4.5 Locations of VES Points and Water Samples	55

4.6	Sounding Curve for VES 1	57
4.7	Geoelectric Sections for VES 1 – 5	58
4.8	Geoelectric Sections for VES 6 – 10	58
4.9	2D Inverse Resistivity Models for Profile 1	59
4.10	2D Inverse Resistivity Models for Profile 2	60
4.11	Grading Curve for Sample L1 at 0.0 m	61
4.12	Concentration of pH compared with NSDWQ (2007) and WHO (2010)	66
4.13	Concentration of Turbidity compared with NSDWQ (2007) and WHO (2010)	67
4.14	Concentration of EC compared with NSDWQ (2007) and WHO (2010)	68
4.15	Concentration of TDS compared with NSDWQ (2007) and WHO (2010)	69
4.16	Concentration of Chloride compared with NSDWQ (2007) and WHO (2010)	70
4.17	Concentration of Nitrite compared with NSDWQ (2007) and WHO (2010)	71
4.18	Concentration of Bicarbonate compared with NSDWQ (2007) and WHO	72
4.19	Concentration of Sulphate compared with NSDWQ (2007) and WHO (2010)	73
4.20	Concentration of Sodium compared with NSDWQ (2007) and WHO (2010)	74
4.21	Concentration of Calcium compared with NSDWQ (2007) and WHO (2010)	75
4.22	Concentration of Magnesium compared with NSDWQ (2007) and WHO (2010)	76
4.23	Concentration of Potassium compared with NSDWQ (2007) and WHO	

	(2010)	77
4.24	Concentration of Magnesium compared with NSDWQ (2007) and WHO (2010)	78
4.25	Concentration of Zinc compared with NSDWQ (2007) and WHO (2010)	79
4.26	Concentration of Chromium compared with NSDWQ (2007) and WHO (2010)	80
4.27	Concentration of Iron compared with NSDWQ (2007) and WHO (2010)	82

LIST OF PLATES

Plate		Page
I	Geophysical Surveying within the Study Area	37
II	Digging of the Trial Pits and a Trial Pit within the Study Area	43
III	The Barikin-Sale Dumpsite	48
IV	Photomicrograph of Granite (a) Plane Polarized Light (b) Cross Polarize Light (X40)	51
V	Photomicrograph of Granite (a) Plane Polarized Light (b) Cross Polarize Light (X40)	51
VI	Photomicrograph of Granite (a) Plane Polarized Light (b) Cross Polarize Light (X40)	52

CHAPTER ONE

1.0

INTRODUCTION

1.1 Background to the Study

Groundwater forms an important part of the water resources across the world particularly in the arid regions. It is used for household functions because it is of high quality and require slight or no remedy prior to usage. According to Martins (2001), bacteria, fungi and other biological contaminants are in nature filtered and attenuated as the water infiltrate or permeate across the soil. Another reason why groundwater is made use of domestically is that the providing clean water through the scheme of water made available is hideously insufficient for the requirements of the public. The result of lackadaisical management and/or discarding of hazardous materials have greatly decreased fresh groundwater supplies. The setback of ecological contamination is a major concern of earth scientists today, and investigators from other associated disciplines across the world.

According to Ige (2013), there is disproportionate increase in waste generated in Nigerian cities with increase in social-economic development. Rapid industrialization and the unrestrained escalation of the city population effect in the creation of substantial noxious solid remains. Municipal desecrate items, principally household trash, are habitually thrown away improperly on surfaces of land, superficial excavation, drainage, channels of river and stream thus making the groundwater susceptible to pollution. Solid trash landfills represent an essential piece of the hydrological structure of the soil (Rosqvist *et al.*, 2003), therefore poses a severe danger of infecting mutually the groundwater and the surface water downstream. Therefore, there is need of understanding and quantifying the landfills

hydraulic behavior. Groundwater pollution happens generally as a result of the percolation of fluvial water and the penetration of pollutants into the soil underneath a garbage dumping sites. The noxious waste is a liquid resulting from the putrefaction of municipal solid wastes. Contamination takes place when the leaking aqueous liquid, known as the leachate reaches the groundwater table, consequently affecting the quality of the groundwater. The ecological contamination and healthiness risk related to exposed dumpsites cannot be overemphasised (Aderemi *et al.*, 2011).

United Nations Environment Programmed (UNEP, 2002), said that 0.5 kg of solid trash is generated by each person daily on the average. Accordingly, in Barikin-Sale area, the municipal waste and refuse generated daily are in thousand metric tonnes. The Barikin-Sale waste disposal site is an open dump type (it has no top protector which stop rain water from inflowing forming leachate and base coat to avoid the leachate departure in the site of waste dump), and it is situated between populated residential areas which consequently creates severe problems to local ecological value and community health. As a result, Barikin-Sale area might encounter serious crisis of contamination of groundwater assets in future if the dilemma of indiscriminate dumping of waste at the dumpsite is not sufficiently tackled.

An essential frequent need in city areas includes identifying the locality and degree of pollution spaces in laces occupied by landfills. Within this context, applying geotechnics, hydrogeology and geophysical approaches gives a significant means in the estimation and categorization of pollutants created by urban remains (household and/or industrial). The particle size grading of soils underlying the dumpsite will give an insight into the rate of movement and percolation of leachates across the area. Geotechnics and geoelectrical

methods have been found very appropriate for such type of ecological studies. This is because usually, ionic intensity of leachate from landfill is a lot beyond that of groundwater and thus as soon as the leachate penetrates the aquifer, a great difference in electrical properties will be experienced and the methods will recognize these regions as an irregularity and it allows the detections of the leachate trail. The use of geology, hydrogeology, geotechnical and geophysical methods as used in the studies of landfills are documented properly (Ige *et al.*, 2011; Rowe, 2011; Porsani *et al.*, 2004; Karlik and Kaya, 2000; Mukhtar *et al.*, 2000, Fatta *et al.*, 2000 and Benson *et al.*, 1997).

The setback of environmental contamination is a major concern of planet scientists today, and investigators from associated area of study all over the globe. Haphazard dumping of untreated garbage is harmful to health since it produces unhygienic surroundings which have bad effects for city inhabitants. Wherever sanitary services are in short supply, domestic solid garbage is likely to be combined with fecal material; thereby complexing the health risks. Most of these waste disposal sites are located in open spaces within the vicinity of human settlements where several wells and boreholes are found. Indiscriminate dumping and inappropriate managing of household and industrial wastes will affect harmfully the environment and wellbeing of the inhabitants. Transmittable infections associated with deprived ecological setting exterminate one in every five African children, with acute respiratory diseases and diarrhea as the two main cause of death (WHO, 1979). Ailments like typhoid, cholera, guinea worm, trachoma, bilharzias, polio, hookworm, and tapeworm are related to drinking of poor quality water and sanitation (Boadi and Kuitunen, 2005). As a result of industrial advancement and urbanization in recent time, there is tremendous increase in the population of people living in Barikin-Sale, and this has led to

exceptional increased in the waste generation, therefore refuse dumpsites become a common feature in the city.

Groundwater contamination within a waste disposal site results from the infiltration of leachates through the soil. The leachates are created once rain falls on the landfill site, percolate into the garbage and carries pollutants as it leaches down (Egbai *et al.*, 2015). The frequent thin aquifer found in the environments of basement complex is typically opened to external and near-external pollution (Aweto, 2011). Having been affirmed that immediately an aquifer is extremely exhausted or polluted, the harm is basically unending and pains to remedy the pollution are exceptionally expensive (Jegade *et al.*, 2013). Within the study area and the surrounding environs, groundwater is gotten from boreholes and wells (hand-dug) at depths occasionally as thin as 5 m as the major supply of water for household uses in the area. The contamination becomes obvious resulting from the hydraulic link relating the harmful substances of the groundwater and leachate plumes (Nasir *et al.*, 2010).

Basically, two distinctive methods can be used in investigating the level of contaminants in groundwater. Firstly, the destructive method which requires sampling utilizing soil auger/core sampler in which case the area's geology is constantly altered. Secondly, the non-destructive method which makes use of geophysical method where the geology of the area is not disturbed (Oyedele, 2009). One of the recognized geophysical methods is the electrical resistivity method which gives beneficial and non-devastating course to recognize delineate and map the sub-surface defining leachate contaminant plumes from dumpsites. This method is based on leachate electrical conductivity which is likely to be above that of groundwater (Cristina *et al.*, 2012). Researches have also proven that resistivity method is a

tool for identifying, delineating and mapping of leachate contaminant plumes (Cristina *et al.*, 2012; Porsani *et al.*, 2004; Meju, 2000 and Loke, 1999;).

Direct Current (DC) electrical resistivity techniques of exploration geophysical are trendy and have proven to be thriving and dependable in the areas of geo-environment, hydrogeology, engineering's and contaminant hydrology. Lately, a recent improvement is in the application of 2-D techniques of electrical imaging to map places having moderate to difficult geology (Griffths and Barker, 1993). Also, mapping of changes in the recorded resistivity in the vertical and also the horizontal trend, gives a more precise pattern of the underground in two-dimension (2-D). Electrical resistivity methods for contaminant studies have a broad range of function on thin resources of groundwater, and the advantages include the reduction in the require for intrusive methods and complete sampling, produces intrinsic properties (electrical conductivity/resistivity) of groundwater chemistry that gives information on contamination, reasonably economical, and optimization of the requisite amount of observation wells (Ebraheem *et al.*, 1990; and EL-Mahmoudi, 1999). The objective of the study is to apply geoelectric technique implementing the vertical electrical sounding and the 2-D subsurface electrical imaging (2D resistivity tomography), employing the Wenner techniques to identify and outline leachate trail from an uncontrolled solid trash disposal site in Barikin-Sale Minna, North-central Nigeria.

1.2 Statement of the Research Problem

Water is a fundamental requisite of human and industrial development and it is the main fragile piece of the surroundings (WHO, 2010). Hence, a nonstop observation of quality of water is extremely necessary to ascertain the status of effluence in our rivers, hand dug wells and boreholes. Every human on earth has the tendency to generate waste, but the

management of the waste produced has constantly posed a challenge to the society at large, mostly in developing nations such as Nigeria. The indiscriminate disposal of waste has seriously added to environmental degradation.

Contamination of water by bacteria and trace metals is a significant feature in equally environmental health and geochemical cycling of metal. Trace quantities of heavy metals are constantly existing in fresh waters of terrigenous supplies for example rock weathering which result to geochemical re-cycling of elements of heavy metal in these ecological units (Amadi *et al.*, 2015). When the waste disposal site is not situated on an appropriate earth, it might allow the permeation and relocation of waste produced leachate into the resources of groundwater thus changing the water attribute harmfully. City waste resources, largely household trash, are frequently disposed off on surface ground, thin excavation, stream and river drains which put the groundwater at extreme threat of being contaminated. The significant increase in human population is apparently associated with the corresponding generation of huge amount of solid waste resulting from socio-economic activities within the metropolis. Solid trash landfills represent a vital element of the soil hydrological structure (Rosqvist *et al.*, 2003), therefore, poses a severe risk of contaminating together the subsurface and downstream surface water.

1.3 Justification for the Study

Groundwater is the major supply of potable water within the Barikin-Sale area and efforts should be geared towards protecting it from contaminants. latest detections of many noxious chemicals in groundwater in the United States of America as a result of municipal solid waste leachate accumulation shows that 32 natural chemicals initiate cancer, 13 result to birth defects, 22 hereditary effects whilst around 10 inorganic chemicals instigate

ailments such as nervous systems defects, cancer of the bladder, kidney/liver defects, central nervous system defects, circulatory system defects, and skeletal impairment US environmental protection agency (EPA,1994).

Furthermore, the World Health Organization (WHO) 1996 fact sheet no.112 projected universally that no less than a child died from a water connected illness each eight seconds and that annually over five million persons died from sicknesses connected to insecure intake water or poor hygiene. Ecological degradation and pollution of groundwater possibly owing to leachate produced from exposed dumpsites and several human actions (Oyediran and Iroegbuchu, 2013 and Amadi, 2009). The far recognized technique for solid waste dumping that requires a least endeavor and expenditure in Nigeria is the exposed dumpsites. Obstacles to such facilities are moderately obvious, particularly to those possessing the adversity of living near the dumpsites. Open dumpsite does not only pollute groundwater, they are also unattractive, unhygienic, and in general stinking.

1.4 Study Area

The location is Barikin-Sale area of Minna headquarters of Niger State (Figures 1.1). It is bounded by longitudes 6° 31'E and 6°33'E of the Greenwich Meridian and latitudes 9°34'N and 9°36'N of the Equators and the dumpsite is located within the area.

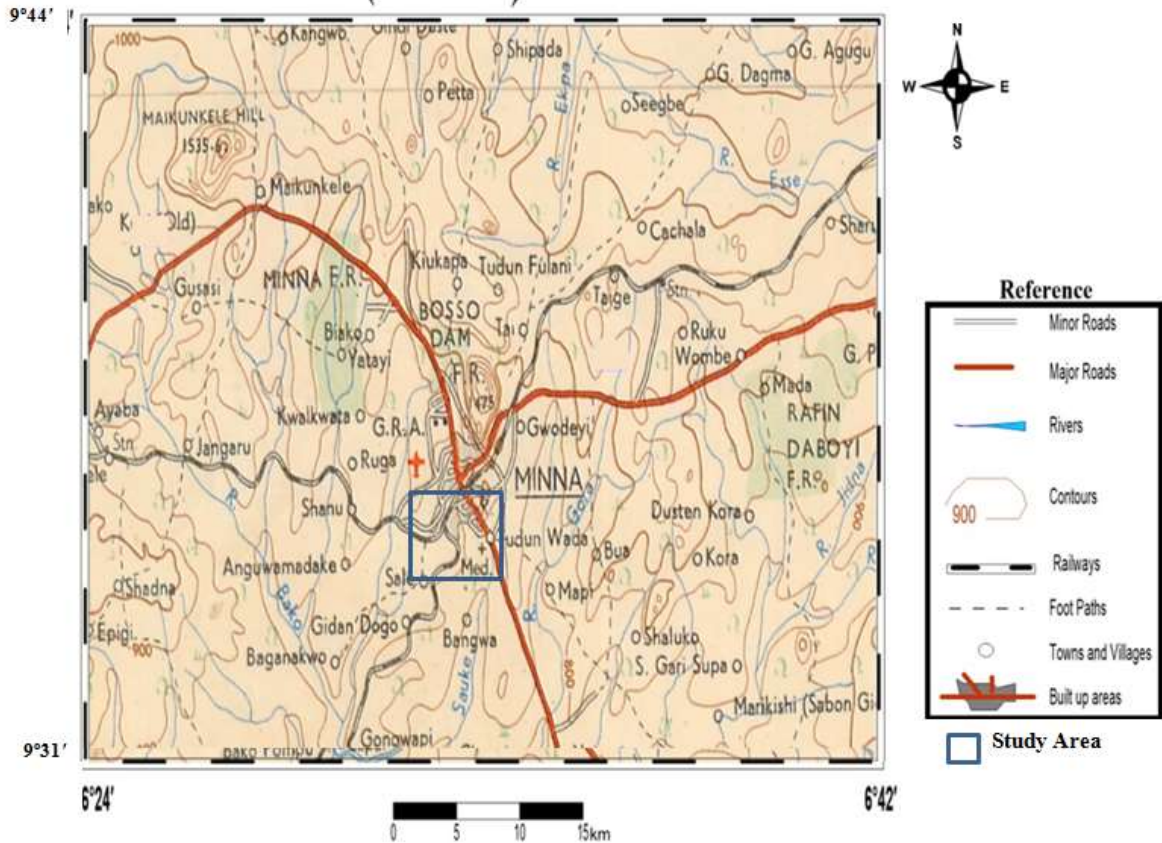


Figure 1.1: Topography of Minna and the study area (Modified after Amadi *et al.*, 2015)

The investigated section lies in the Nigerian Basement Complex topography. This environment is illustrated by three lithofacies: i. the older granites, ii. the low metasedimentary schist and iii. the migmatite gneiss complex (Oyawoye, 1972 and Rahaman, 1976). Significant to the section is the granite-gneiss, granite and schist with residue of quartz trace and pegmatite's as slight incursions fundamental to the area. Rocks of granite occupy almost 95 % of the section in study. The rocks are generally uncovered on the western segment of Minna Township. It appears as elevated batholiths that are broad in dimension. The granite exposures are foliated, fractured and jointed.

The rocks are comprised of minerals that are bright and dark in colour; quartz, feldspar and biotite-mica correspondingly. The mineral colour alteration describes the gneissose bands.

In several circumstances the rocks are fractured and weathered. The quartzite and pegmatites veins appearing as small mineral invasive rock as well outline some part of the region. The rocks of granites and gneisses largely function as the mass rock on which the veins of quartzite and pegmatite minerals. They are delineated by coarse textures. In terms of minerals, they are made up of feldspars, quartz and various valuable minerals of prominent value which consist of aquamarine, emerald, epidote and tourmaline (Ajibade, 1982 and Wright, 1985). The basement sections hydrogeology is easy given that there is an intrinsic restraint to groundwater occurrences. Although, where there is deep regolith and there are intense systems of fractures, the possibilities for the gathering of groundwater within the rocks of basement complex can raise. Preferably, the region can be separated into two components, that is, the aquiferous region found in the weathered overburden lying on the fresh basement rocks and the area of aquifer inside the extremely fractured systems of joint in the partly weathered basement (Omale *et al.*, 2016).

1.4.1 Relief and Drainage

The relief of the research region is typically level lying, with rather rising and falling ridges contained by the area. There is no most important river that draws off the locale water but there are a number of petite streams running/traversing the region. The structure of drainage in the examined region is structurally restricted. The total streams found in the district are seasonal; they run all through the rainy season and withered as dry season sets in. The outline of drainage of the area can be described naturally as dendritic (Figure 1.2). The elevation of the area ranges from 219 to 245 m (Author's fieldwork).

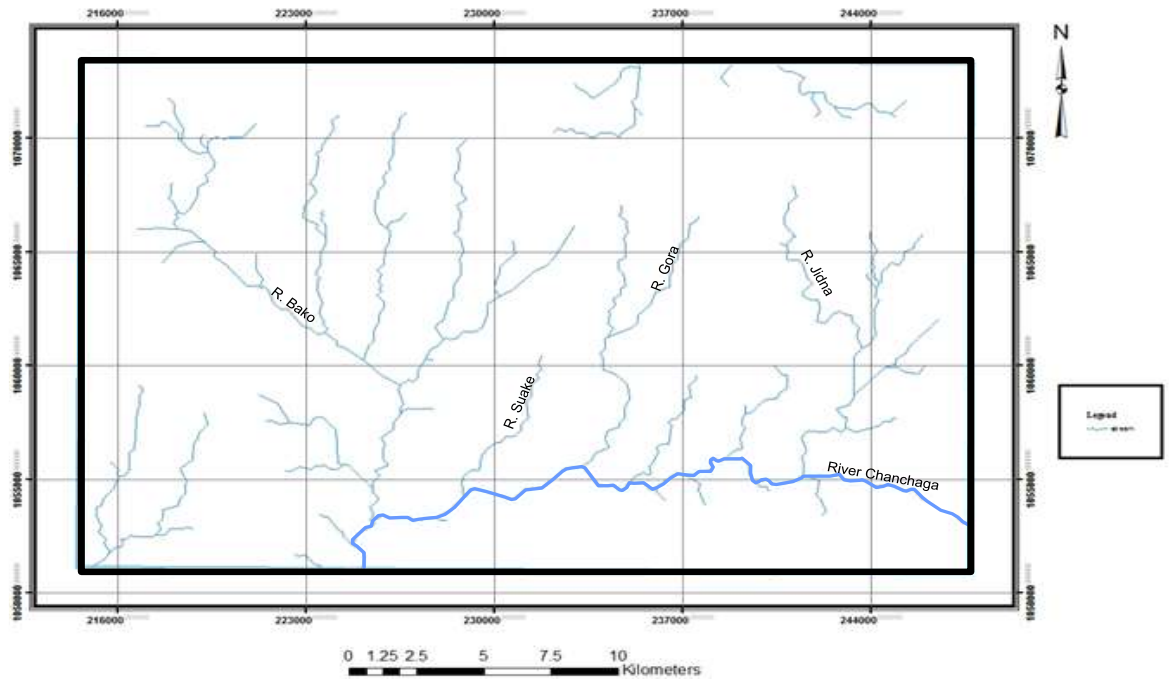


Figure 1.2: Drainage Pattern of Minna Metropolis

1.4.2 Climate and Vegetation

The investigated region has an archetypal savannah climate with diverse wet and dry seasons (Ajibade, 1982). The rainy season starts in April and stop within October which is roughly six months phase (Federal Meteorological Agency, Minna, 2011). Maximum of about 1,300 mm and minimum of about 1,000 mm respectively are the annual rainfall distribution pattern of the area. The area’s climate is predisposed by two wind systems, the south-west downpour emerging from the Atlantics. The subsequent is the dry sandy wind of north-east also known as the “harmattan wind” which emerged from the Sahara Desert. The maximum temperature is at (around 35 °C) between March and June and at its minimum (about 21 °C) in December and January (Ajibade, 1982).

The study area flora is grouped in the savannah variety. The savannah plants are deemed as intermediary between the Guinea savannah of northern Nigeria and the southern rain forest

correspondingly. Rainfall reaches a high peak in August. Somewhere else, the soil is amenable to the farming of vegetables and other food crops plus foraging by animals.

1.4.3 Settlement and Land Use

The examined region is characterized by a nucleated settlement variety inhabited mainly by the Nupe speaking tribe with other dialect scattered among the population. There are supply of some essential public facilities sometimes such as supply of tap water, electricity and road systems within and communication set-ups. There major source of water supply is hand dug wells and boreholes. The major activities of the people within the area are farming, cultivation of crops like maize, groundnuts, guinea corn, yam and millet.

1.5 Scope the Study

The investigation is structured to assessing the effect of the dumpsite in Barikin-Sale on the groundwater within the area of study. The structure of the work is defining the geology of the area, geotechnical properties of soil samples collected from different locations in the field, geophysical and hydrogeological characteristics of the Barikin-Sale area.

1.6 Aim and Objectives

The aim of the research is to investigate leachate infiltration pattern of Barikin-Sale dumpsite.

The specific objectives of the study are to;

1. Carry out geologic field mapping.
2. Delineate the aquifer system and produce hydraulic distribution map.
3. Determine the hydraulic conductivity beneath refuse dump.
4. Investigate the behavior of leachate migration in the subsurface.

5. Determine the suitability of the water for human consumption.

1.7 Regional Geological Setting

The geology of Nigeria is divided into three main litho-petro-stratigraphical units (Figure 1.3). They are the Precambrian aged Basement Complex; the Younger Granite which are Jurassic and the Cretaceous to Recent in ages Sedimentary Basins.

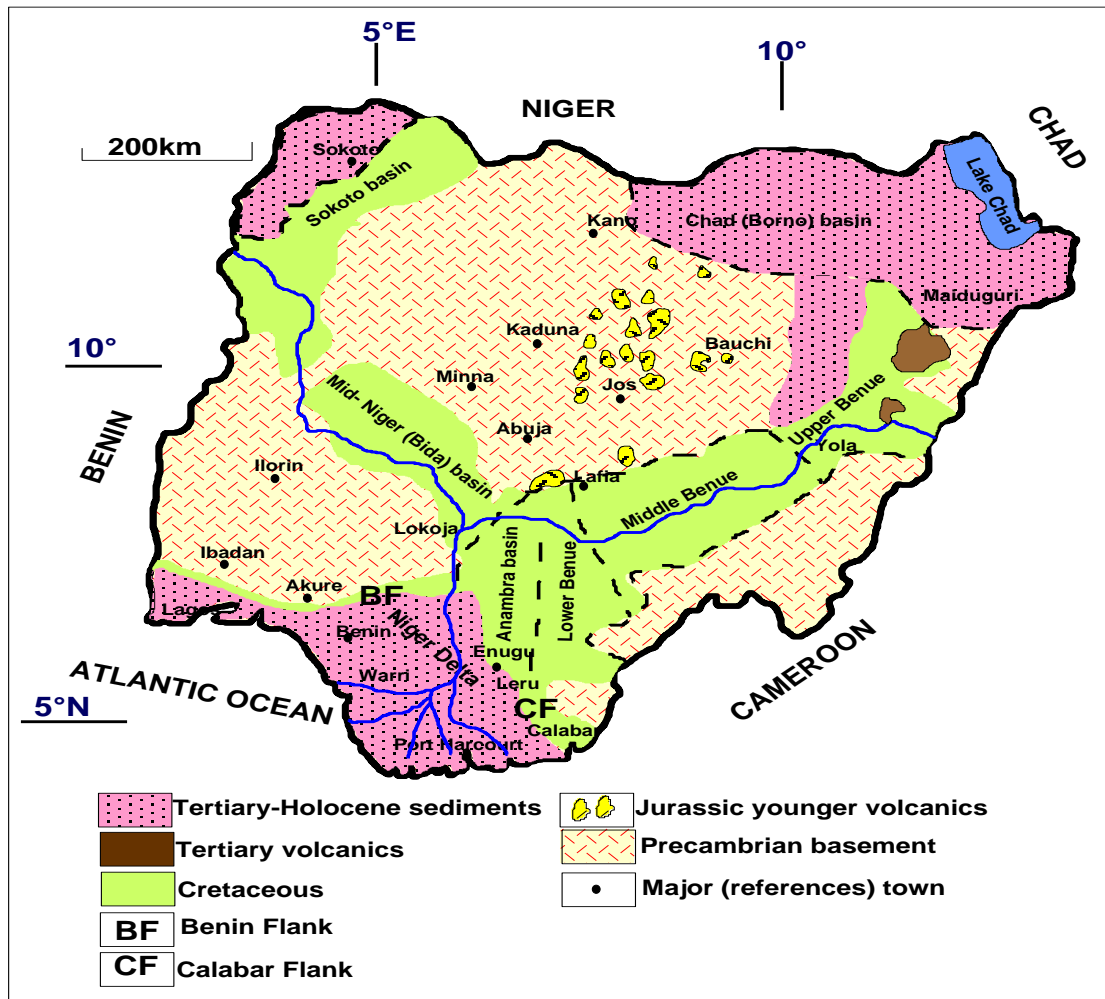


Figure 1.3: Broad geology of Nigeria (NGSA, 2009)

1.7.1 The Basement Complex

Black (1980) affirmed that the Nigerian Basement Complex (Figure 1.3) resulted from the Pan-African movable belt. It is to the south of the Tuareg Shield, amid the Cratons of West

Africa and the Congo. The development of the Basement Complex occurs over no less than events of four orogeny episodes, it consists of $2800 \pm 200\text{Ma}$ Liberian, $2000 \pm 200\text{Ma}$ Eburnian, $1100 \pm 200\text{Ma}$ Kiberan and $600 \pm 150\text{Ma}$ Pan-African (Oyawoye, 1972; Rahaman, 1976). The episodes of Liberian, Eburnian and Kiberan were connected to extreme warp and then by regional metamorphism. The Pan-African period of warp was complemented by a regional metamorphism, complemented by the processes of migmatization, granitization and gneisses formation (Abaa, 1983). Regional warp of fracturing and faulting discern the stop of the orogeny. The Younger Granites of Jurassic age of Jos plateau has abundant ring complexes of calc-alkaline intruding the Basement complex. The Basement Complex is overlaid unconformably by the Cretaceous and younger sediments at numerous localities inside and all-around Nigeria (Olayinka, 1992 and Obaje, 2009). Obaje (2009) said the 600Ma Pan-African orogeny influenced the Nigeria basement complex. There was an impact involving the dynamic Pharusian continental boundary and the West African craton inactive continental boundary. The continental impact is thought to be accountable for the Basement Complex creation (Burke and Dewey, 1972). The Basement Complex of Nigeria is illustrated in four petro-lithological sections, this includes;

- a. The Precambrian Older Granite
- b. The Migmatite/Gneiss Complex
- c. Undeformed Acidic and Basic Dykes.
- d. The Low grade Schist Belt

The stratigraphic succession of the Nigerian Basement Complex is exemplified in Table 1.1.

Table 1.1: Succession of stratigraphy of the Nigeria Basement Complex (McCurry, 1976)

PERIOD	LAYERING	COMPOSITION
Recent to Tertiary	Surface	Laterite, clay and alluvial sand-silt
Cambrian to Upper Precambrian	Metasediment	Phyllite, quartzite hornfels, semi-pelitic schist, schist amphibolites
Precambrian	Crystalline	Migmatite complex, gneiss, feldspathic quartzite, calcareous schist

1.7.1.1 The Older Granite

The Nigerian older granite (Figure 1.3) intersects the gneiss/migmatite complex and the belts of schist. They are believed to be formed in the magmatic phases that come with the 750–450 Ma orogeny of Pan-Africa. They are made up of broad mineral varieties (Obaje, 2009). The older granite is the mainly distinct of the whole episode of Pan-African orogeny (Rahaman, 1988). Rahaman (1988) classified the suites of the Older Granite on the bases of their petrofabric attribute below.

- a) The migmatite granite;
- b) The granitic gneiss;
- c) The early on pegmatitic and fine grained granite;
- d) The uniform to coarse porphyryl granite;
- e) Pegmatitic aplites that are to some extent distorted with veins of quartz; and
- f) Undeformed pegmatite, two-micaceous granites and quartz intrusion.

On a universal degree, the older granites are believed to be intrusions of elevated height (Rahaman, 1988).

1.7.1.2 The Migmatite/gneiss Complex

The age of the migmatite gneiss complex varied from 600 Ma Pan-African to around three billion years Eburnean. It is a united component made up series of metamorphosed rocks that are basic and ultrabasic, migmatites, orthogneisses and paragneisses (Obaje, 2009). The migmatite-gneiss mineral composition is considered to being recrystallized by the incomplete melting process that influenced the basement complex. The migmatic-gneiss complex encompasses around 60 % of the exterior area of the Nigerian basement complex. Proof of its domination can be noted in the Nigerian Northwest and North-south (Rahaman, 1988 and Obaje, 2009). The migmatic-gneiss complexes rocks are related to the three main episodes of geological which includes;

- a. Natural crust development and growth of crustal an outcome of orogeny and sedimentation 2,500 Ma.
- b. The $2,000 \pm 200$ Ma Eburnean, manifest by granitic gneisses of Ibadan variety and
- c. The 900 to 450 Ma Pan-African episodes (Rahaman and Ocan, 1978; Rahaman and Lancelot, 1984).

1.7.1.3 The Low Grade Schist Belt

The Nigeria Schist is understood in age as Upper Proterozoic. They are infolded into the complexes of the migmatic-gneiss-quartz (Figure 1.3). They are made up of meta-volcanic and meta-sedimentary rocks of low grade (Obaje, 2009). They are suitably uncovered in the Nigerian western half which trend in the of north-south bearing (Figure 1.4).

Nigerian northwest has been ascribed ten sheet belts including the Anka, Kazaure, Kushaka, Kuseriki, Maru, Wonaka, Zungeru-Birnin-Gwari, and Zuru. The Nigerian south western section is ascribed the below sheet belts; Egbe-Isanlu, Ife-Ilesha, Igara, Isheyin-Oyan, Iwo, Kabba-Lokoja (Turner, 1983; Woakes *et al.*, 1987).

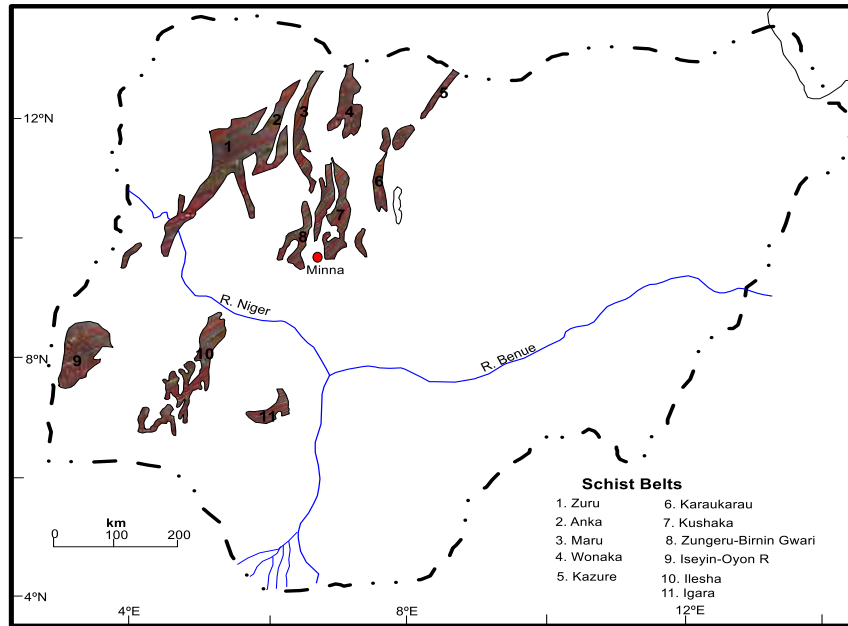


Figure 1.4: Nigeria Schist Belts

1.7.1.4 Undeformed Acidic and Basic Dykes

The acidic and basic undeformed dykes as documented by Obaje (2009) are interrelated to incident of Late to Post tectonic Pan-African episode. They go through the previous elements of the family of the basement complex including; the migmatic-gneiss complexes, the older granites and the belts of schist. The acidic and basic underformed dykes are classified into two categories;

- i. Felsic dykes that are around 580-535 Ma. They are associated to the granitoids of the Pan-African. On a broader level they are connected with rocks and minerals for instance the pegmatites influencing alites, beryl, microgranites, muscovite, syenite and tourmaline (Obaje, 2009).
- ii. The basic dykes age is considered to be roughly 500 Ma. They are considered as the youngest element in the Nigerian Basement Complex. They comprise dykes of lamprophite, dolerite and felsite (Obaje, 2009).

CHAPTER TWO

2.0

LITERATURE REVIEW

Dumping of solid waste on land is the mainly frequent waste techniques of disposal across Nigeria. Groundwater forms an important part of the water resources across the world particularly in the arid regions. It is used for household functions because it is of high value and required slight or no remedy prior to usage. Abimbola *et al.* (2001) and Jegede *et al.* (2013), said that bacteria, fungi and further biological contaminants are in nature filtered and attenuated as the water infiltrate or permeate throughout the soil. The lackadaisical administration and/or discarding of harmful substances, fresh groundwater supplies are decreased greatly.

The menace of groundwater contamination by any leachate is resolved by the factors below:

- i) **Depth to water table:** If there is low water table (far below the ground surface), water will turn out to be partly filtered as it permeates through the soil downward. Water table that is high (near to the surface), the contaminants can go into the groundwater unswervingly devoid of filtration through the soil (Figure 2.1).

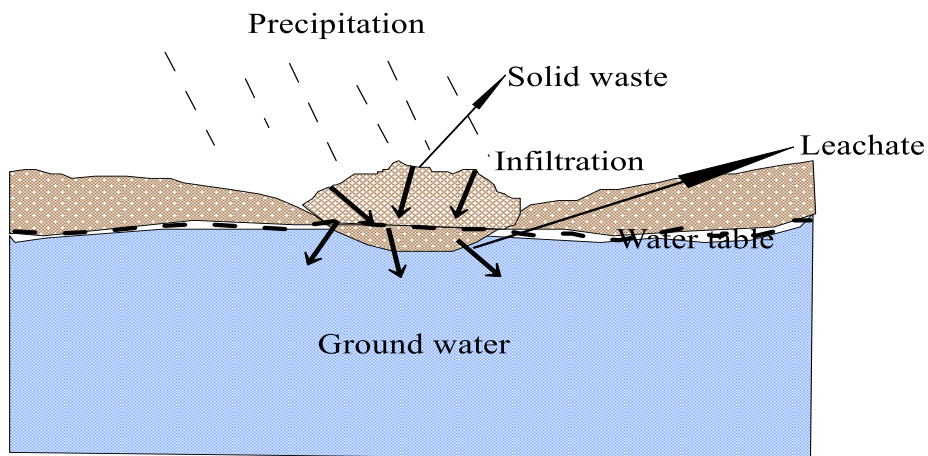


Figure 2.1: Water Tables Intersects Landfill (Montgomery, 2000)

- ii) **Concentration of contaminants:** An elevated contaminants concentration in leachate will make groundwater contamination more possible.
- iii) **Permeability of the geologic strata:** Extremely leaky geologic stratum permit leachate to rapidly infiltrate through, getting slight filtration down the way (Figure 2.2). Strata consisting of moderately impervious resources for instance silt and clay serves as natural impediment to leachate and consequently inhibits the descending leachate percolation.

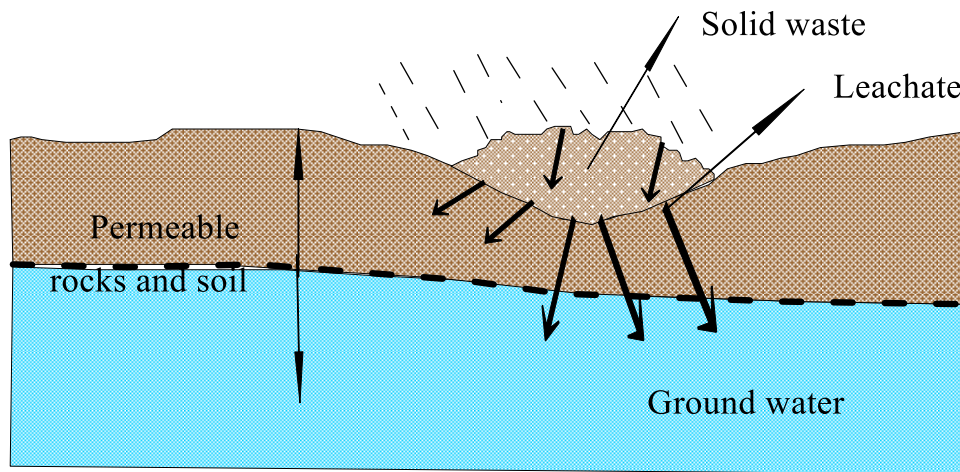


Figure 2.2: Leachate Permeates to Water Table through Permeable Materials beneath Landfill Location (Montgomery, 2000)

- iv) **Type of geologic strata:** A numbers of earth materials, for example clay, are more efficient at sifting out contaminants, not just because they are impervious but as well because chemicals can attach to their units surface. (Table 2.1) illustrates the comparative susceptibility to contamination by hydrologic situation.

Table 2.1: Comparative Susceptibility to Pollution by Hydrologic Setting

(Montgomery, 2000)

Vulnerability	Type of Geological Setting
Intense	1. Aquifers of bedrock snip out (particularly in karsts vicinity); or aquifers of bedrock overlain by soil of under 3 meters 2. Aquifers of unconfined gravel and sand with unsaturated region with thickness of under 3 meters
High	Aquifers of bedrock overlain by 3 meters gravel and sand, 3-10 meters till of sandy, or 3-5 meters clay-rich till or clay
Moderate	Aquifers that are unconfined overlain by 10 meters till of sandy, or 5-10 meters till of clay-rich, peat or clay
Low	Aquifers that are confined overlain by 10 meters till of clay-rich or low permeable rock for example shale

2.1 Review of Related Literatures

2.1.1 Review of Geological and Hydrogeological Related Literature

The work of Iyama and Edori (2019) on the determination of chemical and gross organic pollutant intensities in leachates from accepted waste dumpsites in Port Harcourt city Rivers State, Nigeria indicated from the result that there was no considerable disparity in sequential measurement but high level spatial distinction in most parameters occurred. The research discovered that these dumpsites continued to be main sources of polluting to the surrounding surface and groundwater regime.

Alawode *et al.* (2019) work on the physicochemical investigation and public effects of heavy metals of leachates from landfills in groundwater of Ogeese community Oyo State Nigeria. The results show that leachates from the landfill dumpsite pollute the groundwater within the Ogeese community in Oyo State. Leachate may become highly contaminated as

a result of the composition and extent of decomposition of the refuse and hydrogeological factors (Qasim and Chiang, 2017).

Zakaria and Aziz (2018) carried out a comparative study of the characteristics of leachate at Alor Pongsu landfill location, Perak, Malaysia. The result of the analysis when compared with WHO (2010) allowable limit reveals that the majority of the factor surpasses the standard expulsion restriction.

Bahroz (2015) carried out groundwater and leachate evaluation at Kirkuk sanitary landfill location in Zindana community, Iraq. He discovered that generation of waste increases after 2003 war event because of extreme population growth and economic development. The results show contamination which lead to severe problem concerning environmental and human health within the area.

Abd El-Salam and Abu-Zuid (2015) carried out the influence of leachate of landfill on the quality of groundwater in Egypt and the result of the physicochemical analysis of leachate established that its distinctiveness were extremely erratic with serious contamination of salts, organics and heavy metals. The ratio of BOD5/COD (0.69) denoted that the leachate was recyclable and unstabilized.

Amadi and Nwankwoala (2013) investigate the assessment of heavy metals in soils from refuse dumpsites of Enyimba in Aba town. The techniques of multivariate statistic and AAS were utilized to examine thirty samples of soil from the environs of the dumpsite. The trace metals total concentration decreases as thus $Cd > Co > Cu > Zn > As > Pb > Mn > Ni > Cr$. Owing to the existence of these trace elements which are possible risk to human

wellbeing, they encourage for the substitution of open dumpsites method with a suitably-engineered solid refuse landfill.

Ige (2013) engaged a two means method; geological and geotechnical, to appraise an exposed refuse site for the building of hygienic landfill in Ilorin, Southwest Nigeria. Geotechnical examinations of four illustrative samples were done on unstable soils from test pits inside the dumpsite. Investigated properties comprise the particle size, compaction, Atterberg consistency limits and the soils permeability prospectivity. Sample gathering, preparation and analyses were executed in order of the British Standard BS 1377:1990. The outcome signifies fresh un-fractured migmatite sufficiently practicable to present adequate assistance for recent solid refuse sanitary landfill which is beneath the area. Considering the geotechnic, the samples of soil above the site shows a mean sand of 51%, clay portion of 33% and gravel size of 3.75%. Samples of soil indicate plasticity of low to medium and activity of clay 0.39. The Maximum Dry Density and permeability coefficient means are 1.80 g/cm^3 and $1 \times 10^{-8} \text{ m/s}$ correspondingly at lighter force of compaction. No matter the depth of the trial pit, all the samples show that the soil is inorganic clay of permeability of low to medium.

Kola-Olusanya (2013) examined the consequence on environment the solid refuse on resources of groundwater in Nigeria. Samples of groundwater were taken in refuse sites vicinity. The outcome point to groundwater contamination, resulting from infiltration of leachate into the system of groundwater attributed to the permeable and porous nature of the soil beneath.

Owoeye and Okojie (2013) perform an environmental review of a refuse site in the settlements of Ugbor, southern Nigeria. They express the economic and physical and characteristics of the research section using a study design of descriptive comparative. The outcome discovered that dumpsite does not fulfill the obtainable federal regulation and laws that guide waste dumpsite in Nigeria. This waste dumpsite cause present a probable threat to quality of groundwater and as a result health of the public.

Aderemi *et al.* (2011) evaluate contamination of groundwater by refuse leachate close to Soluos refuse site in Lagos, southwest Nigeria. This was done to determine the consequence of refuse leachate seepage on the groundwater quality. Physico-chemical and bacteriological assessment of the samples of groundwater from the dumpsite environs were made. Factors like pH, total dissolved solid, electrical conductivity, major anions and cations in addition to *Enterobacteriaceae* were investigated. Observed was noticed that refuse-leachate from the sanitary landfill has little effect on the groundwater structure in the landfill environs. It can be credited to the obtainable features of soil at the location that consist clay minerals with significantly low hydraulic conductivity reducing leachate permeation into groundwater structure.

Abimbola *et al.* (2001) appraised the geochemical distinctiveness of a number of refuse dumpsite on the quality of groundwater and soil in Warri, Niger Delta. This research discovered that waste dump leachate permeate into the subsurface water which was ascribed to the elevated hydraulic conductivity, elevated rate of rainfall and thin water-table in the region. The building of a sanitary landfill with hydrogeological and geological setting that will certify the groundwater and soil was encouraged.

Tijani *et al.* (2002) conducted a widespread examination of the environmental consequence of refuse dumpsite on shallow groundwater surface water resource of a basement complex region, southwest Nigeria. This investigation was performed because of the rise in the inhabitants near the dumpsite and the absence of suitable system of landfill. Representatives' samples of groundwater of around sixty were taken and analyzed for main anions, cations, and a number of heavy metals. Observation made was that the exposed refuse site can have a considerable adverse consequence on the quality of groundwater. If the refuse site is not situated on an appropriate soil, it might allow the permeation and movement of waste produced leachate into the subsurface water reserve thus changing the water quality harmfully.

2.1.2 Review of Geotechnical Related Literature

Oyediran and Iroegbuchi (2013) examined the geotechnical character of clays from southwest Nigerian as obstruction soils for urban solid refuse landfill. Total of forty samples of undisturbed and disturbed soils were taken for grading analysis, permeability tests and limit of consistency. The values of hydraulic conductivity varied from 1.18×10^{-4} to 1.45×10^{-7} cm/s signifying low impermeable and permeable soils. Kaolinite combined with lilies and bentonites were discovered from the mineral analysis of the clay. The capability of the clay to have waste produced leachate was established. Likewise, the clay has high specific surface area which permits low movement of leachate.

Bayewu *et al.* (2012) investigate the geotechnical and textural characteristics of lateritic soils formed over primary bedrocks in Ago-Iwoye region, Southwest Nigeria. It bring to light the consequence of the bed rock feature on soil indicator properties like distribution of particle sizes, California Bearing Ratio (CBR), plasticity index and dry density. Also it's

essential to have knowledge of the primary rock and its attribute before the examination of properties of engineering and activities of soils residues.

Oyediran and Adeyemi (2011) conducted the geotechnical examination of an area in Ajibode, southwest Nigeria, in verifying its aptness for sanitary landfills. Examination of the region geology was carried out to establish the natures of rock in the area. Geotechnical indices factors like characteristic Atterberg consistency limit, particle grain size, permeability and compressive strength were established. The quantity of soil fines varies from (30.0 - 73.0 %) and contents of clay (11.3 – 38.7 %) which are within the minimum 30 % and 10 % particular limits for an appropriate site for sanitary landfill. The soils are properly ranked, signifying plasticity of medium to low. The index of plasticity varied from 9.1 to 20.3 % and low possibility of leakage of 0.3 – 0.4 cm/s. Permeability coefficient varied from 4.7×10^{-8} - 1.9×10^{-6} cm/s and is in the span of 10^{-8} - 10^{-6} cm/s requisite for reduction by natural geological impediments.

Ige (2010) conducted an appraisal of the geotechnical behaviour of laterite from a refuse site in Ilorin Southwest Nigeria, as liners of clay in landfill. The standard of BS: 1377 method was used to examine for the particular strictures of the soil for example characteristics of grain size, permeability and Atterberg limit. The soil was suggested for usage as impediment liner down to the reality that its elevated force of compaction gives lower coefficient of permeability value.

Ige and Ogunsanwo (2009) investigated the geotechnical distinctiveness of soil resulting from granite for additional usage as liner of clay in sanitary landfill within Ilorin, southwest Nigeria. Factors for example distribution of particle size, maximum dry density, Atterberg

consistency limits and permeability coefficient were found out in compliance with the 1990 standard of BSI 1377. The soil was categorized as residual soil of inorganic clay that has high plasticity. This work showed that the location soil has the ability of sustaining hydraulic conductivity that is low. Having permeability coefficient of below 1×10^{-7} cm/s, when stoutly compacted, it have the capability to endure the permeation of leachate into the formation of groundwater.

Adeyemi and Ogundero (2001) examined the soil properties resulting from migmatite-gneiss in Oruu-Ijebu, southwestern Nigeria. Geotechnical characteristics of the soils were established keeping to the British Standard (BS): 1377 process. Parameters like particle size, specific gravity and linear shrinkage of the grains were considerably restricted by the inner soil framework, the grain masses and forms. The research indicated that the soils from the sphere of laterite were found appropriate as liner for landfill.

2.1.3 Review of Geophysical Related Literatures

There exist numerous geophysical researches that have been done by various researchers on landfills and refuse dumpsites. Their outcomes revealed that geophysical methods can be utilized in landfills and refuse dumpsites investigation as a result of its capacity to identify modifications connected to variants in conductivity.

Osazuwa and Abdullahi (2008); Porsani *et al.*(2004); Dahlin and Bing (2003); Mukhtar *et al.* (2000); Buselli *et al.* (1992), all showed the applications and limitations of the geophysical technique in environmental drawbacks linked with contamination of groundwater attributable to movement of leachate.

Omale *et al.* (2016) conducted the appraisal of leachate contamination of groundwater at three most important refuse dumping sites in Minna (Barkin-Sale, FM and Albishiri). The geo-electrical technique (induced polarisation and vertical electrical sounding) and physico-chemical analysis of sampled water were useful to measuring the leachate contamination of the resources underground. There were 18 IP and VES locations at Albishiri, 18 IP and VES locations at Barkin-Sale and 350 IP and VES locations at FM sites correspondingly. The outcome illustrates that the region is in general underlain by three patterns of geology (top soil (laterite), fractured/weathered basement and novel basement) matching the geo-electric prototypes. Conversely, wherever the basement has witnessed intense fracturing which leads to the basement rocks weathering, five and four layer prototypes were achieved. Leachate plume discharge and contamination is at changeable depth and moisture content. The degree of contamination by leachate at the research region is put at 0.3, 0.6 m and 0.7 m for each year for the Barkin-Sale, FM and Albishiri sites in that order.

Jegede *et al.* (2013) employed survey by electrical resistivity to observe the movement of leachate plumes in the underground at ancient cemetery and Tsamiya refuse dumpsite in Zaria, Nigeria. Ten months were utilised in studying the movement of plume of leachate in underground for these two areas. He discovered that plume leachate travel quicker in lateral path than vertical bearing. He concluded that this resulted from the existence of clay inhibiting the movement of leachate. The use of different techniques of geophysical for the examination of pollution of groundwater sites is a reasonably latest improvement.

Survey by electrical resistivity scheme was conducted in Uyo by Akankpo and Igboekwe (2011). They establish a broad array of resistivity variant which ranged from 2.0 Ωm to 60700 Ωm . On the basis of the study outcomes, they explained that the rates of resistivity

below 75 Ωm indicate contamination caused by refuse at Udo and Eka Streets. Furthermore, the high amount of resistivity at mechanic village (60700 Ωm) perhaps is connected to the waste oil put down because of the vehicle repair activities. Likewise, they clarified that a contrast of the values of resistivity and the types of curve at the dumpsites (Udo and Eka Streets) and other sites illustrate that the two dumpsites have a type H curve representing zones of contamination, whilst other areas have a type K curve representing uncontaminated areas.

A resistivity survey of direct current was conducted in Akure South-western Nigeria by Bayode *et al.* (2011) established that the resistivity of topsoil and rate of thickness varies from 5 – 107 Ωm and 0.2 – 2.7 Ωm correspondingly. The values of the weathered stratum resistivity range from 4 – 35 Ωm whereas thickness varies from 1.1 – 12.9 m underneath the refuse site. The deepness to the bedrock ranges from 2.2 – 13.1 m. The rates of resistivity of the zones of fault/fractured varies from 2 – 55 Ωm and the thickness ranges from 10 – 30 m. In addition, they elucidated that the structures of 2D resistivity illustrate that areas with moderately low values of resistivity of < 35 Ωm with a depth extent of 1.1 – 15 m for topsoil, layer weathered and fractured/faulted basement regions are assumed to be as a result of saturation of leachate. As a result of the observed fairly superficial water table of 0.5 – 2.0 m within the refuse sites, the groundwater close to the refuse sites is assumed to have been contaminated. They deduced that the research discloses that underground geologic formations inside the bedrock (faults/fractures) influence the movement of leachate plume surrounding the examined refuse site.

Ibitola *et al.* (2011) carried out vertical electric sounding of Ibadan, South-western Nigeria and elucidated that an incorporated study of qualitative and quantitative elucidation shows

that the lithologies of the underground for VES that have top soil (0.5 - 1.0 m) and resistivity varies from 9.2 - 68.3 Ωm , clayey soil (2.0 m - 11.3 m) with resistivity ranges from 2.2 - 12.30 Ωm , lying atop of the novel basement of unidentified thickness of the individual refuse sites. The product of the VES data presents a qualitative clayey and topsoil lithology (aquitar) that has a low resistivity region $< 100 \text{ Ohm-m}$, underlain by extreme resistive basement. They summated that combining the two explanations acquired from the map of digital elevation and geophysical survey was applied for the founding the health and environmental vulnerabilities linked to passage of groundwater in the underground (saturated and vadose regions) down the two refuse sites.

Nasir *et al.* (2010) elucidated the VES values taken within a dumpsite in Kaduna that reveals plumes of contamination as low areas with rates of resistivity varying between 1 and 12.9 ohm-m broadening from the exterior through the aquifer of superficial subsurface water of below 5 m. They elucidated that reasonable value of conductivity of the underground resources is said to ease passage of the leachate plume across the soils and movement of the contaminants beyond the refuse site and into the superficial aquifer in the region of research.

Ehirim and Ekeocha (2009) adopted resistivity sounding method of azimuthal – offset to outline anisotropic structural components in relation to the incidences of gully erosion. They discovered that the resistivity anisotropic bearings concurred with gully erosions axes.

Mondal *et al.* (2008), demonstrated that electrical resistivity method can give a better picture of the concealed structures than the conventional mapping and apparent resistivity contours using the vertical electrical sounding method.

Chamber *et al.* (2006) and Soupious *et al.* (2007) exploit tomography of electrical resistivity to confirm the geotechnical examination for study of foundation. He applied electromagnetic survey with electrical resistivity imaging to resolve the inhomogeneity in geological outline.

Rao *et al.* (2004) used 2D and 3D electrical resistivity tomography to determine buried quarry site geometry, plotting bedrock contamination and characterized site geology for engineering purpose.

Olayinka and Yaramanci (2002) offered the smooth and sharp-boundary inversion of two-dimensional simulated section figures in the presence of decrease in resistivity with depth. Their inferences present guiding philosophy in arithmetical form of multi-channels resistivity profiling data.

Barker (2001) applied electrical resistivity tomography to resolve environmental setback. He applied this process to outline the contaminated area close to Dindigul town in India. The outcome indicates that electrical resistivity tomography could be used as quick and proficient in resolving environmental drawbacks.

Olayinka and Olayiwola (2001) examined the effect of solid refuse dump site at Ring road area of Ibadan on bordering sources of surface and subsurface water with the usage of electrical imaging and revealed that bodies of water in a downward slope bearing in the near environs of the landfill obtains considerable contribution of organic pollutant.

Michel *et al.* (1999) effectively utilised 2-D wenner electrical imaging to describe the underground composition of eastern Senegal basement complex. From the research, the level of relationship of electrical resistivity tomography figures with product of pit indicate that tomography of electrical resistivity can be utilised as quick and resourceful exploration means to map the broad lateritic weathering mantle in humid basement region with geology of hard rock.

2.2 Principle of Electrical Resistivity Survey

The electrical resistivity principle is commonly on the bases of the well-known Ohm's law. Usually, measurements are done on the earth by distributing current in the earth surface using two current electrodes (C1 and C2). The consequential voltage (V) variation is determined between an additional potential electrodes pairs (P1 and P2) (Figure 2.3). The resistance (R) is resultant from the voltage and current (V and I correspondingly) amounts with the aid of Ohm's law ($R = V/I$).

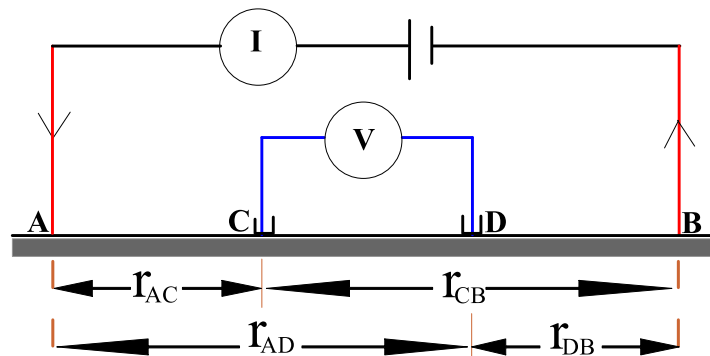


Figure 2.3: General Four Electrodes Array (Lowrie, 2007)

Allowing for the earth to be a consistent half-space, the basis electrode (C1) that provides the current to the earth, there is positive potential and it reduces with space from the supply. The supply will have several lines of electric field which travel outward radially. Within the

sink (C2) the potential terminal to be negative and obtains fewer negative with rising expanse from the electrode submerged. The field outline travel inward radially within the sink (Figure 2.4). When a lone electrode is measured, in that case the equipotential planes surrounding a sink or source electrodes are hemispherical (Lowries, 2007).

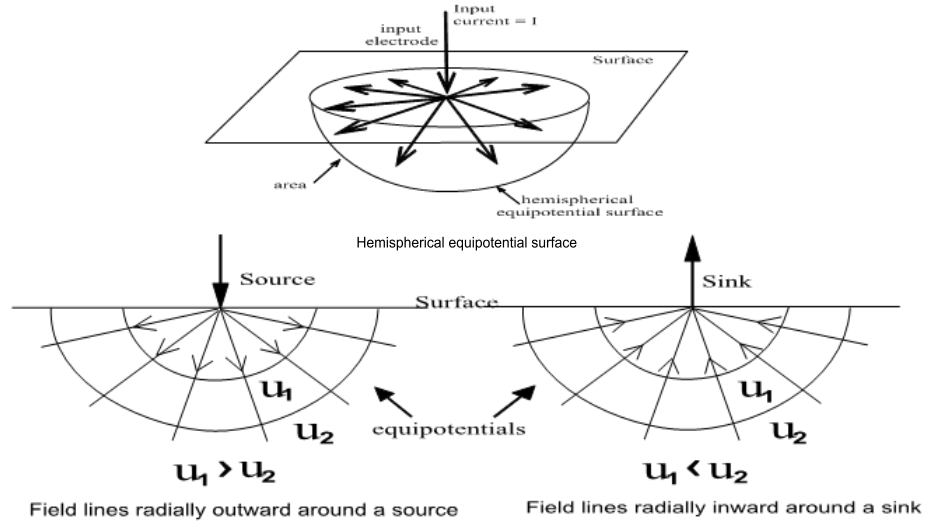


Figure 2.4: Equipotential plane and field lines (Lowrie, 2007)

2.2.1 The General Four Electrode Theory

Considering the configuration of four electrodes, the current electrodes A operate as basis whereas B operates as sink (Figure 2.3). On the revealing potential electrode C, the basis A is $+pI/(2 \pi r_{AC})$, whereas the potential attributable to the sink electrode B is $-pI/(2 \pi r_{CB})$ (Lowrie, 2007). The potential which came together at electrode C is expressed as

$$C_u = \frac{\rho I}{2\pi} \left(\frac{1}{r_{AC}} - \frac{1}{r_{CB}} \right) \quad (2.1)$$

Furthermore the resulting potential difference at D is expressed as

$$C_D = \frac{\rho I}{2\pi} \left(\frac{1}{r_{AD}} - \frac{1}{r_{DB}} \right) \quad (2.2)$$

Hence the variation in measured potential using a numerical voltmeter joined involving C and D is expressed as

$$V = \frac{\rho I}{2\pi} \left\{ \left(\frac{1}{r_{AC}} - \frac{1}{r_{CB}} \right) - \left(\frac{1}{r_{AD}} - \frac{1}{r_{DB}} \right) \right\} \quad (2.3)$$

The entire measurement of parameters is gotten from the earth surface apart from the resistivity (ρ)

$$\rho = 2\pi \frac{V}{I} \left\{ \left(\frac{1}{r_{AC}} - \frac{1}{r_{CB}} \right) - \left(\frac{1}{r_{AD}} - \frac{1}{r_{DB}} \right) \right\}^{-1} \quad (2.4)$$

Two out of the four electrodes techniques were utilised for the project; Wenner and Schlumberger array. These four electrodes in each of the arrangement are collinear but diverse in their intervals and geometry.

In Wenner Array (Figure 2.5)

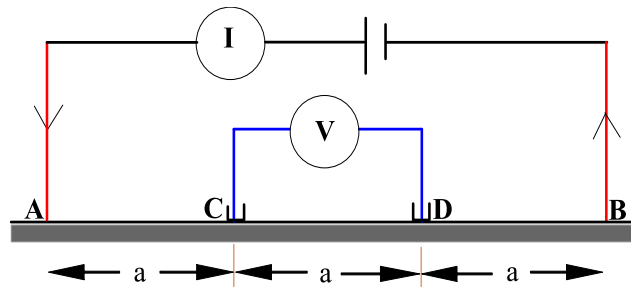


Figure 2.5:Wenner Array

$$\rho = 2\pi \frac{V}{I} \left\{ \left(\frac{1}{a} - \frac{1}{2a} \right) - \left(\frac{1}{2a} - \frac{1}{a} \right) \right\}^{-1} \quad \text{equation (2.5)}$$

$$\rho = 2\pi a \frac{V}{I} \quad \text{equation (2.6)}$$

In Schlumberger array (Figure 2.6)

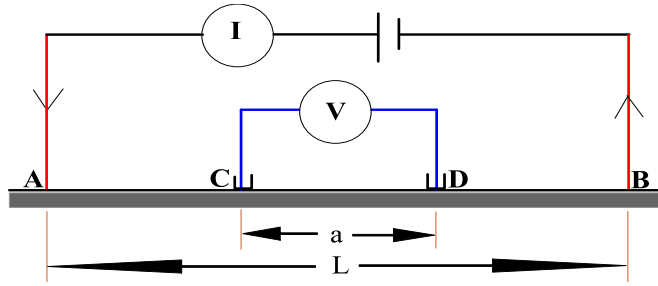


Figure 2.6: Schlumberger Array

In this arrangement, the two potential and current electrodes assign a joint middle but the spacing of inter electrode are not the same.

Taking the partitions between the two electrodes potential and current as L and a , in that order, in that case $R_{AC}=R_{DB}=(L-a)/2$ and $R_{CB}=R_{AD}=(L+a)/2$. Substituting these measures in equation 2.4 yields;

$$\rho = 2\pi \frac{V}{I} \left\{ \left(\frac{2}{L-a} - \frac{2}{L+a} \right) - \left(\frac{2}{L+a} - \frac{2}{L-a} \right) \right\}^{-1} \quad \text{equation (2.7)}$$

$$\rho = \frac{\pi V}{4I} \left(\frac{L^2 - a^2}{a} \right) \quad \text{equation (2.8)}$$

The value of resistivity computed is believed to not be the exact value of resistive of the underground, except an “apparent”. This value of apparent resistivity is the resistivity of a uniform earth that generates the same value of resistance for same electrode array. So as to establish the exact character of the earth resistivity, a computer iteration/inversion of the values of apparent resistivity measured must be conducted (Loke, 1999).

A variety of geological and earth minerals react to resistivity in a different way (Keary *et al.*, 2002). The extent value of resistivity for a number of geological resources is denoted on Figure 2.7.

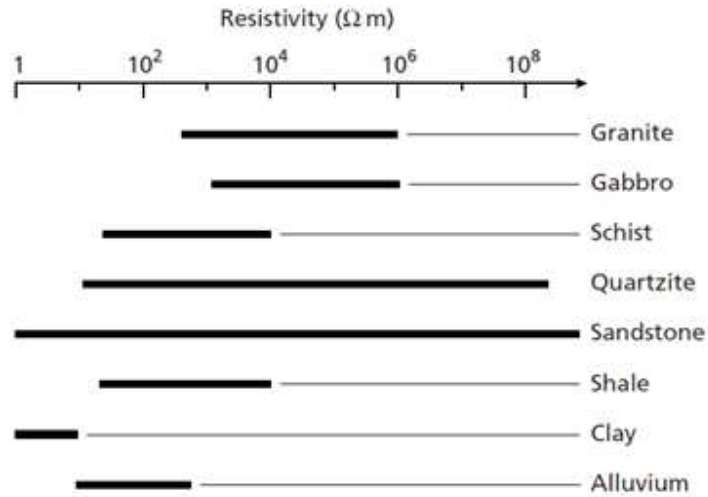


Figure 2.7: Approximate range of resistivity values of some rock types (Keary *et al.*, 2002)

Loke (1999) in his handbook of practical to three-dimensional (3-D) and two-dimensional (2-D) electrical investigation affirmed the significance of 2-D examination for engineering and environmental reasons. He affirmed that the version of 2-D is a more effectual version since mutually the horizontal and vertical paths next to the line of profile undergo the variance in resistance. The investigation by electrical imaging of 2-D is employed for mapping fairly difficult geological landscape in addition to examining underground lithology or variant in strata.

CHAPTER THREE

3.0 MATERIALS AND METHODS

3.1 Materials

Rocks, soil and water samples are the key materials employed for this research. Thin sections were prepared from the rock samples for petrographic analyses, sieve analyses were carried out on the soil samples and the physic-chemical analyses of the water samples were done.

3.2 Methods

Several methods were employed in carrying out the research which is as stated below.

3.2.1 Preliminary Desk Study and Reconnaissance

Existing in-print and unpublished texts, geological map and topographical map of the examined region were reviewed in order to have an outline of the location prior to going to the field for reconnaissance survey. The reconnaissance was conducted to discern the questions that might arise on the field. Possible traversing directions were as well recognized throughout the reconnaissance.

3.2.2 Geological Mapping

A base map on the scale of 1:12,500 was produced from topographic map with scale 1:100,000. GPS was used to acquire co-ordinates of exposed rocks localities on the field. Lithologies of rocks were recognized using grain and mineral constituents. Structural behaviours of linear structures and the rocks were taken with compass clinometers. The data were outlined on the base map. Novel samples of outcrop were acquired from the field and examined micro-photographically. The thin section was prepared at Vineyard

Geological Company and the analyses of petrography analysis were done at the Laboratory of Geology Department of the Federal University of Technology, Minna. The fundamental information incorporated in the geological map is the kinds of rock and essential structural elements like the fault, joints, and strike trend.

3.2.3 Geophysical Mapping

Geophysical examination with the aid of electrical resistivity method of 1 and 2-Dimension resistivity underground imaging was utilised for the investigation of the dumpsite (Plate I). The 2-D resistivity underground imaging shows together the vertical and horizontal information down the route of traverse whereas the explanation of VES sounding curves is prepared on the conjecture of horizontal layering. The VES was done to supplement the 2-D underground imaging for enhanced underground information.



Plate I: Geophysical Surveying within the Study Area

3.2.3.1 Vertical Electrical Sounding (VES)

Resistivity meter was used to measure the resistance of the subsurface layer. Four electrodes were used; the first pair was the current electrodes while the second pair was the potential electrode. Their fundamental purpose was to send current into the subsurface and measure the potential between two positions. There are four reels of cable which were connected to the resistivity meter at one end and the other ends were connected to the electrodes. Electrode spacing was measured using a tape meter and two-thirds of the electrodes were driven below the earth surface using the Schlumberger array.

The Schlumberger arrangement of electrical resistivity technique of examination was utilized for the VES with 30 m as the maximum $AB/2$. The arrangement of Schlumberger adheres to the universal four electrode standard. The middle of the arrangement remained unchanging; with spacing of electrode increment between electrodes to get from the layering of horizontal layering of the underground strata the vertical information. In concluding the layering of the vertical resistivity, the MN potential electrodes were set at near gapped and permanent to the centre of the array whilst the current electrodes AB were outwardly increase. The raise in AB current electrodes indicated a rise in the penetration depth of the underground. Three VES locations were determined on every one of the line of profile formerly confirmed for the measurements of 2D. The locations were created at 1 m, 50 m and 100 m expanses on the navigation route. Quantitative explanations of the figures were done. Assessment visually and conventional curve matching were employed for the physical understanding of the figures from field. Iteration using computer of the data curve matched was done with the aid of Winresist software (Van der Valpen and Sporry, 1992) to produce resolution curves.

An increase in $AB/2$ led to a rapid reduction in potential difference measured at electrodes $MN/2$. In this case, the MN distance was also raised to get a better response in potential. Longitudinal unit conductance was also calculated using Dar-Zarrouk formula ($S_c = h/\rho$) (Maillet, 1947).

3.2.3.2 Two Dimensional (2-D) Electrical Subsurface Imaging

In 2D investigation, the resistivity examination encompasses differences in mutually the horizontal and vertical directions down the survey outline (Loke, 1999). The Wenner electrode arrangement was used for this method. Three key varieties of Wenner arrangement can be utilised for the 2D examination which comprises; Wenner Gamma Figure 3.1(c), Wenner Beta Figure 3.1(b) and Wenner Alpha Figure 3.1(a).

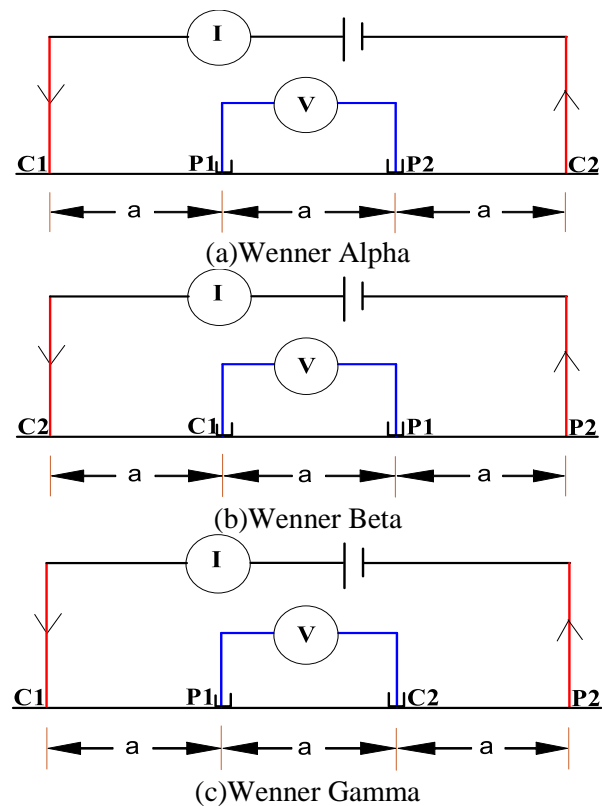


Figure 3.1: Diverse Configurations of Wenner (Loke, 1999)

The arrangement of Wenner Alpha as summarized by Loke (1999) (Figure 3.1a) was used for the investigation. The option of the Wenner arrangement was established as a result of its stout strength of signal.

A sum of twenty one (21) electrodes was employed for the investigation. As a result of the characteristics of the research area, the length of traverse (L) was restricted to a space of 100m. In the initial series of dimension, the intervals between adjoining electrodes (a) at 1a were placed at 5m. For the initial dimension, electrodes numerals 1, 2, 3 and 4 functioned as C1, P1, P2 and C2 correspondingly (Figure 3.2). For the subsequent measurement, electrodes numerals 2, 3, 4, and 5 represents C1, P1, P2 and C2 in that order. This progression was conducted till electrodes 18, 19, 20 and 21 represent C1, P1, P2 and C2 in the same way. When the series were concluded, eighteen middle-points were taken.

The entire measurement process was done again for spacings 3a, 4a, 5a, and 6a. From the initial series of measurement 1a, sum of 18 middle-points were acquired, and the middle-point lowered by three in consequently measured series. Mid-points =15 at 2a, 12 at 3a, 9 at 4a, 6 at 5a and 3 at 6a (Figure 3.2). The quantity of measurement reduces with rise in the spacing of electrode. The overall investigated depth is roughly 18m from surface of ground.

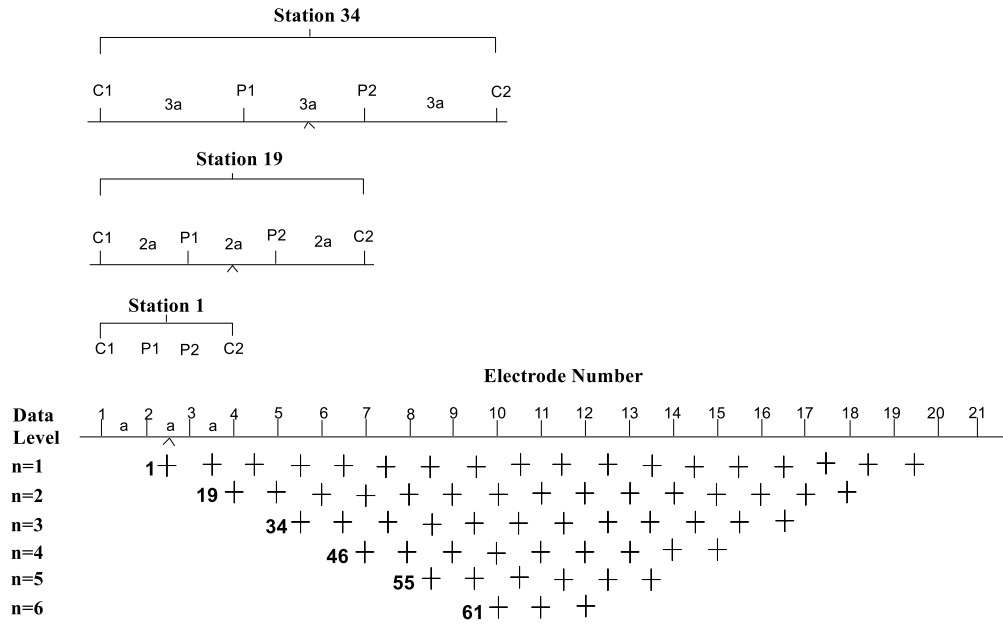


Figure 3.2: Series of 2D Wenner Resistivity Measurement to construct a Pseudo-section (Loke, 1999)

The 2-D Wenner-Schlumberger arrangement was navigated transversely on the dumpsite. The acquired data were elucidated by inversion quantitatively with the software RES2DINV and DIPROWIN. Traverse of four imaging at 100 m expense were instituted. The inter electrode spaces varies from 5 m to 30 m on the ground surface.

3.2.4 Hydrogeological Mapping

Hydrogeological examination was conducted with the aid of diverse means of investigating groundwater with respect to the dumpsite. The depths of well and static water levels were taken within the study area and the coordinates of these points were recorded. Maps of flow direction of groundwater of the locations were produced utilising the golden Surfer 11 software.

For the water sampling, plastic bottles of 1 litre were used for taking the water samples. The bottles were thoroughly washed repeatedly with the water to be sampled for at least

three (3) times at each sampling location. The water samples were filled into the bottle and tightly capped with their covers and they are placed in a cooler containing ice and covered. Immediately the sampling is completed, the samples were taken to the laboratory for the requisite analysis.

3.2.4.1 Groundwater Flow Direction

The map of flow direction of the groundwater was created from the well measurement data acquired from the areas within the dumpsite. The hydraulic head (H) was aided in the design of the map of direction of flow. H is quantified as the mechanical energy that triggers the moving of subsurface water. H can be obtained in two approaches:

- (a.) The addition of elevation and pressure head and;
- (b.) The divergence between ground altitude and depth to water table.

In generating the map of groundwater direction of flow, the coordinate of every well were obtained with global positioning system (GPS). The water table altitudes were established at different positions of well by deducting depth to static water height from the well altitude measurement. The variant in water table altitudes of each well was next established by deducting the wells with high water table from those having low water table. The software golden surfer was employed in plotting the map of groundwater direction of flow, entering X for the latitudes and Y for the longitude coordinates and Z for the difference in water tables data respectively.

3.2.5 Grading Analysis

The grading analysis involved visual evaluation of loads of soil and laboratory evaluations of the samples of soil. The research was related to the evaluation of the overburden/soil

matters below the dumpsite. Soil samples were taken at depths 1.5 m, 1.0 m 0.5 m and 0.0 m and from four (4) pits dug within the surrounding of the refuse site (Plate II). The samples were conveyed in polythene bags to the laboratory so as to sustain their natural moisture contents.



Plate II: Digging of the Trial Pits and a Trial Pit within the Study Area

3.2.5.1 Laboratory Analysis of Soil

The soil test was done at the Geology Laboratory, Federal University of Technology, Minna. The grading (sieve analysis) was carried out to categorize the diverse soil samples on the bases of their physical features. Before getting the sample ready for analysis in the laboratory, the natural moisture content of every soil was verified by weighing the wet sample and then dried in the oven and weighed again to get the moisture.

Sieve analysis

Mechanical sieve analysis was carried out on the soils to verify the proportion of diverse sizes of grain found in the soil. Acquired samples from the field were air dried for at least 24 hours and then it was thoroughly mixed after air drying. The sample was disaggregated

using the mortar and pestle. A quantity of the sample was taken and weighed using the weighing balance. The known weight of sample was poured into the top sieve of the nested column of sieves. The nested column of sieves was positioned on the sieve shaker and shaken for 20 minutes. The brush (hard or soft) was utilised in the removal of soil grains stuck in the sieves apertures.

After the shaking processes, the samples retained on each sieves were weighed and recorded. The overall total of the weight retained was assessed against the first dry soil before sieving. The soil retained percentage on individual sieve was obtained by the division of the retained weight on individual sieve by the first weight of sample. The percentage passing of the soil or finer percentage by dry weight was computed, starting with 100% to attain a cumulative percentage by dry weight of the percentage finer. The plot of passing percentage against sizes of sieve was plotted on a semi-logarithmic scale with the aid of the rockwork software.

The coefficients of curvature (C_k) and coefficient of uniformity (C_u) were then confirmed from the graph.

$$C_k = (D_{30})^2 / (D_{10})(D_{60}) \quad \text{while } C_u = D_{60}/D_{10}$$

3.2.6 Petrographic Studies

The representative rock take from the field is used to prepare the thin sections at Vineyard Geological Company, Minna Niger state. Three samples of rock were taken from the research area and analyzed for petrographic characteristic. The samples were taken as; Sample 1: 6° 31' 56"E, 9° 35' 01"E, Sample 2: 6° 32' 03"E, 9° 34' 46"E and Sample 3: 6° 32' 05E, 9° 35' 10"E

Micrographic thin section preparation

Three representative rock samples thin sections were made. Uniform thickness rock slide was cut from the sample using the diamond saw cutting machine. The cut surface was lapped that is grinded so as to get an even and smooth rock surface to be glued to a glass. A glass piece plate supported on a wooden platform was used for the processes of lapping. The crushed abrasive (Silicon Carbide) was placed to the face of the grinding glass plate and water was poured to create the abrasive slurry. The polishing was begun with abrasive that is coarse and finished with the finer. Following the grinding, the chip was meticulously cleansed with water and allowed to dry.

A glass slide was frosted (grinded) to smoothen it out and coarsen the surface so that the Canada balsam can join suitably. The slide was positioned on the grinding machine in similar direction and smoothly polished till it become translucent. The glass slide was cleaned dry, set for mounting. The rock chip was placed on a hotplate and allowed to be heated before mounting. The lapped side of the rock chip was glued to the glass slide using Canada balsam. The chip of rock cut was positioned on the glass chip and small mild force was used with the aid of a forceps to drive out the trapped air bubbles. The medium was allowed to air dry for little time to allow it reach a strong stage of bond between the slide and the rock chip.

After the rock was mounted on the slide, the trimming saw was utilised in reducing the chip to a size a little lesser than the thin section. The slide was next softly lapped once more to the proper thickness of roughly 0.03 mm. The slide was grounded with carefulness as water was added and constantly inspected under the petrographic microscope till the preferred piece was attained. Once the preferred thickness of 0.03 mm was attained, surplus abrasives

and gum are detached using a blade and systematically washed. A cover slip of glass is used to cover it to enhance the clearness of the slide under the petrographic microscope and to guard it from destruction. And finally, it was labeled and ready for petrography.

3.2.7 Laboratory Analysis of Groundwater Samples

Ten (10) water samples were taken for their physico-chemical analyses. The physical and chemical parameters of these samples were analysed at the Regional Water Quality Laboratory Minna, Niger State using colorimetric method and flame emission photometry. The anions were determined using the method of titration.

Titrimetric method

Titration quantitative chemical analysis method was used in the laboratory to determine the concentration of an analyte identified. The measurements of the volumes perform a fundamental function in titration. Reagent known as the titrator or titrant was made as a standard solution. A definite concentration and titrant volume was reacted with a solution of titrand or analyte to confirm the concentration. The concentrations of the analytes were determined at the end of the titration. Titrimetric analysis systems have the desirable quality of being complete in that the material concentrations are verified from the fundamental theories of chemistry and it does not needs calibration curves. Parameters like calcium, potassium, chloride, sulphide, nitrite, bicarbonate, manganese and zinc were determined by this method.

Colorimetric method

Colorimeter was utilised to determine the solution concentration by determining its absorbance of particular light wavelength. Diverse solutions were prepared, a reference or

control sample of identified concentration typically combination of a solution with distilled water and was packed into a cuvette and positioned in the colorimeter to standardize it. Following the calibration of the concentration or densities of extra mixtures were established. From these the concentrations of the elements were determined. The dimension of the filter is indispensable, as the wavelength of light that is spread by the colorimeter should be identical with the one the solution absorbed. Parameters like arsenic, copper, sulphate and iron were determined by this method.

CHAPTER FOUR

4.0 RESULTS AND DISCUSSION

4.1 Study Area Observations

The size of the Barkin-Sale dumpsite (Plate III) measured 112 m by 73 m and it measured about 7 m at the highest point and it is over 20 years in age. Domestic wastes are the major wastes disposed at the dumpsite that is polythene bags, food remains, metallic objects, electronic wastes, papers, clothing and so on. The studied portion is part of Minna Sheet 164 SE (Figure 4.1).



Plate III: The Barikin-Sale dumpsite at $9^{\circ} 35' 09.8''$ N and $6^{\circ} 32' 04.5''$ E

4.2 Geological Map and Petrography

The outcomes of the geological mapping of the study area reveals granite as the only rock type that make up the local geology of the area (Figure 4.2). The granite outcrops are common and well exposed all across the area. They are light in colour and generally medium to fine grained containing mainly feldspars, quartz and biotite. The effect of

tectonic activities is observable in the field with the presence of features like fractures (faults and joints) which resulted to the modification of the existing rock characteristics. The faults and joints serve as a passage for groundwater movement. Several joint values were taken from the rock outcrops and they are used to generate the rose diagram (Figure 4.3). The principle joint direction from the plot is NNE – SSW. The basement within this area is overlain by overburden in situ materials with varying composition. Persistent chemical weathering of the rocks in the area resulted to clay minerals and lateritic clay in situ to the area.

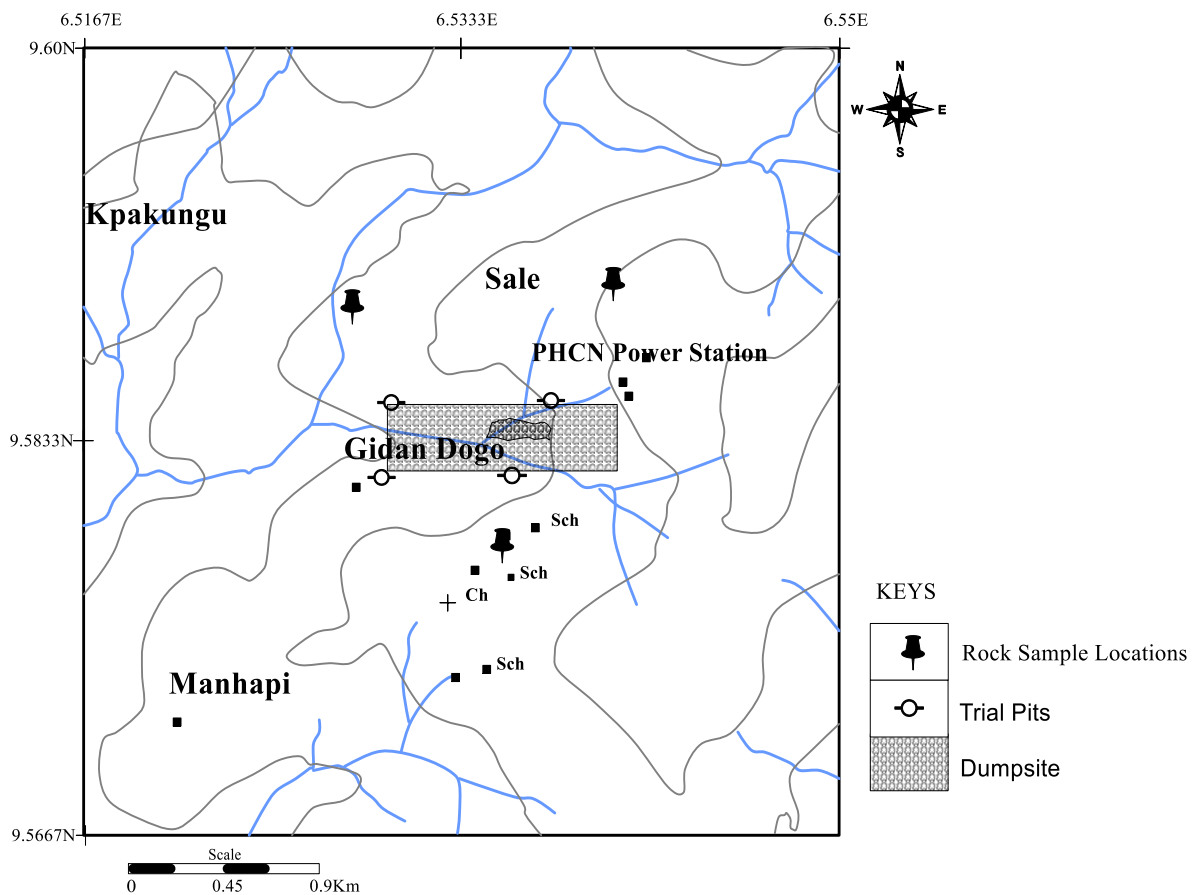


Figure 4.1: Locations of Rock Samples, Trial Pits and Dumpsite

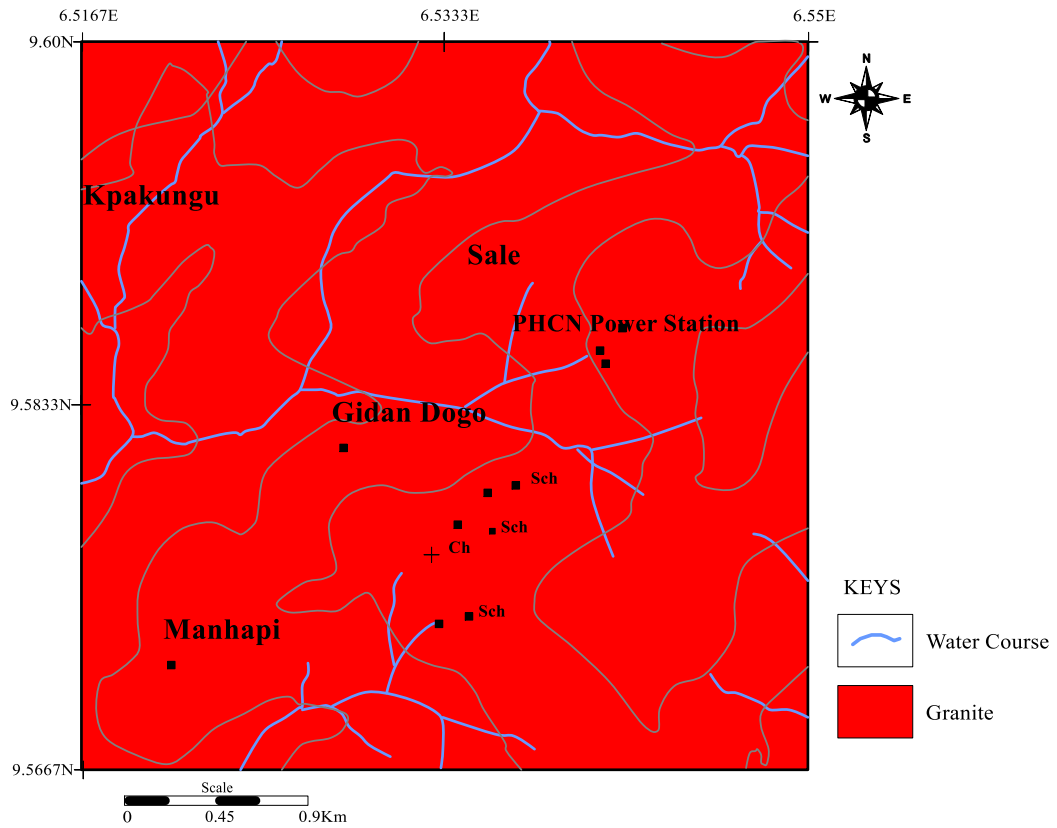


Figure 4.2: Geological Map of the Study Area

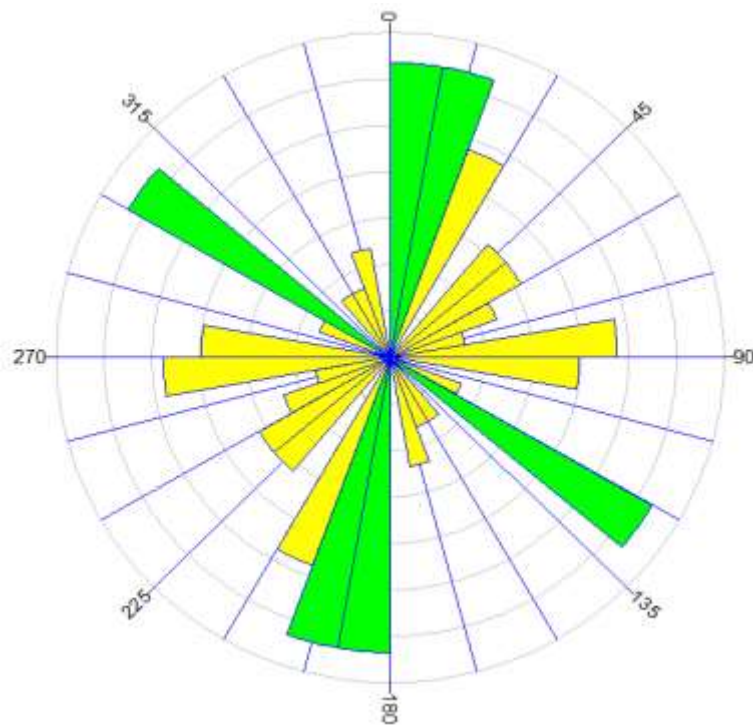


Figure 4.3: Rose Diagram of the Joint Directions from the Study Area

Samples were taken from rock outcrops in three different locations within the study area. The thin section analysis of the three granitic rock samples from the study area is presented in Plates IV, V and VI respectively. They were viewed under plane and cross polarized light. The result revealed the presence of quartz, biotite, plagioclase, orthoclase and other accessory minerals which include hypersthene, epidote and sericite.

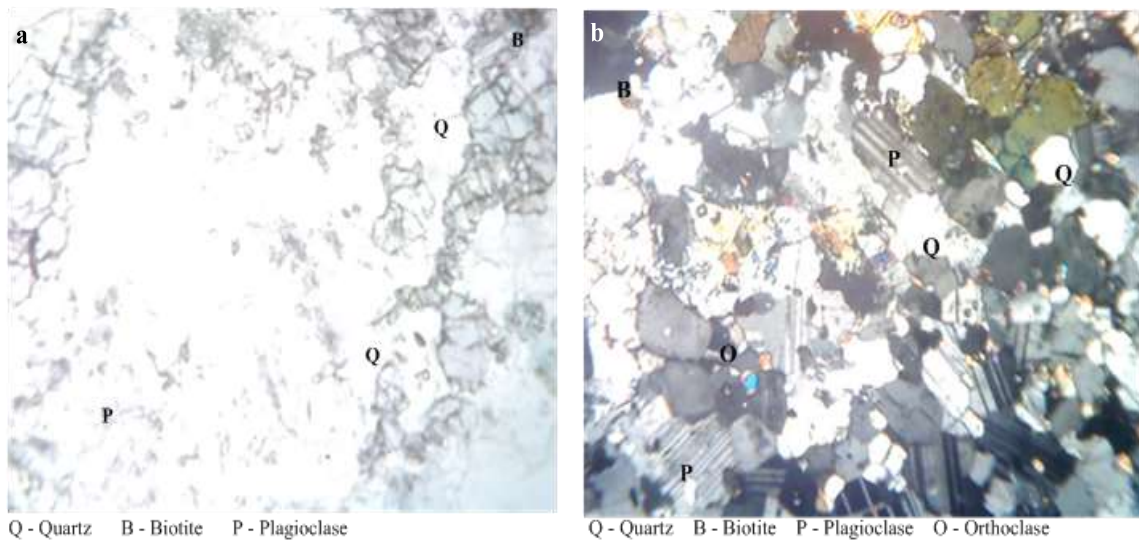


Plate IV: Photomicrograph of Granite1 (a) Plane Polarized Light (b) Cross Polarize Light (X40)

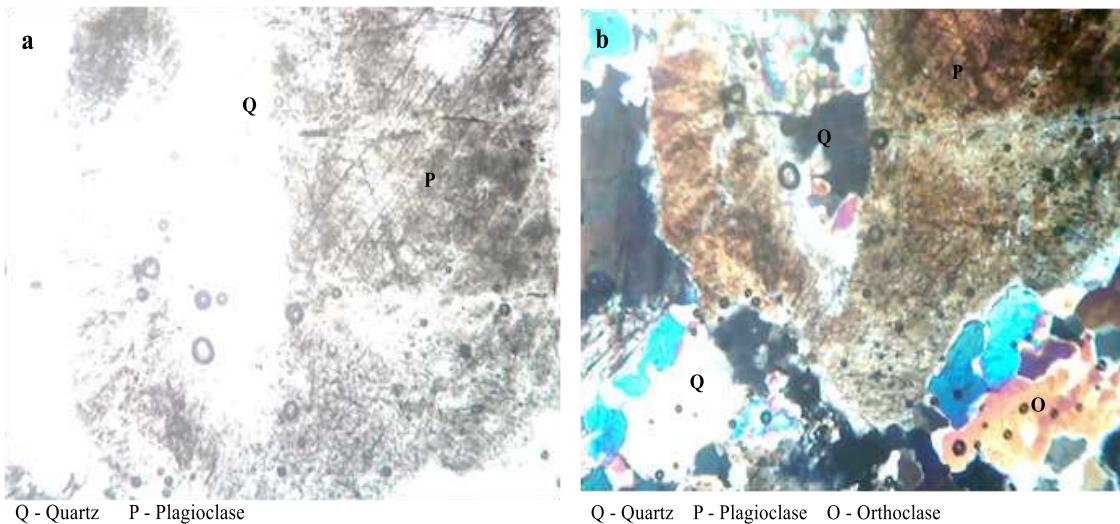


Plate V: Photomicrograph of Granite 2 (a) Plane Polarized Light (b) Cross Polarize Light (X40)

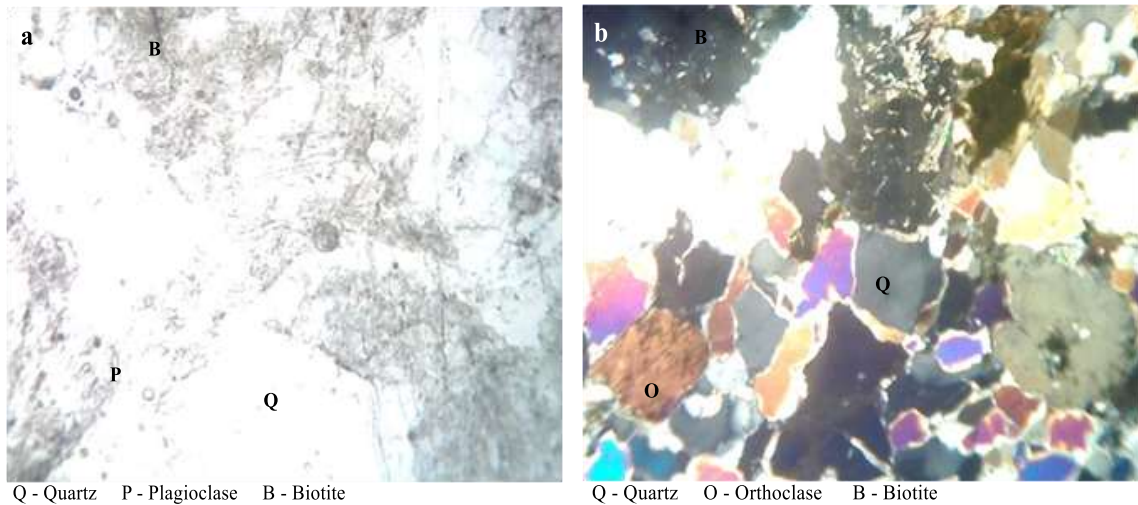


Plate VI: Photomicrograph of Granite 3 (a) Plane Polarized Light (b) Cross Polarize Light (X40)

From the thin section micrographic analysis, the entire rock is considered to be granitic rocks containing majorly of quartz, feldspar (plagioclase and orthoclase) and biotite. The quartz under plane polarize light exhibit colourless colour, anhedral crystal shape. It shows unbroken irregular shapes of crystal and parallel extinction under the cross polarized light.

The orthoclase display Carlsbad twinning, with some patchy texture. Under plane polarized light, plagioclase has relief of low negative to low positive which is colourless and euhedral to subhedral in shape. Under cross polarized light, it exhibits bright polysynthetic/albite twinning, oblique extinction and interference colour of first order yellow under the cross polarized light.

It was observed that biotite under plane polarized light displays brown colouration with medium relief and mica cleavage (one cleavage directional) whilst in cross polarized light it showed extinction that is parallel. The biotite showed mica cleavage in the thin sections. The accessory mineral identified on the petrographic thin sections is sericite; a product of feldspar alteration, epidote and hypersthene; products of amphibole alteration.

4.3 Well Parameters

Table 4.1 shows the well parameters for the study area.

Table 4.1: Well parameters for the study area

Location	Latitude	Longitude	Elevation (m)	Depth (m)	SWL (m)	Hydraulic Head (m)
L1	9° 35' 10"	6° 32' 05"	230	3.8	2.9	227.1
L2	9° 35' 12"	6° 32' 03"	233	3.0	2.0	233
L3	9° 35' 13"	6° 32' 03"	232	7.2	2.3	229.7
L4	9° 35' 14"	6° 32' 03"	229	4.2	1.8	227.2
L5	9° 35' 13"	6° 32' 01"	231	3.6	2.4	228.6
L6	9° 35' 08"	6° 32' 06"	225	4.1	1.6	223.4
L7	9° 35' 09"	6° 32' 05"	227	4.3	1.3	225.7
L8	9° 35' 06"	6° 32' 04"	231	6.1	1.7	229.3
L9	9° 35' 03"	6° 32' 04"	219	3.7	1.2	217.8
L10	9° 35' 03"	6° 32' 02"	223	4.9	0.3	222.7
L11	9° 35' 02"	6° 31' 57"	225	2.4	1.4	223.6
L12	9° 35' 00"	6° 31' 58"	220	3.1	0.7	219.3
L13	9° 35' 00"	6° 31' 56"	219	4.8	1.4	217.6
L14	9° 34' 59"	6° 31' 54"	220	5.0	0.7	219.3
L15	9° 34' 58"	6° 31' 53"	221	5.9	0.8	220.2
L16	9° 35' 58"	6° 31' 51"	225	4.4	0.5	224.5
L17	9° 34' 56"	6° 31' 50"	227	3.5	0.7	226.3
L18	9° 34' 58"	6° 31' 50"	225	5.3	1.6	223.4
L19	9° 35' 01"	6° 31' 52"	227	5.1	2.3	224.7
L20	9° 35' 00"	6° 31' 51"	221	3.6	1.1	219.9
L21	9° 35' 03"	6° 31' 55"	227	4.7	1.3	225.7
L22	9° 35' 04"	6° 32' 01"	245	4.3	0.2	244.8
L23	9° 35' 05"	6° 32' 01"	240	5.3	0.9	239.1
L24	9° 35' 07"	6° 32' 01"	235	6.3	1.9	233.1
L25	9° 35' 08"	6° 32' 03"	235	4.4	1.3	223.7
L26	9° 35' 10"	6° 32' 02"	236	4.6	1.5	234.5
L27	9° 35' 09"	6° 32' 05"	235	3.6	1.5	233.5
L28	9° 35' 09"	6° 32' 07"	232	3.4	1.0	231
L29	9° 35' 07"	6° 32' 09"	231	5.4	1.7	229.3
L30	9° 35' 12"	6° 32' 09"	233	7.6	1.5	231.5

The parameter was used to plot the water level elevation map of the area (Figure 4.4). On the acquired data, the mean depth to the water table in the examined area is around 1.5 m.

The wells' depth is in the extent of 0.3 m to 2.9 m which is dependent on the overburden thickness. This could mean that the depth to the groundwater within dumpsite area is unsafe, as a result of possible infiltration of leachate into the subsurface groundwater.

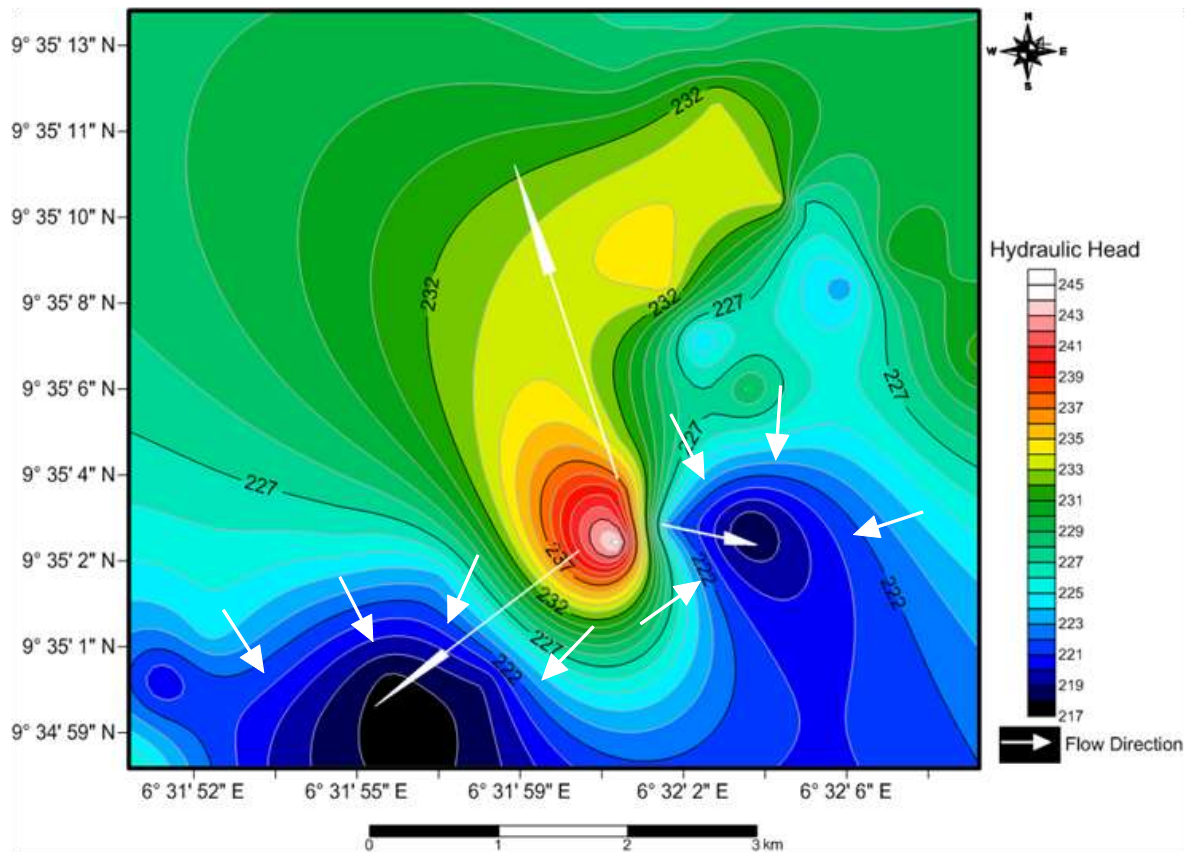


Figure 4.4: Hydraulic Head Distribution Map

From Figure 4.4, the dark section of the map indicates the areas with lower elevation and the water level in those locations are high and as the colour change progress upward, the depth to water level increases. The outcome of equivalent level contour map (Figure 4.4) indicates a North-South direction of flow within and the recharge point is within the northern section of the study area. Areas within the center part of the study area have high elevation and the water tends to flow from there to the other parts of the area indicating a radial flow direction but essentially the flow direction in N-S direction.

4.4 Geophysics

4.4.1 Vertical Electrical Sounding (VES)

Ten (10) points were located within the dumpsite area and vertical electrical sounding was carried out at those ten points (Figure 4.5). Figure 4.6 show the sounding curve for VES 1 and Appendix A for VES 2 to 10 iterated using the WINResist software. The curves for VES 2 to VES 10 are contained in Appendix A. Table 4.2 shows the VES parameters and lithologic delineation of the VES points of the study area. The Figures 4.7 and 4.8 show the geoelectric sections of the VES data.

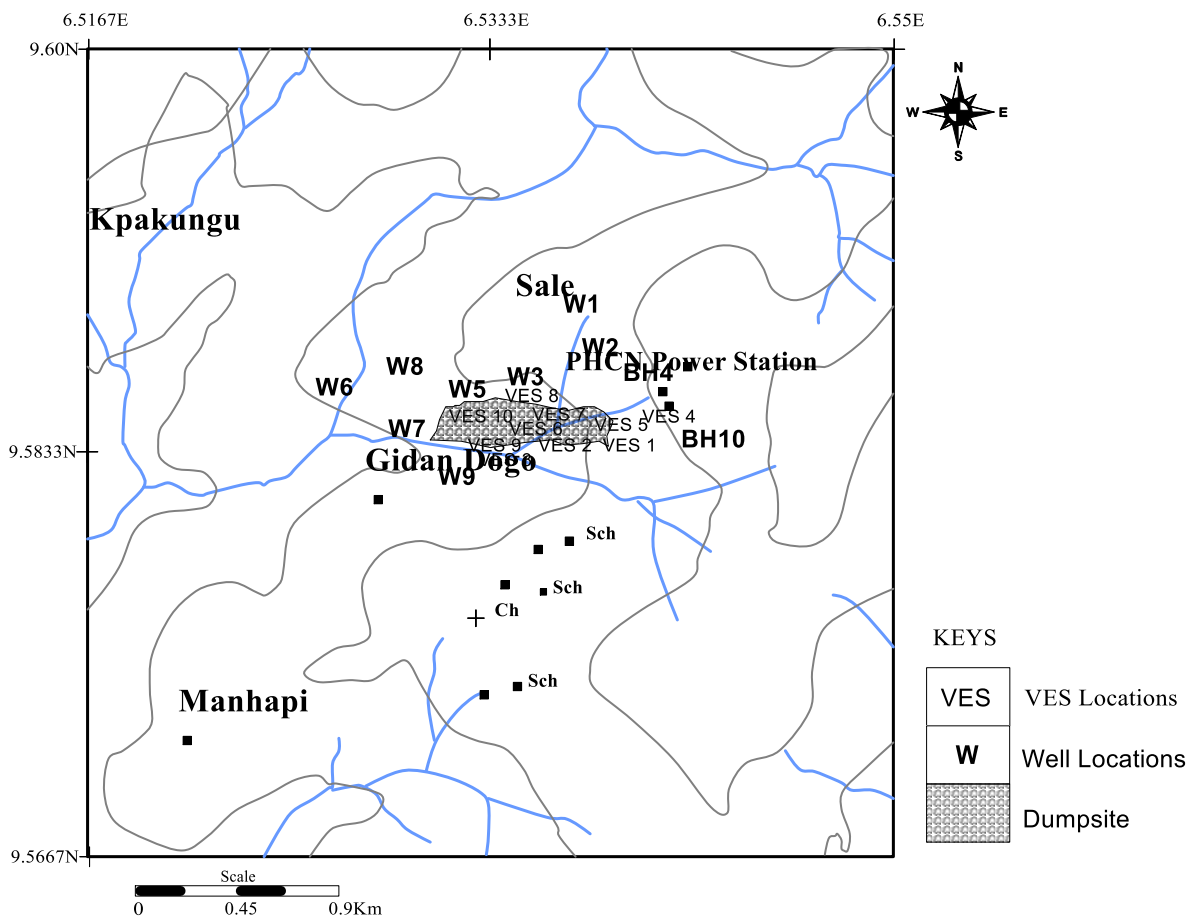


Figure 4.5: Locations of VES Points and Water Samples

The longitudinal conductance (S_L) were computed and illustrated in Table 4.2.

Table 4.2: VES Parameters and Lithologic Delineation of the Study Area

VES No.	Coordinates	Layer	Resistivity, ρ (Ωm)	Thickness (m)	Longitudinal Conductance, S_c ($\Omega^{-1}\text{m}$)
1	9° 35' 10.2" N 6° 32' 04.7" E	1	71.7	1.0	0.014
		2	33.4	5.0	0.150
		3	137.8		
2	9° 35' 10.2" N 6° 32' 04.4" E	1	27.9	1.1	0.039
		2	25.1	4.6	0.183
		3	106.8		
3	9° 35' 10.2" N 6° 32' 04.0" E	1	65.3	1.6	0.025
		2	23.9	4.6	0.192
		3	134.4		
4	9° 35' 09.9" N 6° 32' 03.6" E	1	52.9	1.8	0.034
		2	23.3	4.3	0.185
		3	166.4		
5	9° 35' 09.3" N 6° 32' 03.3" E	1	19.4	1.1	0.057
		2	30.3	4.1	0.135
		3	93.5		
6	9° 35' 09.1" N 6° 32' 02.7" E	1	34.7	1.5	0.043
		2	25.5	5.0	0.196
		3	113.3		
7	9° 35' 09.8" N 6° 32' 04.5" E	1	27.0	1.3	0.048
		2	18.2	4.1	0.225
		3	166.1		
8	9° 35' 08.0" N 6° 32' 02.7" E	1	76.0	0.9	0.012
		2	29.7	4.8	0.162
		3	124.4		
9	9° 35' 08.4" N 6° 32' 03.1" E	1	122.6	0.9	0.007
		2	22.0	5.3	0.241
		3	120.5		
10	9° 35' 08.8" N 6° 32' 03.5" E	1	102.4	1.6	0.016
		2	21.7	4.3	0.198
		3	166.3		

The sounding curves obtained consists of three layers that correspond to three lithologic layers, topmost layer being the top soil (figure 4.6) with a depth range between 0.90 m and 1.80 m, the second layer being the weathered basement with depth range of 4.0 m and 5.3

m and the third being the fractured/fresh basement which is the aquifer unit. The remaining curves obtained from the study area are presented in appendix A.

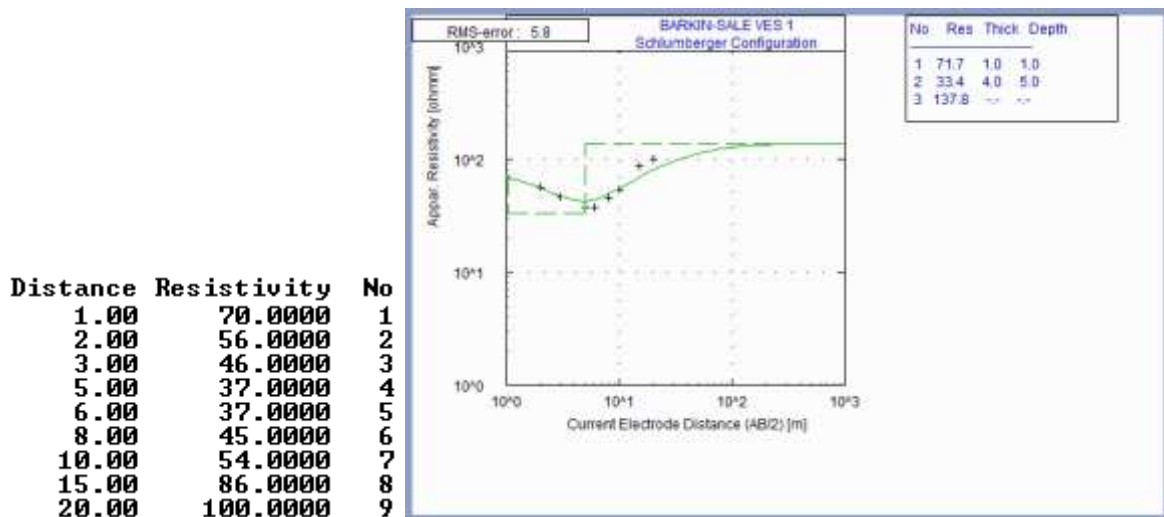


Figure 4.6: Sounding Curve for VES 1

The geoelectric sections were generated for the ten (10) VES stations in the study area and it reveal three distinct layers namely topsoil, weathered basement and the fractured/fresh basement (Figures 4.7 and 4.8). The topsoil resistivity varies from 19.4 to 112.6 Ωm , with thickness of 0.9 to 1.8 m respectively. The topsoil is composed of clayey sand/sandy clay. The low resistivity values obtained beneath the dumpsite is due to infiltration and accumulation of leachates from the dumpsite or as a reason that the charged surfaces (feature of clay) and connected border layers of ions that are attracting.

The unit shows that the uppermost level at all the points of VES pare generally sandy, whilst the second layers are filled by clayey sand. The second layer is in general lean at all the VES spots, therefore giving slight or no shield at all to the aquifer underneath it. Table 4.2 Overburden that is clayey is typified by area of moderately raised longitudinal unit conductance which gives shield to the aquifer lying beneath. From Table 4.2, the

longitudinal conductance for Layer 1 is $0.0295 \Omega^{-1}\text{m}$ while that of Layer 2 is $0.1867 \Omega^{-1}\text{m}$. From Henriet (1976) and Oladapo *et al.* (2004), Layer 1 has poor protective capacity and Layer 2 has weak protective capacity. Therefore, leachate can easily move within the study area. It is stated that substances like gravel and sand have low longitudinal conductance ensuing from their elevated values of resistivity as well of possessing low aquifer protecting ability (Farid *et al.*, 2017). This prevailing condition in the research location could enhance the infiltration into the aquifer possible contaminants. From the stated above, it is observed that the aquifer in the refuse dump region is susceptible to contamination. Obviously, the shallow aquifer in the vicinity can be effortlessly polluted by contaminated runoff water at the surface in the area.

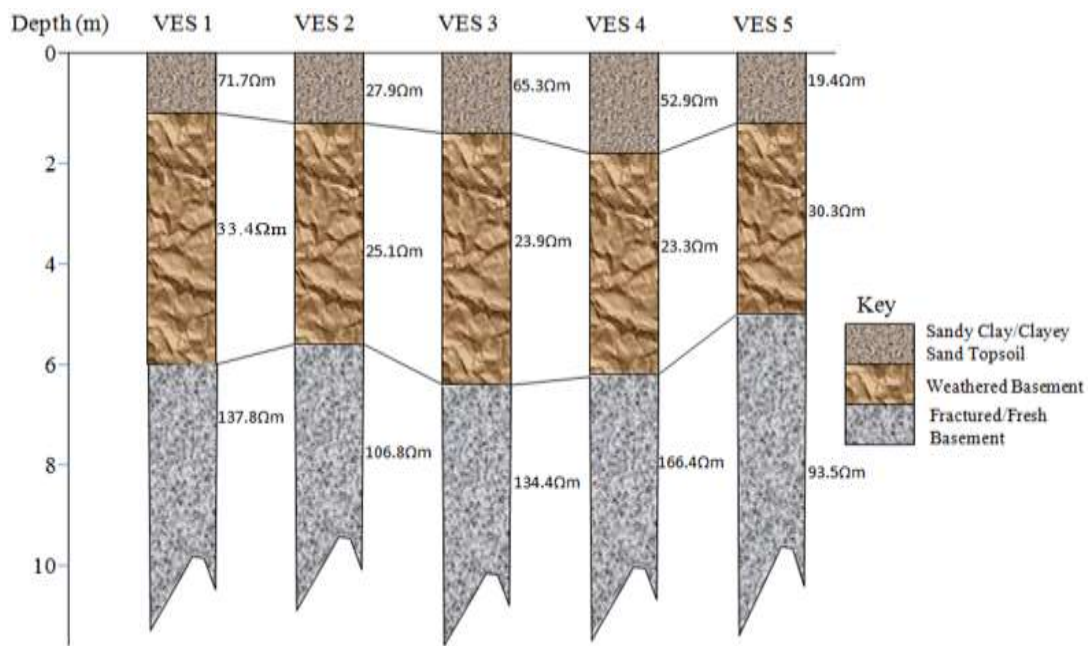


Figure 4.7: Geoelectric Sections for VES 1 – 5

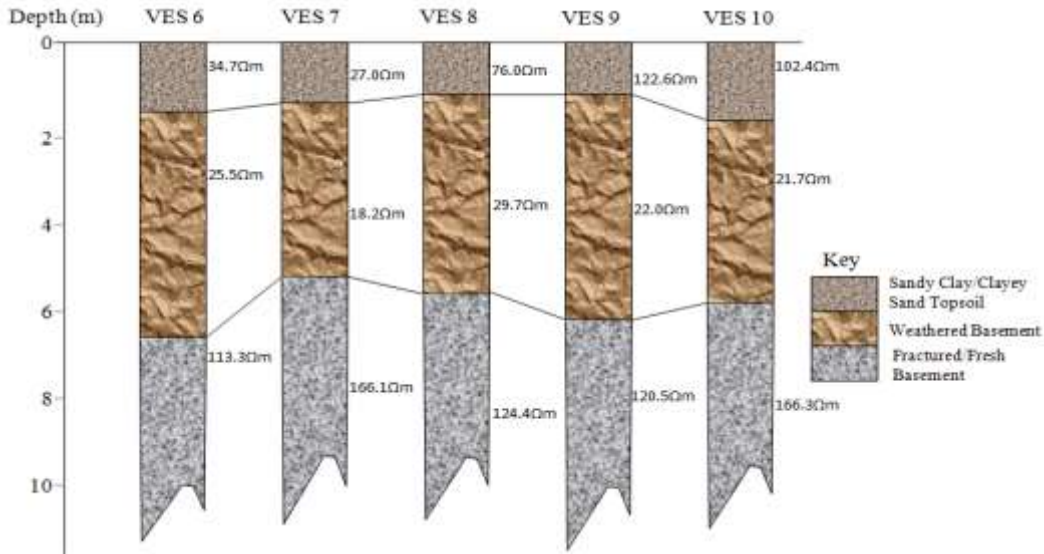


Figure 4.8: Geoelectric sections for VES 6 – 10

4.4.2 Two Dimensional (2D) Resistivity Subsurface Imaging

The 2D subsurface images recognized dissimilar lithologic layers which are discernible on the basis of colouration (Figure 4.9).

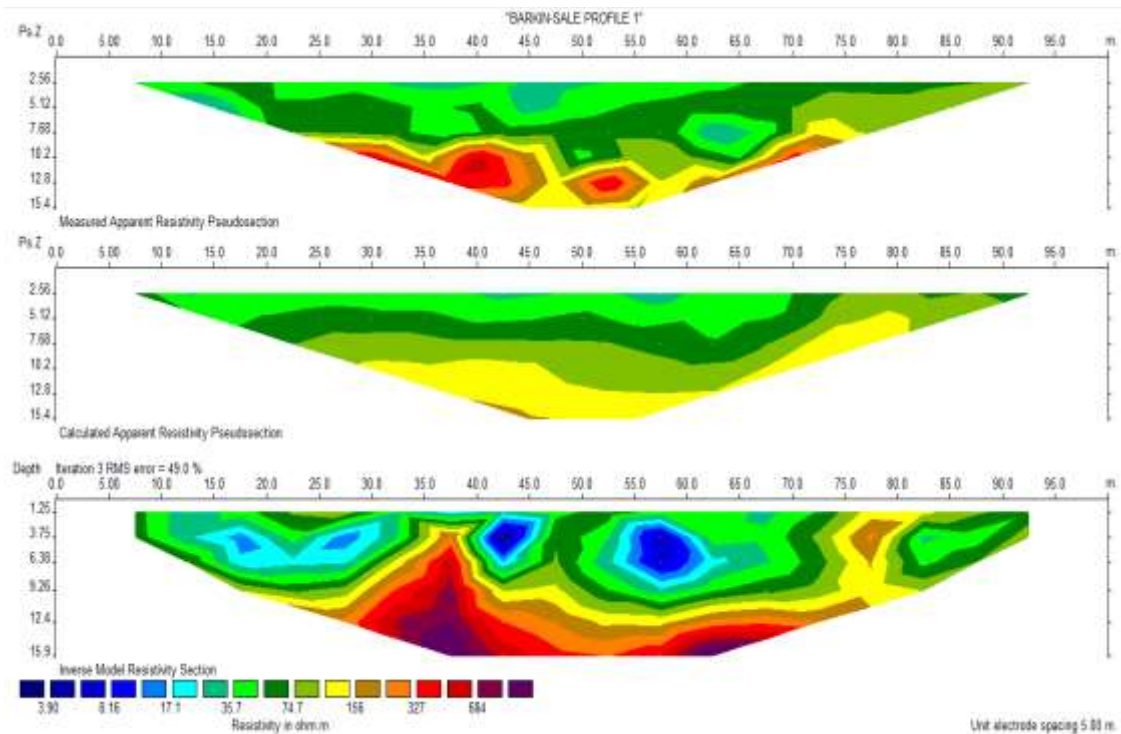


Figure 4.9: 2D Inverse Resistivity Models for Profile 1

The 2D inverted resistivity models were generated from measurements along the two perpendicular traverses across the dumpsite area (Figures 4.9 and 4.10) using the RESDINV software. The 2D inverted resistivity sections image shows the subsurface geologic sequence and the structural disposition of the layer. This was used to identify and map possible migration of the leachate across the dumpsite area. The profiles show very low resistivity across the 2D section (Figures 4.9 and 4.10). This can be attributed to contamination of the top-most soil as a result of accumulation of leachate plume. The sections reveal basically a maximum of three subsurface layers, which is in agreement with the results of the VES geoelectric section. The resistivity of the various layers ranges from 35.7 to 2,860 Ωm . However, a low resistivity structure is found at a depth of about 3.75 m with resistivity ranging from 3.91 to 42.3 Ωm which indicates the presence of leachate from the dumpsite. This shows that the leachate in the study area migrate laterally with ease and vertically with little resistance.

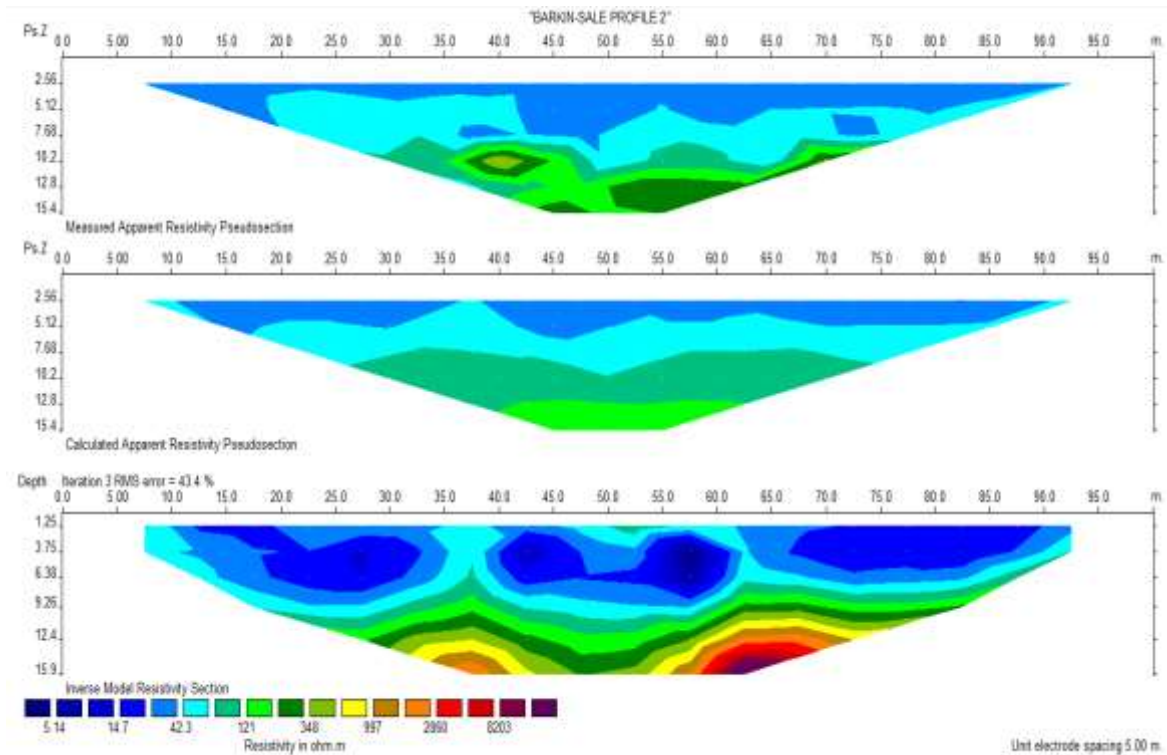


Figure 4.10: 2D Inverse resistivity models for profile 2

4.5 Grain Size Distribution

4.5.1 Sieve Analysis

Sieve analyses of soil samples obtained at 1.5 m, 1.0 m, 0.5 m and the surface respectively from four different pits were carried out so as to determine the distribution of the particle sizes (Table 4.3 and Figure 4.11). All the soil samples fall within medium to fine sands. The remaining results for the sieve analyses are presented on Appendix B. From the sieve analysis, the hydraulic conductivity of the soil was computed using the HydrogeoSieveXLv2.3 software (Devlin, 2016).

Table 4.3: Grain Size Distribution Parameters for Soil Sample L1 at 0.0 m

Initial Dry Mass	272.76	
Total Final Mass	272.57	
Mass Lost	0.19 (0.1%)	
Screen	Screen Mass	Cumulative

Name	Size (mm)	Retained	% Retained	% Retained	% Finer
#10	2.00	88.06	32.3	32.3	67.7
#20	0.85	23.05	8.5	40.7	59.3
#40	0.42	41.22	15.1	55.8	44.2
#60	0.25	32.21	11.8	67.7	32.3
#80	0.18	25.29	9.3	76.9	23.1
#100	0.15	12.48	4.6	81.5	18.5

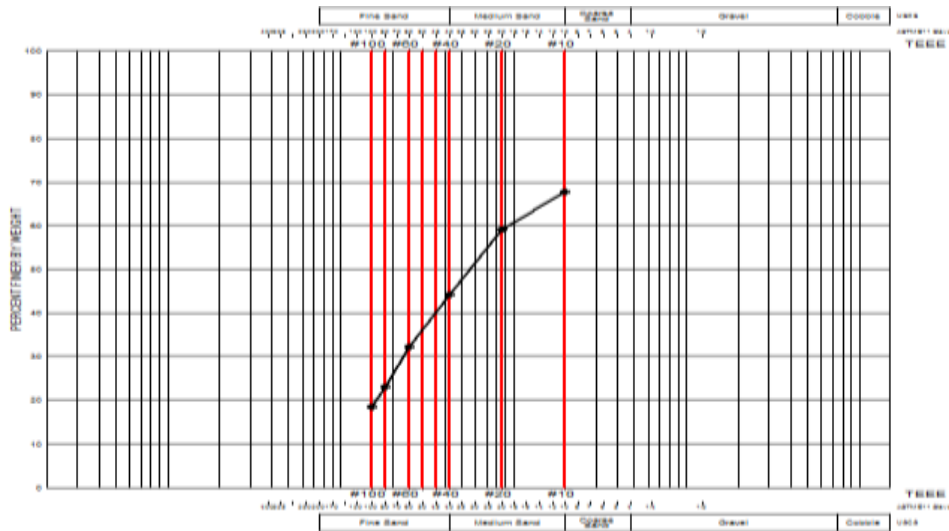


Figure 4.11: Grading Curve for Soil Sample L 1 at 0.0 m

4.5.2 Hydraulic Conductivity

The result of the hydraulic conductivity calculated from the sieve analysis of soil samples from the research location is given on Table 4.4 below. Table 4.4 shows that the hydraulic conductivity ranges between 0.974×10^{-4} and 0.100×10^{-3} m/s. According to Macaulay (2008), these values are high implying that the studied soils are permeable. This could lead to downward movement of possible leachate, resulting in contamination of the aquifer.

Table 4.4: Hydraulic conductivity (K) from the sieve analysis

Locations	Depth(m)	Hydraulic conductivity(K)	
		meter/second	meter/second
L1	0.0	0.657E-04	0.657×10^{-4}
	0.5	0.890E-04	0.890×10^{-4}
	1.0	0.142E-03	0.142×10^{-3}
	1.5	0.541E-04	0.541×10^{-4}
L2	0.0	0.890E-04	0.890×10^{-4}
	0.5	0.769E-04	0.769×10^{-4}
	1.0	0.974E-04	0.974×10^{-4}
	1.5	0.197E-03	0.197×10^{-3}
L3	0.0	0.563E-04	0.563×10^{-4}
	0.5	0.120E-03	0.120×10^{-3}
	1.0	0.563E-04	0.563×10^{-4}
	1.5	0.127E-03	0.127×10^{-3}
L4	0.0	0.252E-04	0.252×10^{-4}
	0.5	0.100E-03	0.100×10^{-3}
	1.0	0.115E-03	0.115×10^{-3}
	1.5	0.643E-04	0.643×10^{-4}

High values of hydraulic conductivity indicate that the soil is permeable and leachates can easily move through the interconnected pore spaces of the soil underlying the waste dumpsite. Therefore, the leachates can move gradually through the soil and if the dumpsite is not relocated or completely evacuated from the area, the adjoining aquifer and surrounding will be susceptible to contamination. The dump site has to be properly designed in order for it to serve as the community dump site.

4.6 Laboratory Analyses of Groundwater

Physicochemical and heavy metal analyses of the groundwater samples were carried out in the laboratory and the result is presented in Table 4.5. Table 4.6 is the statistical summary of those analysed water samples compared with the Nigerian Standard for Drinking Water Quality (2007) and WHO (2010) acceptable standards.

Table 4.5: Physico-chemical and heavy metals parameters analyzed in the water sample from the study area

Parameters (mg/l)	W1	W2	W3	BH W4	W5	W6	W7	W8	W9	BHW10	NSDWQ (2007)	WHO (2010)
pH	6.58	6.87	6.51	7.25	7.17	6.62	6.51	6.06	6.11	6.06	6.5 – 8.5	6.5 – 8.5
Turbidity (NTU)	0.00	6.0	0.00	5.0	7.0	4.0	3.0	3.0	3.0	5.0	5.0	5.0
EC (µS/cm)	2,040	3,500	3,120	960	1,700	1,200	1,380	1,020	940	240	1000.0	1000.0
TDS	1,367	2,345	2,090	643	1,139	804	925	683	630	161	500.0	500.0
Chloride	152.1	207.2	239.6	17.5	80.2	71.9	83.9	56.2	49.8	6.50	250.0	250.0
Nitrite	0.000	4.172	0.117	0.083	0.024	0.037	0.404	0.040	0.039	0.013	0.2	0.2
Bicarbonate	79	260	93	111	40	40	61	59	32	12	250.0	Variable
Manganese	0.036	0.194	0.023	0.007	0.001	0.000	BDL	0.005	0.002	0.000	0.2	-
Zinc	0.008	0.000	0.003	BDL	BDL	BDL	BDL	BDL	BDL	0.000	3.0	5.0
Sodium	123	173	147	47	80	79	94	57	59	8	200.0	200.0
Chromium	0.00	0.00	0.01	0.00	0.02	0.02	0.01	0.01	0.03	0.00	0.05	0.05
Arsenic	0.000	0.000	0.000	0.000	0.000	0.000	0.000	0.000	0.000	0.000	0.01	0.01
Calcium	85.8	71.3	165.1	37.7	72.9	52.1	52.9	32.9	33.7	8.8	-	75.0
Copper	BDL	BDL	BDL	0.000	0.000	0.001	0.000	BDL	BDL	0.00	1.0	2.0
Magnesium	11.2	4.5	26.4	17.1	18.5	2.4	4.9	17.1	7.32	2.4	20.0	50.0
Sulphate	21	55	24	46	18	14	18	10	6	13	100.0	100.0
Potassium	3	56	3	3	7	3	7	13	9	3	-	55.0
Iron	0.17	0.23	0.19	0.25	0.47	0.26	0.21	0.22	0.21	0.27	0.3	0.3
Carbonate	0.00	0.00	0.00	0.00	0.00	0.00	0.00	0.00	0.00	0.00	-	-
Cadmium	0.000	BDL	0.000	0.000	BDL	BDL	0.000	0.000	0.000	BDL	0.003	-
Lead	0.000	BDL	0.000	BDL	BDL	0.000	0.000	0.000	0.000	0.000	0.01	0.01

Table 4.6: Statistical summary of groundwater parameters in the study area compared with NSDWQ (2007) and WHO (2010)

Parameter (mg/L)	Min.	Max.	Mean	Median	NSDWQ (2007)	WHO (2010)
pH	6.06	7.250	6.570	6.550	6.5 – 8.5	6.5 – 8.5
Turbidity (NTU)	0.0	7.000	3.700	3.500	5.0	5.0
Conductivity ($\mu\text{s/cm}$)	240.0	3500.0	1616.0	1290.0	1000.0	1000.0
TDS	161.0	2345.0	1078.7	864.50	500.0	500.0
Chloride	6.5	239.6	96.490	76.050	250.0	250.0
Nitrite	0.0	4.172	0.4929	0.039	0.2	0.2
Bicarbonate	12.0	260.0	78.700	60.00	250.0	Variable
Manganese	0.0	0.194	0.0268	0.004	0.2	-
Zinc	0.0	0.008	0.0011	0.000	3.0	5.0
Sodium	8.0	173.0	86.700	79.50	200.0	200.0
Chromium	0.0	0.030	0.0100	0.010	0.05	0.05
Arsenic	0.0	0.000	0.000	0.000	0.01	0.01
Calcium	8.8	165.1	61.320	52.50	-	75.0
Copper	0.0	0.001	0.0001	0.000	1.0	2.0
Magnesium	2.4	26.40	11.182	12.21	20.0	50.0
Sulphate	6.0	55.00	22.50	18.00	100.0	100.0
Potassium	3.0	56.00	10.70	5.000	-	55.0
Iron	0.17	0.470	0.248	0.225	0.3	0.3
Carbonate	0.0	0.000	0.000	0.000	-	-
Cadmium	0.0	0.000	0.000	0.000	0.003	-
Lead	0.0	0.000	0.000	0.000	0.01	0.01

4.6.1 Physical Parameters

The physical parameters analyzed for in the groundwater samples are pH, turbidity, electrical conductivity and total dissolve solids (Tables 4.5 and 4.6) and they are therefore discussed below.

Hydrogen ion concentration (pH)

The pH quantifies the concentration in water of hydrogen ion (acid). Neutral pH has a value of 7, and above this is alkaline or basic and below is acidic. The values of the pH of water sample from the area of study is in the range of 6.06 to 7.25 with a median of 6.55 compared to the permissible limit of 6.5 to 8.5 recommended by (WHO, 2010) and (NSDWQ, 2007) (Table 4.6). All the water samples from Locations W1 to W7 are within the permissible limits but Locations W8 to W10 samples are slightly acidic (Table 4.5, Figure 4.12). Acidic water boosts the rate of chemical weathering and the dissolution of rocks and this may result to metal enrichment of water within the area.

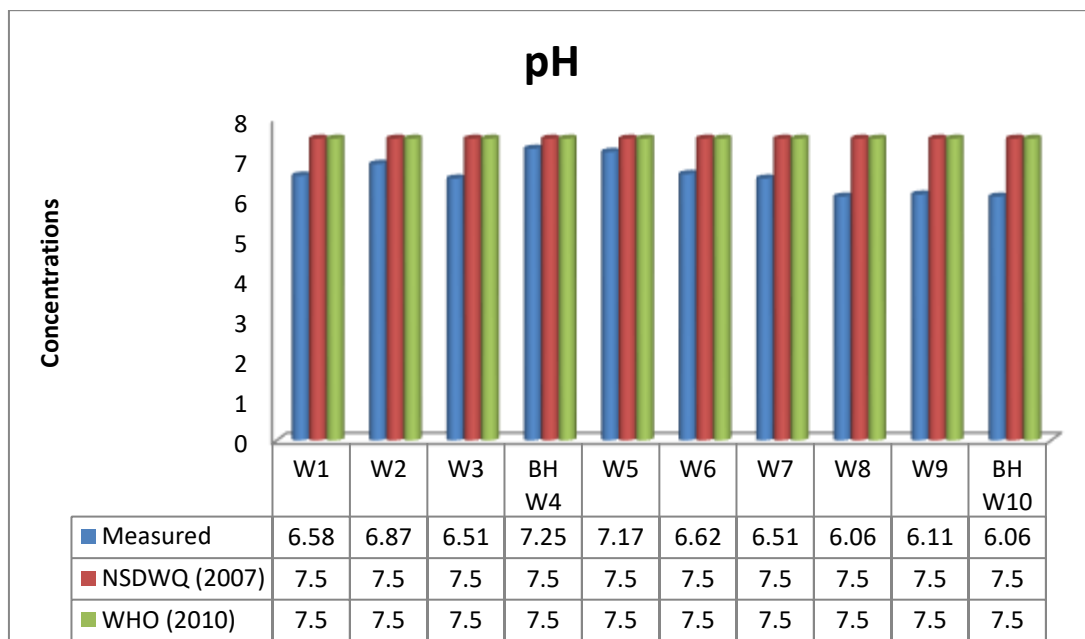


Figure 4.12: Concentration of pH compared with NSDWQ (2007) and WHO (2010)

Turbidity

Turbidity is the degree of clarity of a water sample. Samples from locations W2 and W5 are slightly above the recommended value (Table 4.5, Figure 4.13) indicating contamination. The median concentration of the turbidity is 3.5 NTU with a range of 0.0 to 7.0 NTU (Table 4.6). The median value is within the acceptable boundary of 5.0 NTU (NSDWQ, 2007 and WHO, 2010).

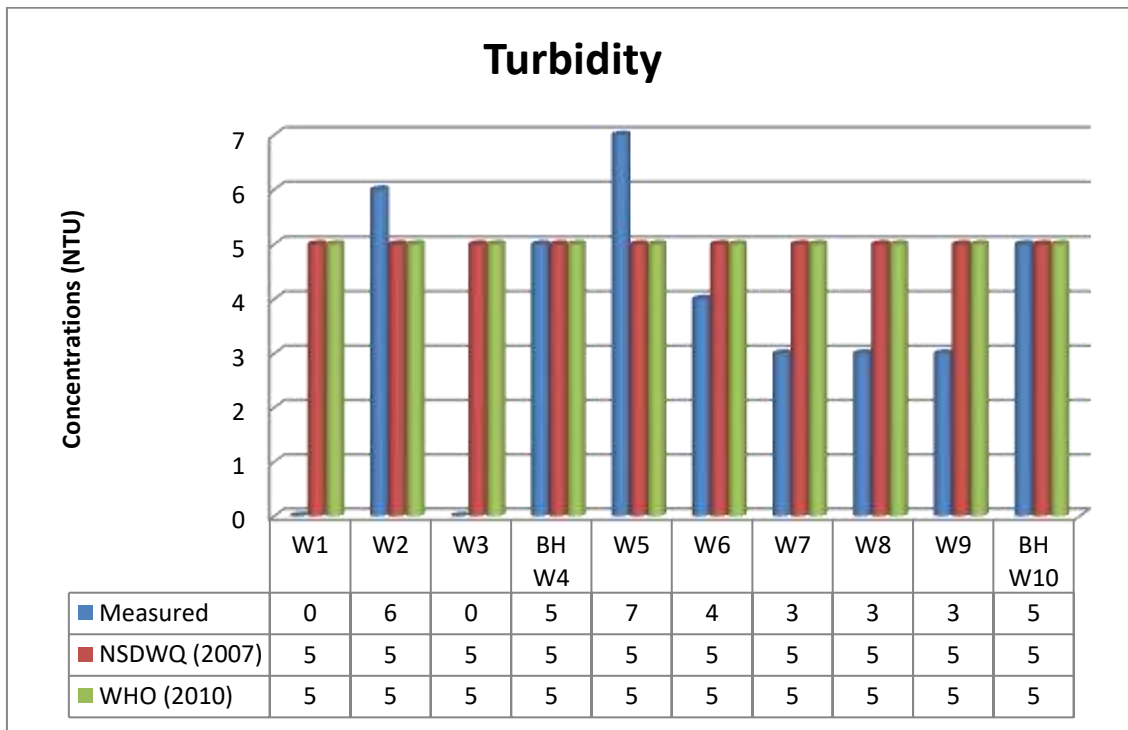


Figure 4.13: Concentration of turbidity compared with NSDWQ (2007) and WHO (2010)

Electrical conductivity

Conductivity is linked to the ionic substance of a sample which is a function of the amount of liquefied minerals in water. The concentration of electrical conductivity (EC) ranged from 240.0 to 3500 $\mu\text{s}/\text{cm}$ with a median estimate of 1290 $\mu\text{s}/\text{cm}$ (Table 4.6). Most of the locations exceed the maximum permissible limit of 1000 $\mu\text{s}/\text{cm}$ recommended by NSDWQ,

(2007) and WHO (2006) except BHW4, W9 and W10 which have concentrations below the recommended values indicating no contamination in those areas (Table 4.5, Figure 4.14).

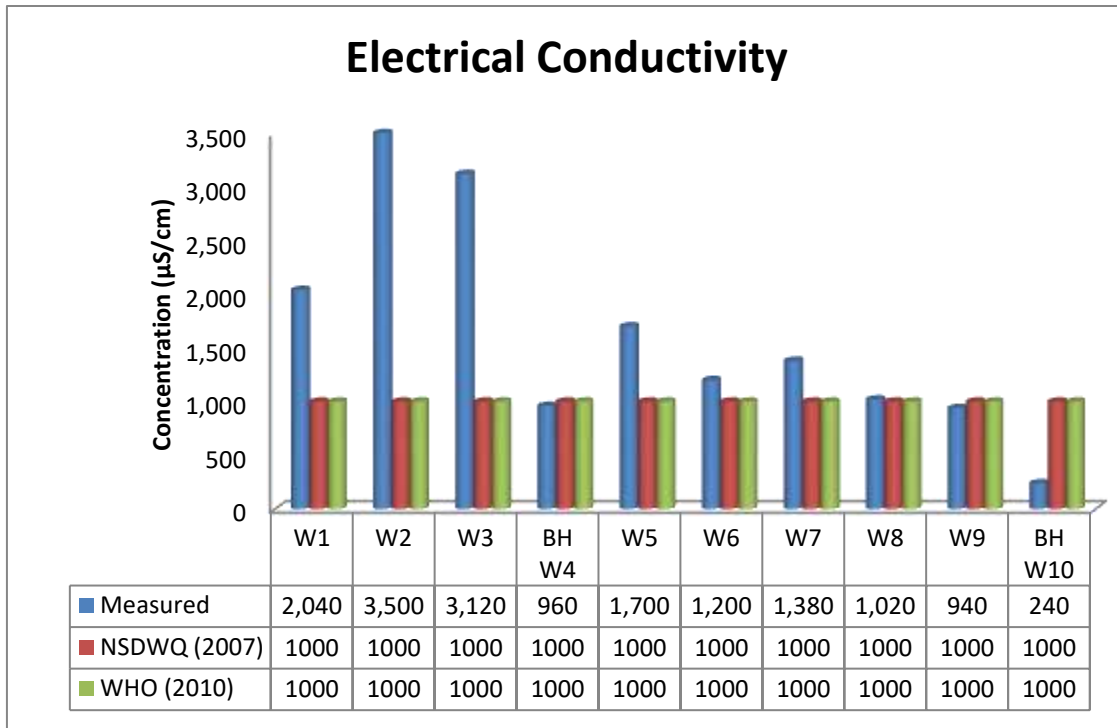


Figure 4.14: Concentration of EC compared with NSDWQ (2007) and WHO (2010)

Total dissolved solids

It is the measurement of all soluble solids in waters. Nutrients like nitrates, phosphates and salts dissolved for instance sodium chloride add to total dissolved solids. Total dissolved solids (TDS) from the analyzed sample range from 161 mg/l to 2,345 mg/l with value of average 1078.7 mg/l and median of 864.5 mg/l which are above 500.0 mg/l recommended by WHO (2010) and NSDWQ (2007) (Table 4.6). All the locations shows considerable contamination by dissolved solid except Location BHW10 only that have concentration value below the recommended value (Table 4.5, Figure 4.15).

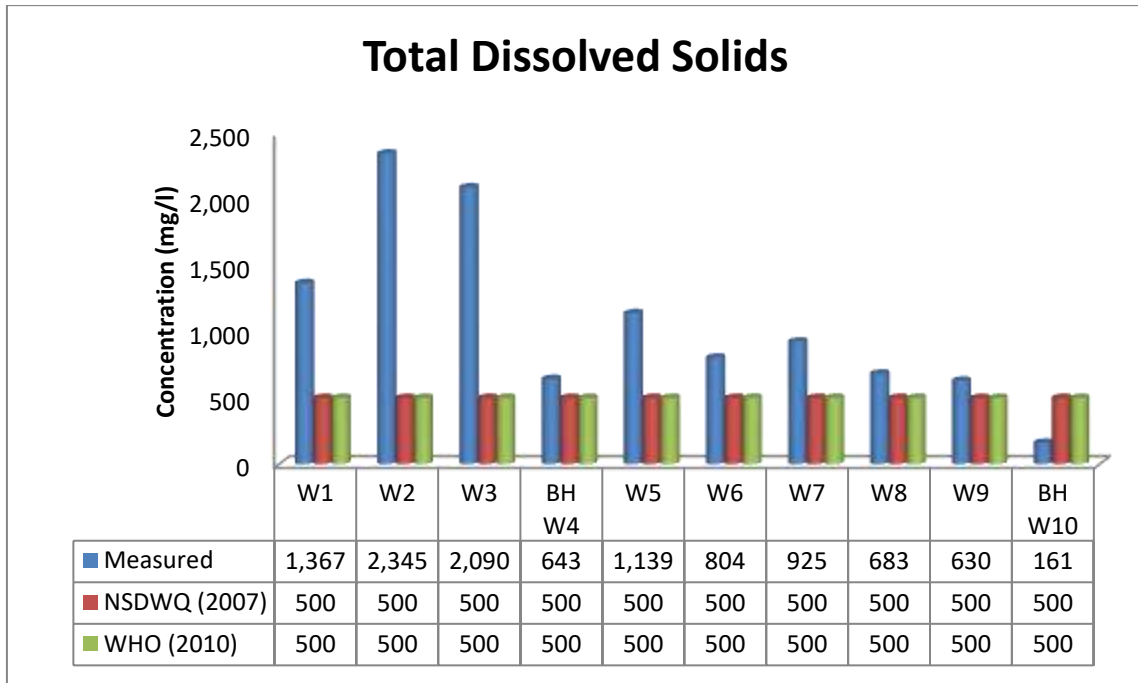


Figure 4.15: Concentration of TDS compared with NSDWQ (2007) and WHO (2010)

4.6.2 Chemical Parameters

4.6.2.1 Anions in the Water

Some of the analyzed anions in the samples of water include chloride, nitrite, bicarbonate, sulphate and carbonate (Table 4.5).

Chloride

The concentration of chloride in the water sample is in the extent of 6.5 mg/l to 239.67 mg/l and a median of 76.05 mg/l (Table 4.6). The outcome illustrate that the chloride concentrations in all the sites are lesser than the suggested permissible maximum threshold of 250.00 mg/l of NSDWQ (2007) and WHO (2010) (Table 4.5, Figure 4.16).

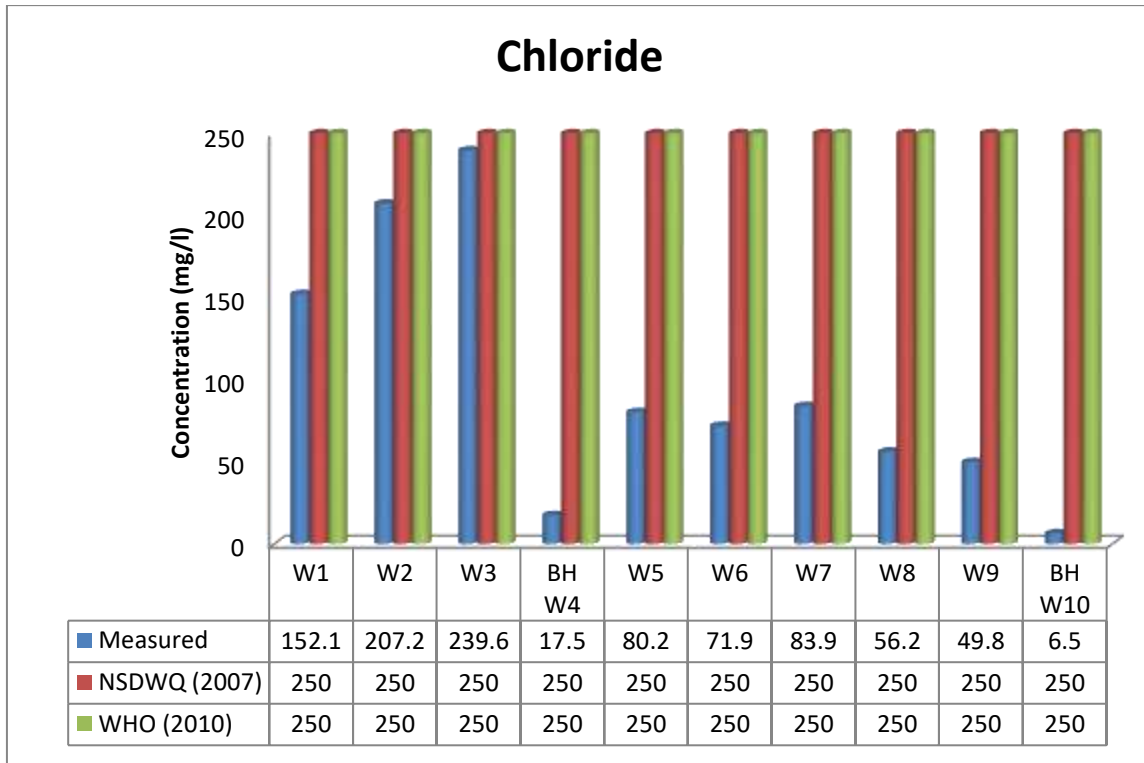


Figure 4.16: Concentration of Chloride compared with NSDWQ (2007) and WHO (2010)

Nitrite

Nitrite concentration ranged from 0.0 mg/l to 4.172 mg/l with a median concentration of 0.0395 mg/l (Table 4.6). The concentration of nitrite within the locations are beneath the minimum acceptable limits of 0.2 mg/l of WHO (2010) and NSDWQ (2007) except Locations W2 and W7 that are highly above the recommended values (Table 4.5, Figure 4.17). Asphyxia (blue-baby syndrome) and cyanosis in newborns below three months is as a result of high nitrite and nitrate concentration in drinking water (Chapman, 1992) and it is also known as infant methaemoglobinaemia (Amadi, 2010).

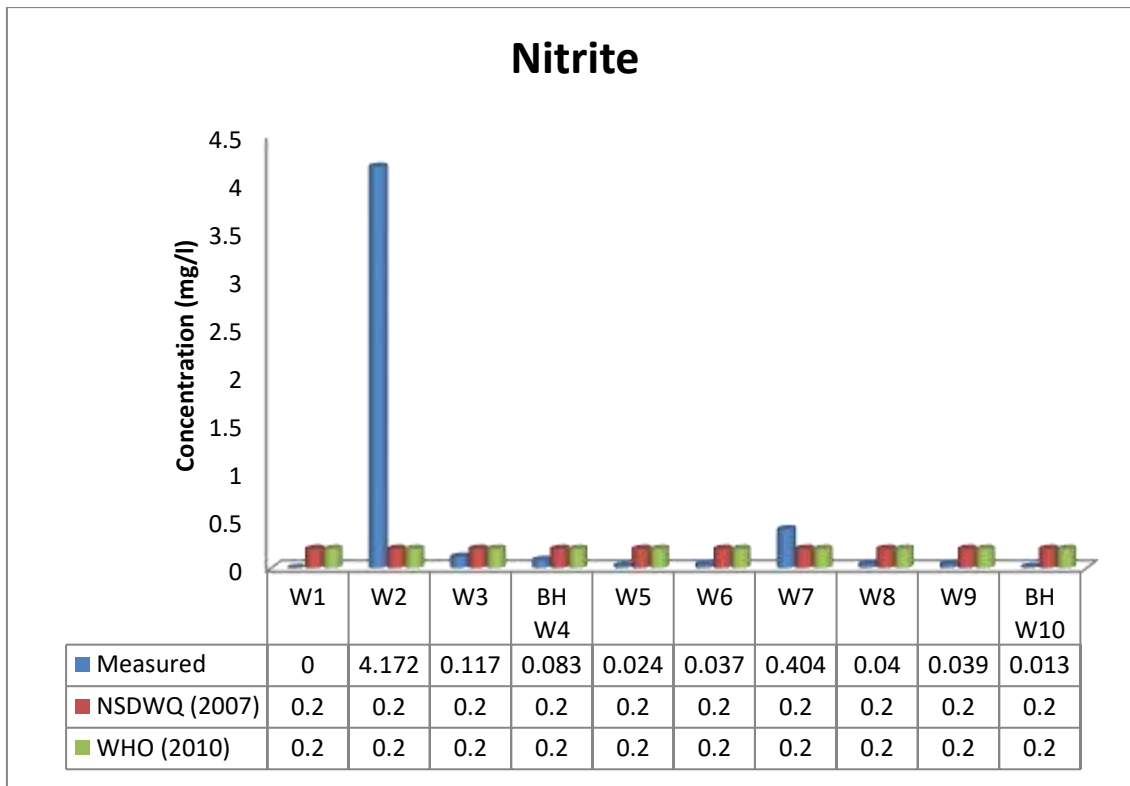


Figure 4.17: Concentration of Nitrite compared with NSDWQ (2007) and WHO (2010)

Bicarbonate

The concentration of bicarbonate varied between 12.0 mg/l and 260.0 mg/l with an average and median values of 78.7 mg/l and 60.0 mg/l respectively (Table 4.6). All the values of the concentration of the water samples from all the locations are beneath the acceptable bound of 250 mg/l of NSDWQ (2007) except Location W2 that is slightly above the limit (Table 4.5, Figure 4.18).

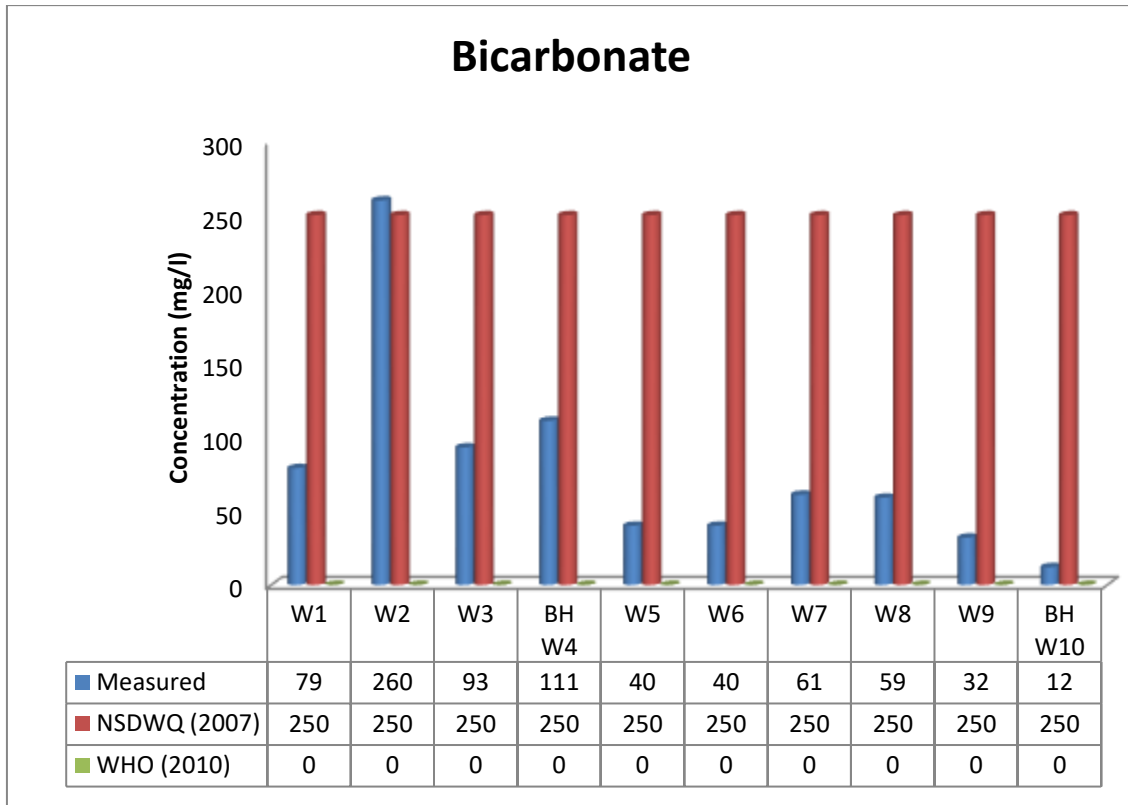


Figure 4.18: Concentration of bicarbonate compared with NSDWQ (2007) and WHO (2010)

Sulphate

Sulphate concentration ranges from 6.0 mg/l to 55.0 mg/l and an average and median values of 22.5 mg/l and 18.0 mg/l in that order (Table 4.6). There is no sulphate contamination within the study area since all the values are within the minimum tolerable limits of 100 mg/l of both WHO (2010) and NSDWQ (2007) (Table 4.5, Figure 4.19). When sulphate concentration in groundwater is high, it might be caused by dissolution of bedrock and/or city contamination evolving from anthropogenic actions.

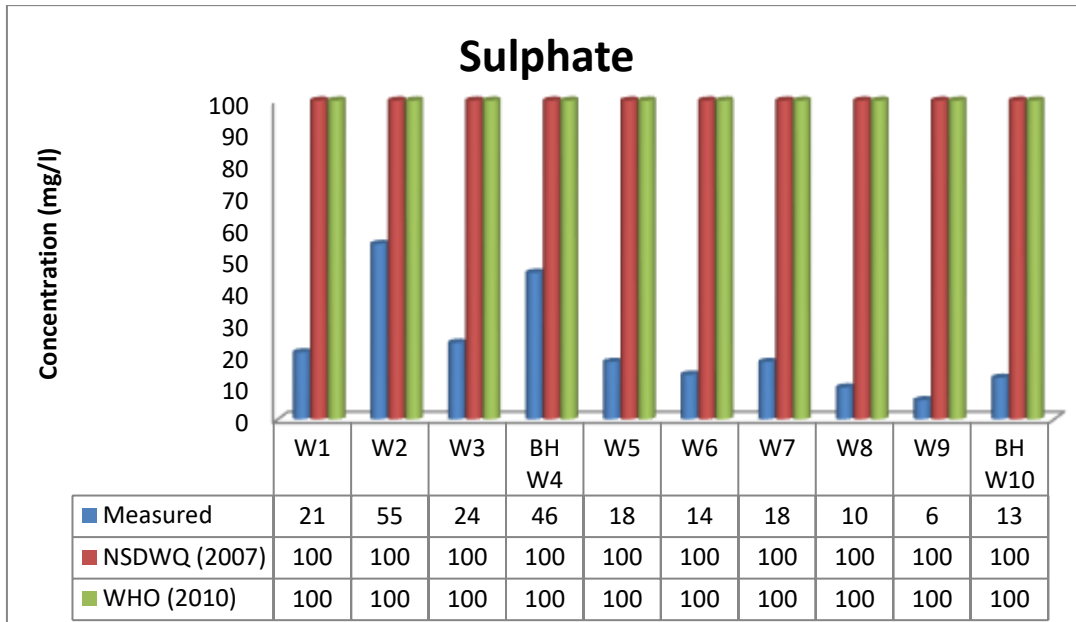


Figure 4.19: Concentration of Sulphate compared with NSDWQ (2007) and WHO (2010)

Carbonate

The concentration of carbonate spans from 0.0 mg/l to 0.0 mg/l indicating no contamination at all within the study area (Table 4.5). All the samples analyzed do not give any significant value for the presence of this anion.

4.6.2.2 Cations in the water

The principal cations analyzed for in the samples of water are sodium, calcium, magnesium and potassium (Table 4.5). Concentrations of cation in water are resultant from the course of interaction of rock-water as groundwater evolves chemically by interrelating with minerals in aquifer or inner mixing amid diverse flow directions of groundwater in the subsurface.

Sodium

The concentration of sodium in the water samples extends from 8.0 mg/l to 173.0 mg/l with median concentration of 79.5 mg/l (Table 4.6). The concentration estimate of the sodium

are within the tolerable level of 200 mg/l on rules for quality of drinking water by Nigerian Standard for Drinking Water Quality (NSDWQ, 2007) and World Health Organization (WHO, 2010) (Table 4.5, Figure 4.20). This shows no contamination by the alkali metal sodium.

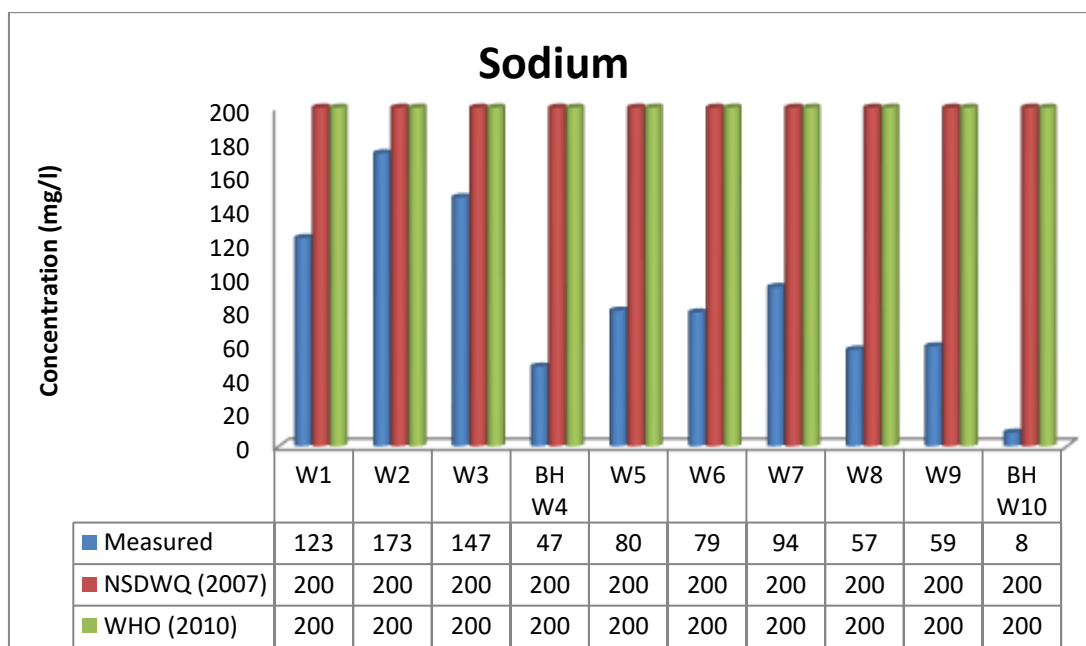


Figure 4.20: Concentration of Sodium compared with NSDWQ (2007) and WHO (2010)

Calcium

From the results, the values of calcium concentration range from 8.8 mg/l to 165.1 mg/l with a medium concentration of 52.5 mg/l (Table 4.6). Locations W1 and W3 have concentrations over the permitted level of 75mg/l recommended by WHO (2010). NSDWQ (2007) does not specify any limit for calcium in drinking water (Table 4.5, Figure 4.21). Calcium is a dietary necessity for all humans. It is a construction rock of skeletons of the majority of marine organisms, and lenses of eye. Calcium deficiency causes osteoporosis, an ailment in which the bones happen to exceedingly porous and vulnerable to fracture and heal gradually (Amadi, 2010).

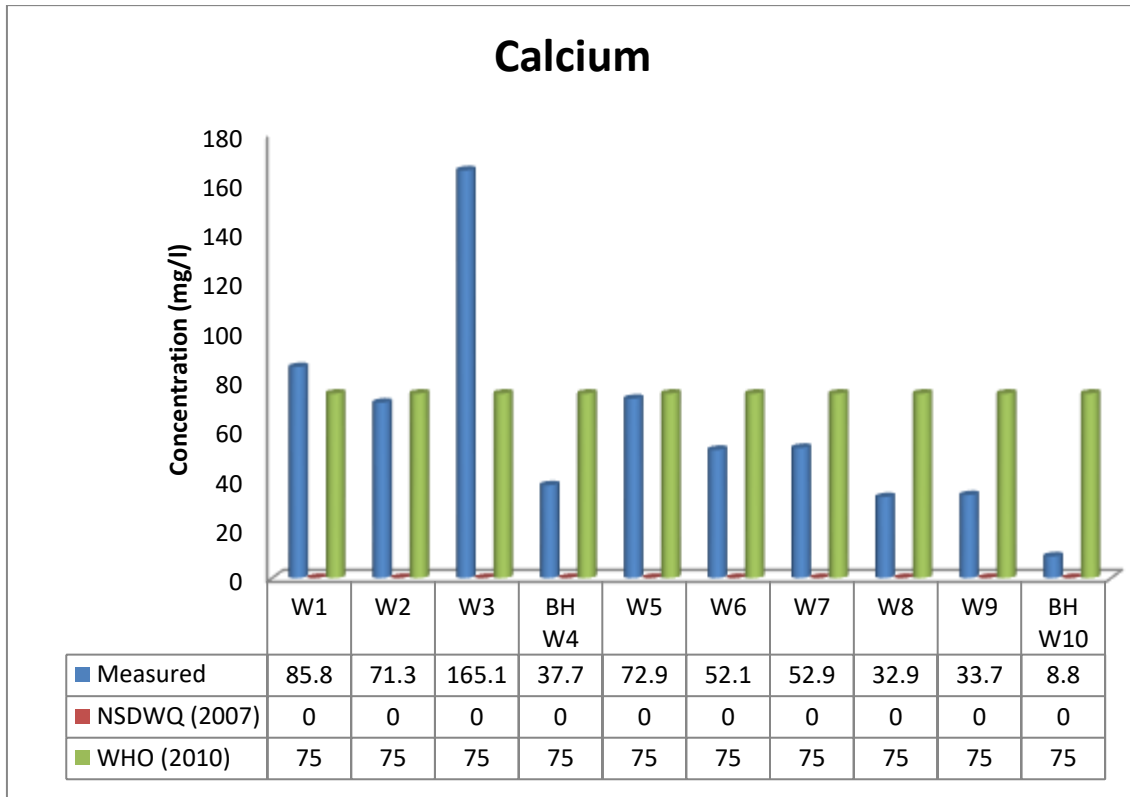


Figure 4.21: Concentration of calcium compared with NSDWQ (2007) and WHO (2010)

Magnesium

The concentration of magnesium extends from 2.4 mg/l to 26.4 mg/l and concentration of the median is 12.21 mg/l (Table 4.6). It is inside the tolerance value of 50 mg/l for WHO (2010) and 20 mg/l of NSDWQ (2007). For Location W3 which has concentration that slightly exceeded the permissible value of 20 mg/l of NSDWQ (2007) (Table 4.5, Figure 4.22). Generally, the area is free from magnesium contamination.

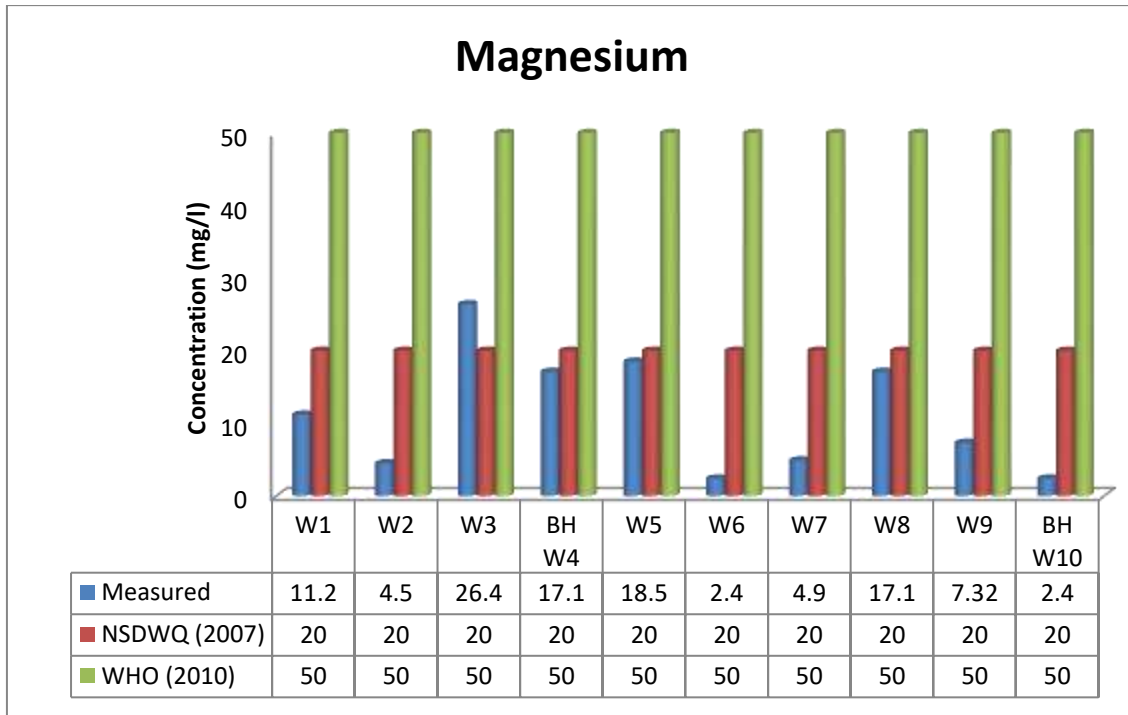


Figure 4.22: Concentration of Magnesium compared with NSDWQ (2007) and WHO (2010)

Potassium

The concentration of potassium ranged from 3.0 mg/l to 56.0 mg/l with median concentration of 5.0 mg/l (Table 4.6). This indicates that there is no potassium contamination within the study area. Although at Location W2, the concentration recorded is slightly higher at 56 mg/l than 55 mg/l recommended for drinking water quality by WHO (2010) (Table 4.5). There is no discernible potassium contamination within the area.

From the analyses, the cations are within the (WHO, 2010) limits for drinking water quality except for calcium that has slightly higher concentration from two locations (Table 4.5, Figure 4.23). The cations (Ca, Na, Mg and K) are crucial parts of water and essential for human health and metabolism and must therefore exist in regular drinking water. When

the permissible limits of Ca, K, Na and Mg in drinking water are exceeded, it can cause intestinal disorder which can lead to complicated health issues.

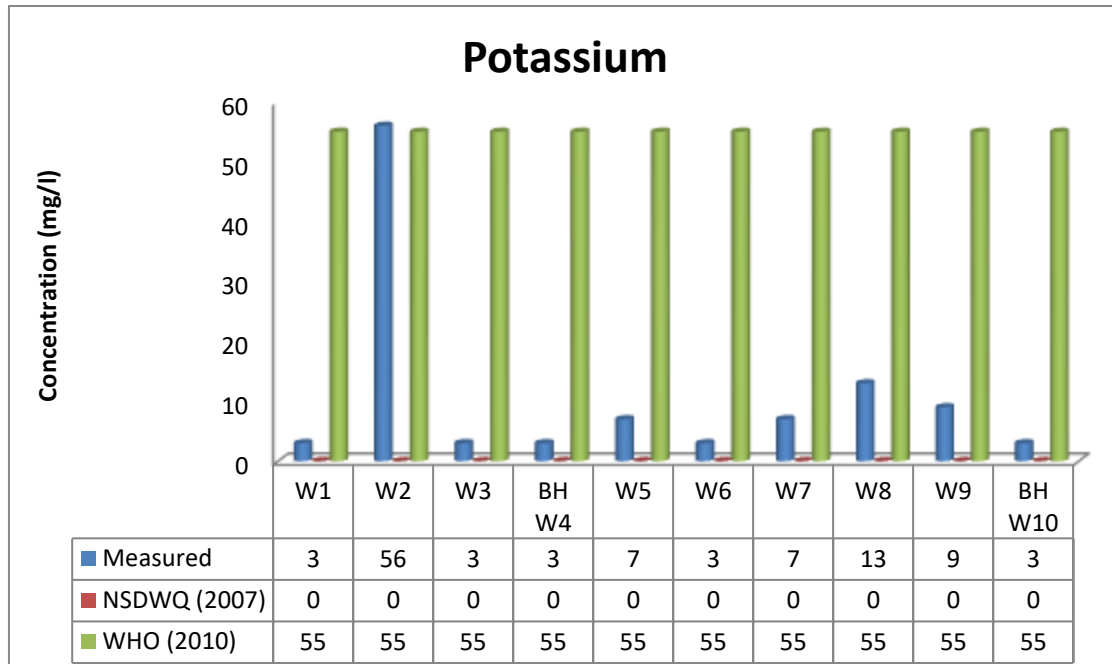


Figure 4.23: Concentration of potassium compared with NSDWQ (2007) and WHO (2010)

4.6.2.3 Heavy Metals

These are chemical element that are metallic and have a comparatively high density (or specific gravity) usually greater than 5.0 and can be rather toxic in small concentrations (Martin *et al.*, 1982). The heavy metal concentration in the samples of subsurface water samples from the area of research are illustrated on Table 4.5. Heavy metal pollution usually results from a range of sources viz; industrial wastewater, solid waste dumpsites, urban surface water runoff and discharges from natural resources mines into the aquatic environment, geological formation, weathering and agricultural activities (Gupta *et al.*, 2009). The heavy metals analyzed for in the groundwater samples are manganese, zinc, chromium, arsenic, copper, iron, cadmium and lead.

Manganese

The concentration of manganese from the analyzed samples varies from 0.0 mg/l to 0.194 mg/l and with a mid value concentration of 0.0035 mg/l (Table 4.6) and it is below the minimum acceptable limit 0.2 mg/l of NSDWQ (2007). There is no contamination by manganese from the area. All the groundwater samples have concentration values lower than the WHO and NSDWQ tolerable level of 0.2 mg/l (Table 4.5, Figure 4.24). Manganese is important for animals and plants, and is used in effects like glass, batteries and firecrackers (Aboud and Nandini, 2009).

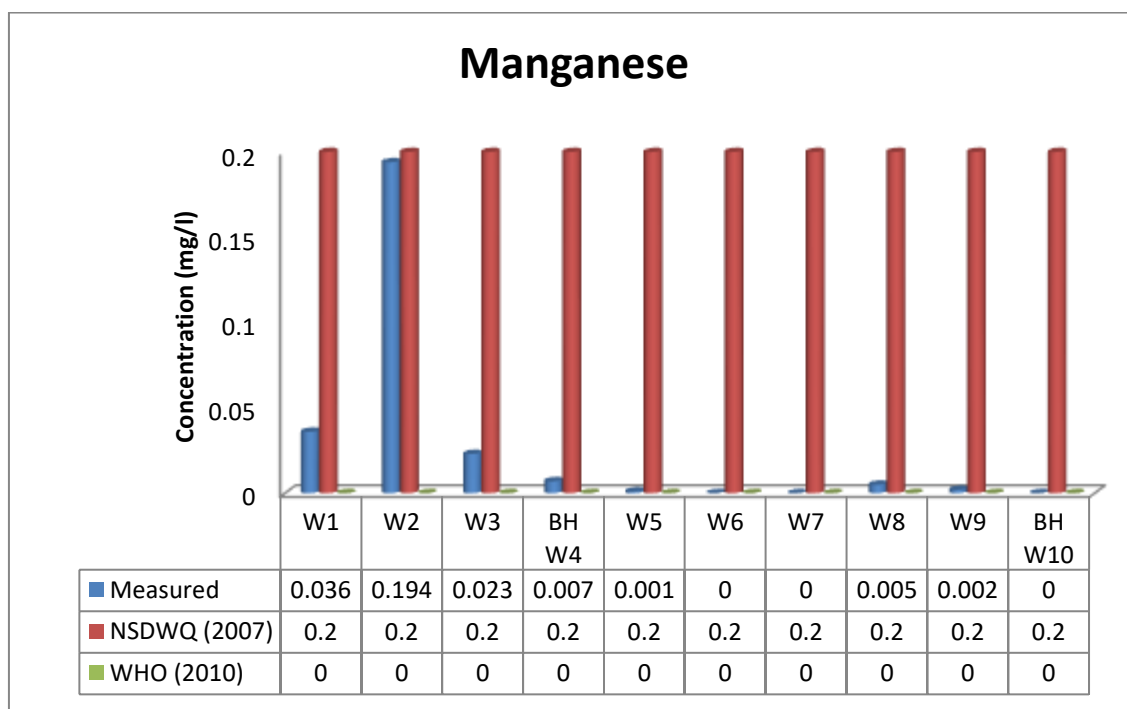


Figure 4.24: Concentration of magnesium compared with NSDWQ (2007) and WHO (2010)

Zinc

Zinc concentration in surface water extends from 0.0 mg/l to 0.008 mg/l and an average and median values of 0.0011 mg/l and 0.00 mg/l (Table 4.6). The general and mean

concentration values for the groundwater samples falls under the tolerable level of 3.00 mg/l (NSDWQ, 2007). In Locations BHW4, W5, W6, W7, W8 and W9, the concentration is beyond detectable limit (Table 4.5, Figure 4.25). The WHO recommended nutritional tolerance of zinc for men is 15 milligrams/day (15 mg/day); for women 12 mg/day; for children 10 mg/day; and for infants 5 mg/day (WHO, 2008; Lee *et al.*, 2007). Zinc is an indispensable constituent in human diet. Inadequate zinc can result in health problems, but surplus zinc is also risky. Severe toxicity might bring about sweet taste, dryness of throat, weakness, chills, nausea, generalized aching, fever and vomiting. Chronic toxicity can result to stomach cramps, vomit, nausea, anemia and pancreas harm (Nouri *et al.*, 2008).

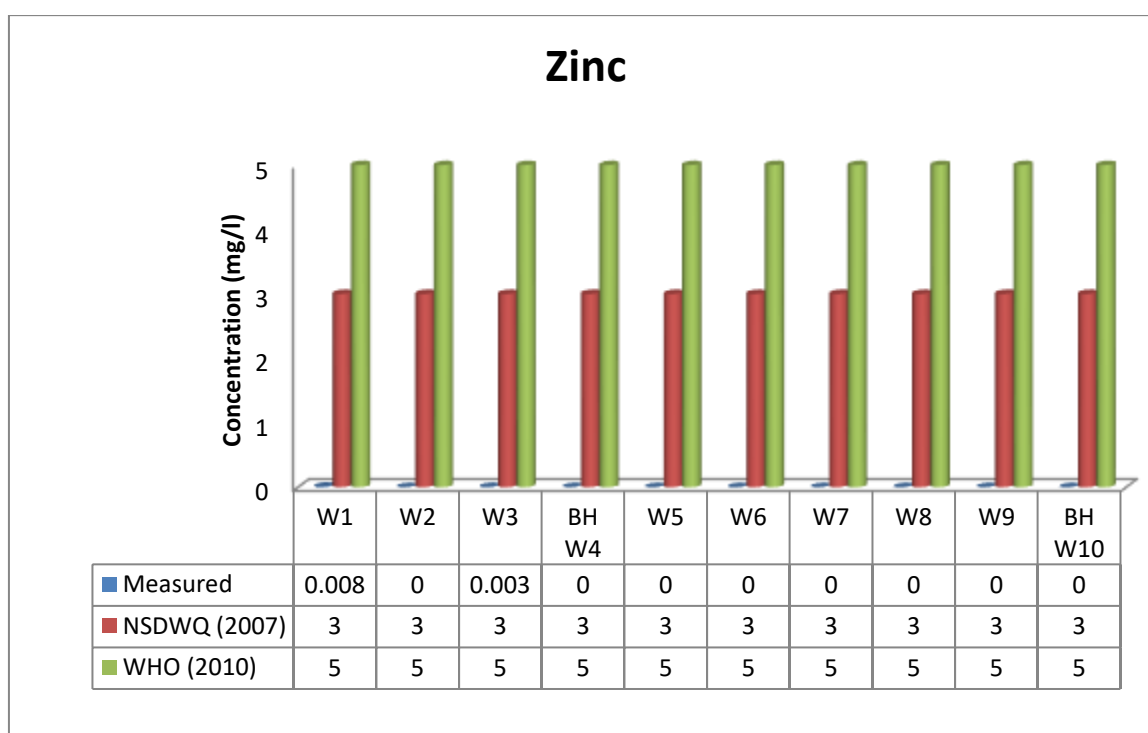


Figure 4.25: Concentration of zinc compared with NSDWQ (2007) and WHO (2010)

Chromium

The concentration of chromium in the examined groundwater samples extends from 0.0 mg/l to 0.03 mg/l with median concentration of 0.01 mg/l (Table 4.6). This is below the

minimum permissible level of 0.05 mg/l for both NSDWQ (2007) and WHO (2010) (Table 4.5, Figure 4.26). Chromium enrichment in water causes cancer (Aboud and Nandini, 2009).

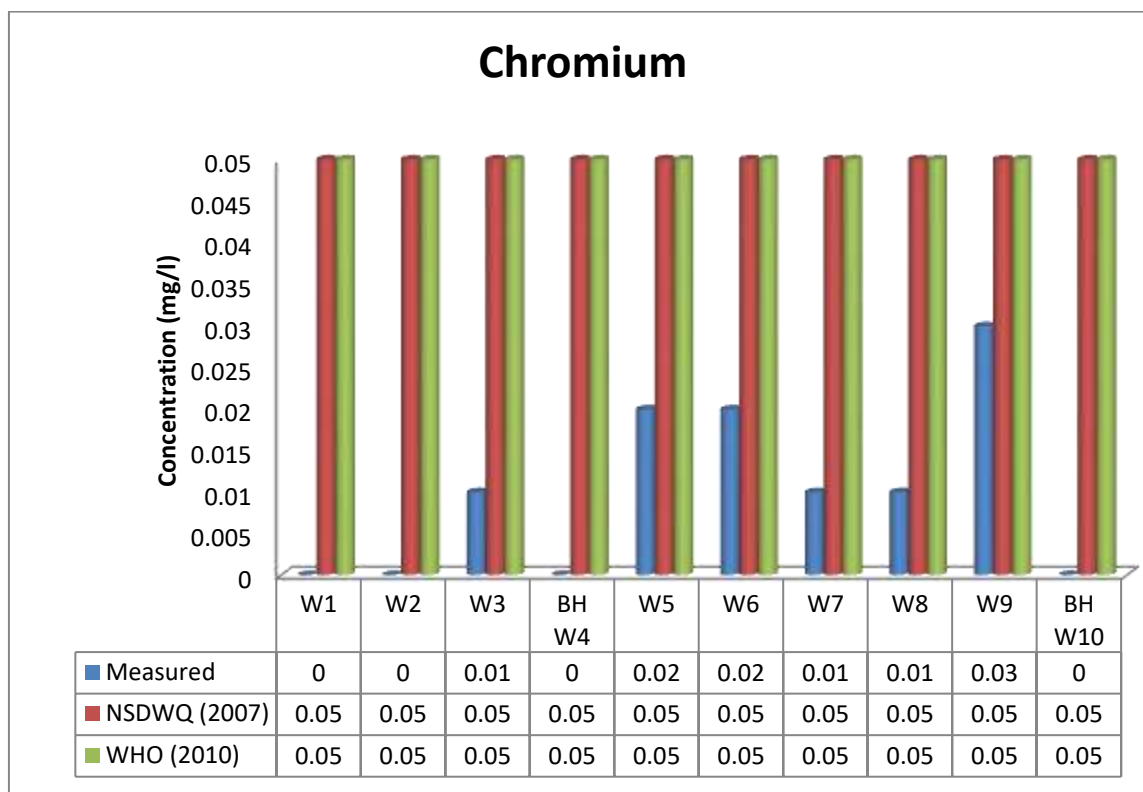


Figure 4.26: Concentration of chromium compared with NSDWQ (2007) and WHO (2010)

Arsenic

There was no contamination by arsenic because all the analyzed water samples concentrations were 0.0 mg/l (Table 4.5). Arsenic is the main causes of severe heavy metal fatality in grown-ups and can be freed into the surroundings through mining as a pathfinder element to gold. When arsenic goes into the surroundings, it does not vanish, rather it can be sucked up by the soil through pesticides application on farm lands, infiltrate into groundwater system or surface water via run off (Karbassi *et al.*, 2008; Sekabira *et al.*, 2010).

Copper

Copper concentration extends from 0.0 mg/l to 0.001 mg/l and has a median value of concentration of 0.0001 mg/l (Table 4.6). It has numerous functions which range from roofing sheets, electrical wiring, cooking pots, alloy pigments, electroplating to insecticides and preservation of wood. Copper serve as supplementary to feeds of animal and fertilizer as nutrient supply to maintain the development of animals and plants (Pascual *et al.*, 2004). The appraised copper concentration in the region of research lies within the tolerable limit of 1.0 mg/l recommended by NSDWQ (2007) and WHO (2010). Elevated copper concentration in water directs to gastrointestinal syndrome (NSDWQ, 2007).

Iron

The concentration of iron in groundwater samples of the area extend from 0.17 mg/l to 0.47 mg/l with a median concentration of 0.225 mg/l (Table 4.6). The concentrations of the subsurface water samples is within the highest tolerable limit of 0.3 mg/l (NSDWQ, 2007 and WHO, 2010) except for Location W5 (0.47 mg/l) which is slightly beyond the 0.3 mg/l of NSDWQ (2007) and WHO (2010) (Table 4.5, Figure 4.27). Iron permeates into the subsurface water as a consequence of chemical eroding of rock/laterilization thus considerable amounts of iron might hence exist in groundwater. The body of human requires iron for fundamental activities of metabolism as it is a valuable constituent of the blood, iron deficiency in the body can result to goitre (WHO, 2006).

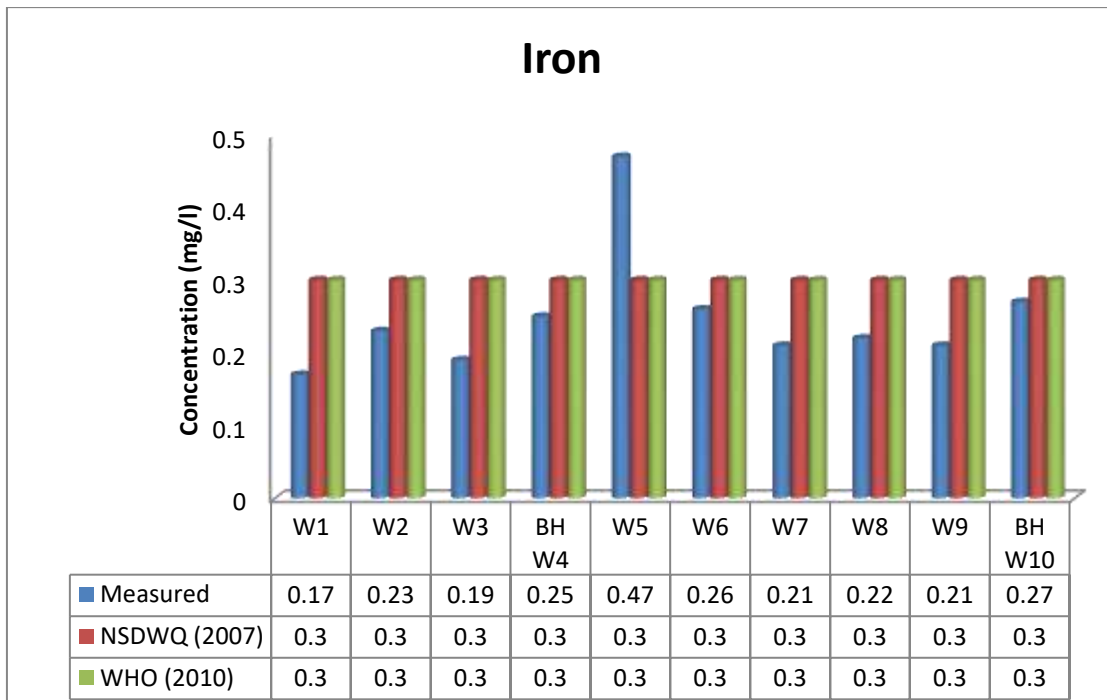


Figure 4.27: Concentration of iron compared with NSDWQ (2007) and WHO (2010)

Cadmium

The concentration of cadmium extends from 0.0 mg/l and 0.0 mg/l with some location beyond detectable limits (Table 4.5). The maximum allowable limit is 0.003 mg/l for NSDWQ (2007) (Table 4.6). There is no cadmium contamination within the study area.

Lead

The groundwater's lead concentrations ranges from 0.0 mg/l to 0.0 mg/l and mid concentration level is 0.0 mg/l (Table 4.6). The concentration of lead in some area is beyond detectable limit and there is no lead contamination within the study area. The maximum recommended limit for NSDWQ (2007) and WHO (2010) is 0.01 mg/l. High intensities lead in the body is able to harm several body systems and organs. It can be particularly hazardous to infants, young children and the unborn.

CHAPTER FIVE

5.0 CONCLUSION AND RECOMMENDATIONS

5.1 Conclusion

The geology, geophysical, geotechnical and hydrogeological studies were applied in the mapping of a public waste disposal site in Barikin-Sale Minna, Nigeria and the geological map of the area was produced. This was done to unravel potential groundwater pollution that could arise from leachate associated with the dumpsite. The petrographic thin sections of the samples of rock carried out shows the existence of quartz, plagioclase, orthoclase and biotite that are minerals found on the surface of the earth which shows that the area is underlain by granitic rocks. From the sieve analysis, the soil outline in the examined area from crest to base is composed of; sandy clay/clayey sand topsoil, weathered basement and the fractured/fresh basement rocks, from the top to the bottom. The hydraulic distribution map was produced. The hydraulic conductivity of the soils indicates that the soil in the area is porous and can easily serve as conduit for the movement of leachates from the dumpsite into the surrounding aquifers. The outcome of the vertical electrical sounding and 2D inverse model resistivity sections indicates a thin to thick electrically conductive clayey/sandy layer underlain by weathered basement rock which overlies the rocks of the fresh basement. The hydrogeological analysis also shows that there is gradual contamination of the groundwater system within the area.

The outcome of all the analyses carried out revealed that the gaping dumpsite in the area is underlain by substances of weak shielding capacity for the aquifers. This indicates that as time goes on, the aquifer in the area will continue to receive loads of contaminants. Therefore, the aquifer structures in the region are susceptible to contamination from

permeation of leachate from decaying refuses discarded at the location and the water in the area is not suitable for human consumption.

5.2 Recommendations

From the results of all the analyses carried out, the following recommendations are made:

To ensure safe consumption of potable groundwater in the area, wastes should be evacuated from the area because the area is vulnerable to pollution and as a result of the shallow depth of the aquiferous unit.

Further and continue dumping of waste in the area should be discontinued.

Also, the outcomes and generated data from this research must be brought into concern when setting up development plan that employs the subsurface surrounded by and outside the refuse-site such as water boreholes, farms and health facilities, inhabited and commercial facilities.

Exclusively, it is suggested that pre-drilling geophysical explorations should be done prior to embarking on any water borehole projects around and within the dumpsite.

Certainly, contemporary engineered landfills with base liner for sustainable and secure refuse dumping and management should be introduced in the study area.

REFERENCES

- Abaa, S. I., (1983). The Structure and Petrography of Alkaline Rocks of the Mada Younger Granite Complex, Nigeria. *Journal of African Earth Science*, 3, 107–113.
- Abd El-Salam, M. M., & Abu-Zuid, G. I. (2015). Impact of Landfill Leachate on the Groundwater Quality: A Case Study in Egypt. *Journal of Advanced Research*, 6(4), 579-586. doi.org/10.1016/j.jare.2014.02.003
- Abimbola, A. F., Oke, S. A., & Olatunji, A. S. (2001). Environmental Impact Assessment of Waste Dumpsites on the Geochemical Quality of Water and Soil in Warri Metropolis, Southern Nigeria. *Water Resource Journal of Nigerian Association of Hydrogeologist*, 13, 6-11.
- About, S. J., & Nandini, N. (2009). Heavy Metal Analysis and Sediment Quality Values in Urban Lakes. *America Journal of Environment Science*, 5(6), 678 – 687.
- Aderemi, A .O., Oriaku, A. V., Adewumi, G. A. & Otitolaju, A. A. (2011). Assessment of Groundwater Contamination by Leachate near a Municipal Solid Waste Landfill. *African Journal of Environmental Science and Technology*, 5(11), 933-940.
- Adeyemi, G. O., & Ogundero O. C., (2001). Some Geotechnical Properties of Soil Developed Over Migmatite Gneiss in Oru-Ijebu, Southwestern Nigeria. *Journal of Applied Sciences*, 4 (3), 2140-2150.
- Ajibade, A. C. (1982). The Origin of the Older Granites of Nigeria: Some Evidence from the Zungeru Region. *Nigerian Journal of Mining and Geology*, 19, 223-230.
- Akamkpo, A. O., & Igboekwe, M. U. (2011). Monitoring Groundwater Control Using Surface Electrical Resistivity and Geochemical Methods. *Journal of Water Resources and Protection*, 3, 318 – 324.
- Alawode, O. I., Ojo, I. O., & Adeuyi, O. B. (2019). Physico-Chemical Analysis and Social Impacts of Heavymetals from Landfill Leachates in Groundwater: A Case Study of Ogeese Community, Oyo State, Nigeria. *International Journal of Environmental Science and NaturalResources*, 17, 103-108. doi-10.19080/IJESNR.2019.17.555964.
- Amadi, A. N., & Nwankwoala, H. O., (2013). Evaluation of Heavy Metal in Soils from Enyimba Dumpsite in Aba, Southeastern Nigeria Using Contamination Factor and Geo-Accumulation Index. *Energy and Environment Research*, 3(1), 125-134.
- Amadi, A. N. (2009). Evaluation of Surface and Groundwater Quality in Owerri Metropolis, Southeastern Nigeria. *International Journal of Chemical Sciences*, 2 (2), 212 – 219.
- Amadi, A. N., (2010). Effects of Urbanization on Groundwater Quality: A Case Study of Port-Harcourt, Southern Nigeria. *Natural and Applied Sciences Journal*, 11(2), 143 – 152.

- Amadi, A. N., Okunlola, I. A., Eze C. J., Jimoh, M. O., Unuevho, C. I., & Abubakar, F. (2015). Geotechnical Assessment of Clay Deposits in Minna, North-Central Nigeria for Use as liners in Sanitary Landfill Design and Construction. *American Journal of Environmental Protection*, 3, 67-75. DOI:10.12691/env-3-3-2.
- Aweto, K. E.. (2011). Aquifer vulnerability assessment at Oke-IIa area, Southwestern Nigeria. *International Journal of Physical Sciences*. 6. 10.5897/IJPS11.933.
- Bahroz, A. (2015). Leachate and Groundwater Assessment at Kirkak Sanitary Landfill Site in Zindana Village, Iraq. *International Journal of Environmental Research*, 9(2), 457 – 466.
- Barker, R. D. (2001). *Principle of Electrical Imaging*. University of Birmingham, United Kingdom.
- Bayewu, O. O., Olountola, M. O., Mosuro, G. O. & Adeniyi, S. A. (2012). Petrographic and Geotechnical Properties of Lateritic Soils Developed Over Different Parent Rocks in Ago-Iwoye Area, Southwestern Nigeria. *International Journal of Applied Sciences and Engineering Research*, 1(4), 584-595.
- Bayode, O. J. A., Adewunmi, E.A. & Odunwole, S. (2011). Environmental Implications of Oil Exploration and Exploitation in the Coastal Region of Ondo State, Nigeria: A Regional Planning Appraisal. *Journal of Geography and Regional Planning*, 4(3) 113-116.
- Benson, A. K., Pane, K. L., & Stubben, M. A. (1997). Mapping Groundwater Contamination Using DC Resistivity and VLF Geophysical Methods: A Case Study. *Geophysics*, 62(1), 80-86
- Black, R. (1980). Precambrian Geology of West Africa. *Episodes*, 1980, no. 4 (Dec), 3 – 8.
- Boadi, K. O., & Kuitunen, M. (2005). Environmental, wealth, inequality and the burden of disease in the Accra metropolitan area, Ghana. *International Journal of Environment and Health Resources* 15 (3) 2005, 193-206.
- Burke, K. C., & Dewey, J. F., (1972). Orogeny in Africa, In Dessauvage, T.F.J. and Whiteman, A.J. (EDs.). *African Geology*, Geology Dept., University of Ibadan, 583-608.
- Buselli, G., Bareber, C., Davis, G. B. & Saama, R. SB. (1992). Detection of Groundwater Contamination Near Waste Disposal Sites with Electromagnetic Methods. *Geotechnical Environmental Geophysics*, 11, 73-79.
- Chambers, J. E., Kuras, O., Meldrum, P. I., Ogilvy, R. D. & Hollands, J. (2006). Electrical Resistivity Tomography Applied to Geologic, Hydrogeologic and Engineering Investigation at a Former Waste-disposal Site. *Geophysics*, 71(6), 231 - 239.
- Chapman, D. (1992). Water Quality Assessment: In D. Chapman (ed.) on behalf of UNESCO, WHO and UNEP, London, Chapman and Hall.

- Cristina, P., Cristina, D., Alicia, F., Pamela, B. (2012). Application of Geophysical Methods to Waste Disposal Studies. 10.5772/29615
- Dahlin, T., & Bing, Z. (2003). A Numerical Comparison of 2D Resistivity Imaging with Ten Electrode Arrays. *Revised version for Geophysical Prospecting*, 1, 43 – 47.
- Devlin, J. F. (2015). HydrogeoSieveXL: An Excel-based Tool to Estimate Hydraulic Conductivity from Grain-Size Analysis. Developed April 29, 2014, Most Recent Update September, 2016.
- Ebraheem, M. H., M. W., Bayless, E. R. & Krothe, N. C. (1990). "A Study of Acid Mine Drainage Using Earth Resistivity Measurements", *Ground Water*, 28 (3), 361-368.
- Egbai, J. C., Efeya, P. & Iserhien-Emekeme, R. E. (2015). 2D Geoelectric Evaluation and Imaging of Aquifer Vulnerability of Dumpsite at Ozoro Isoko South LGA of Delta State. *Journal of Natural Sciences and Resources*, 5: 1.
- Ehirim, C. N. & Ekeocha, N. E. (2009). Anisotropic Type Determination and Soil Structure Evaluation in Parts of the Gully Erosion Zones of SE Nigeria using Azimuthal-Offset Resistivity Sounding Technique and Erodibility Characterization. *Pacific Journal of Science and Technology*, 10(2), 709-715.
- El Mahmoudi, Ahmed. (1999). Geoelectric Resistivity Investigations of Kafr Saqr Sheet, Sharrqiya Governorate, East Nile Delta. *Journal of Petroleum and Mining Engineering*. 2. 84-108.
- Environmental Protection Agency (EPA) United States. (1994). Use of Airborne, Surface and Borehole Geophysical Techniques at Contaminated Sites. Reference Guide.EPA/625/R-92/007.
- Farid, H. U., Mahmood-Khan, Z., Ali, A., Mubeen, M. & Anjum, M. N. (2017). Site-Specific Aquifer Characterization and Identification of Potential Groundwater Areas in Pakistan. *Pol Journal of Environmental Studies*, 26, 17-27.
- Fatta, D., Naomi, C., Karlis, P. & Loizidou, M. (2000). Numerical Simulation of Flow Sand Contaminant Migration at a Municipal Landfill. *Journal of Environmental Hydrology*, 8(6), 1-10.
- Federal Meteorological Agency (2011). Minna Weather Report. Unpublished.
- Griffiths D. H. and Barker, R. D. (1993) Two-Dimensional Resistivity Imaging and Modeling in Areas of Complex Geology. *Journal of Applied Geophysics*, 29, 21-26. [http://dx.doi.org/10.1016/0926-9851\(93\)90005-J](http://dx.doi.org/10.1016/0926-9851(93)90005-J)
- Gupta, A., Rai, D.K., Pandey, R.S. & Sharma, B. (2009). Analysis of Some Heavy Metals in the Riverine Water, Sediments and Fish from River Ganges at Allahabad. *Environmental Monitoring Assessment*, 157,449-458.
- Henriet, J. P. (1976). Direct Application of Dar-Zarrouk Parameters in Ground Water Surveys. *Geological Prospecting*, 24, 344 - 353.

- Ibitola, M. P., Ehinola, A. O. & Akinnigbagbe, A. E. (2011). Electrical Resistivity Method in Delineating Vadose and Saturated Zone in Some Selected Dumpsites in Ibadan Part of Southwestern Nigeria. *International Journal of Geomatics and Geosciences*, 2(1), 164 – 178.
- Ige, O. O., & Ogunsanwo, O. (2009). Assessment of Granite-derived Residual Soil as Mineral Seal in Sanitary Landfills. *Researcher*, 1(6), 80-86. Retrieved from <http://www.sciencepub.net/researcher>
- Ige, O. O. (2010). Assessment of Geotechnical Properties of Migmatite-gneiss Derived Residual Soil from Ilorin, Southwestern Nigeria, as Barrier in Sanitary Landfills. *Continental Journal of Earth Sciences*, 5 (1), 32 – 41.
- Ige, O. O. (2013). Geological and Geotechnical Evaluation of an Open Landfill for Sanitary Landfill Construction in Ilorin, Southwestern Nigeria. *Journal of Environment and Earth Science*, 3 (3), 9-17.
- Ige, O. O., Ogunsanwo, O. & Iyang, H. I. (2011). Characterization of Terrain and Biotite Gneiss-Derived Lateritic Soil of the Ilorin, Nigeria, for Use in Landfill Barriers. *Global Journal of Geological Sciences*, 9(1), 1-9.
- Iyama, W. A., & Etori, O.S. (2019). Comparative Analysis of the Water Quality Status of the Bassan Rivers in Bayelsa State, Nigeria. *International Journal of Chemistry and Chemical Engineering*. 6(1), 59 – 69.
- Jegede, S. I., Iserhien-Emekem, R. E., Iyoha, A. & Amadasun, C.V.O. (2013). Near Surface Investigation of Groundwater Contamination in the Regolith Aquifer of Palladan, Zaria using Borehole Log and Tomography Techniques. *Research Journal of Applied Sciences & Engineering Technology*, 6, 537-543.
- Karbassi, A. R., Monavari, S. M., Nabi-Bidhendi, G. R., Nouri, J. & Nematpour, K. (2008). Metal Pollution Assessment of Sediment and Water in the Shur River. *Environmental Monitoring and Assessment*, 147(2), 107-116.
- Karlik, G., & Kaya, A. M. (2000). Investigation of Groundwater Contamination Using Electric and Electromagnetic Methods at an Open Waste Disposal Site: A Case Study from Isparta, Turkey, *Environmental Geology*, 40(6), 725-731.
- Kearey, P. Brooks, M. & Hill, I. (2002). *An Introduction to Geophysical Exploration*. Blackwell Science Ltd. Third Edition. United Kingdom.
- Kola-Olusanya, A. (2013). Impact of Municipal Solid Waste on Underground Water Resources in Nigeria. *European Scientific Journal*, 8(11), 1-19.
- Lee, C. L., Li, X.D., Zhang, G., Li, J., Ding, A. J. & Wang, T. (2007). Heavy Metals and Pb Isotopic Composition of Aerosols in Urban and Suburban Areas of Hong Kong and Guangzhou, South China Evidence of the Long-range Transport of Air Contaminants. *Environmental Pollution*, 41(1), 432-447.

- Loke, M .H. (1999). *Time-lapse Resistivity Imaging Inversion*. Proceedings of the 5th Meeting of the Environmental and Engineering Geophysical Society European Section.
- Lowrie, W. (2007). *Fundamental of Geophysics*. New York, Cambridge University Press.
- Macaulay, O. O. (2008): Revision notebook on hydrogeological practices (with application to Nigeria groundwater terrains. PIOS publications.
- Maillet, R. (1947). The Fundamental Equation of Electrical Prospecting. *Geophysics*, 12, 529 - 556.
- Martin, M. H., Duncan, E. M. & Coughtrey, P. J. (1982). The distribution of heavy metals in a contaminated woodland ecosystem. *Environmental Pollution* 3, 147–57.
- Martins, O. (2001). Water Resource Management and Development in Nigeria – *Issues and Challenges in a New Millennium*, (pp. 11-20).
- McCurry, P. (1976). A General Review of the Geology of the Precambrian to Lower Paleozoic Rocks of Northern Nigeria. A Review. In Kogbe C. A. (ED.) *Geology of Nigeria*,(pp.15-38). Ibadan, Elizabeth Publication Company.
- Meju, M. A., (2000). Environmental geophysics: tasks ahead. *Journal of Applied Geophysics*, 44, p. 63-65.
- Michel, R. Jean-Claude, P., Diout, S. Beauvais, A. Dione, F. & Niany, M. (1999). Electrical Imaging of Lateritic Weathering Mantles over Granitic and Metamorphic Basement of Eastern Senegal. *West Africa Journal of Applied Geophysics*, 41, 335-344.
- Mondal, N. C. Rao, V. A. Singh, V. S. & Sarwade, D. V. (2008). Dealineation of Concealed Linearment Using Electrical Resistivity Imaging in Granitic Terrain. *Current Sciences*, 94(3), 277-283.
- Montgomery, C. L. (2000). *Environmental Geology*. 5th Edition, McGraw Hill. Higher Education Publication.
- Mukhtar, A., Ibrahim, S., Abdullatif, P. & Hanafi, M. (2000). Detection of Groundwater Pollution Using Resistivity Imaging at Seri Petang Landfill, Malaysia. *Journal of Environmental Hydrology*, 8, 1-8.
- Nasir, K. A., Isaac, B. O. & Abraham, O. (2010). Detecting Municipal Solid Waste Leachate Plumes through Electrical Resistivity Survey and Physicochemical Analysis of Groundwater Samples. *Journal of American Science*, 6(8), 18-35.
- Nigerian Geological Survey Agency (2009). Geological Map of Nigeria, Federal Republic of Nigeria. *Nigeria Geological Survey Agency Publication*, 2009.
- Nouri, J., Mahvi, A. H., Jahed, G. R. & Babaei, A. A. (2008). Regional Distribution Pattern of Groundwater Heavy Metals Resulting from Agricultural Activities. *Environmental Geology*, 55(6), 1337-1343.

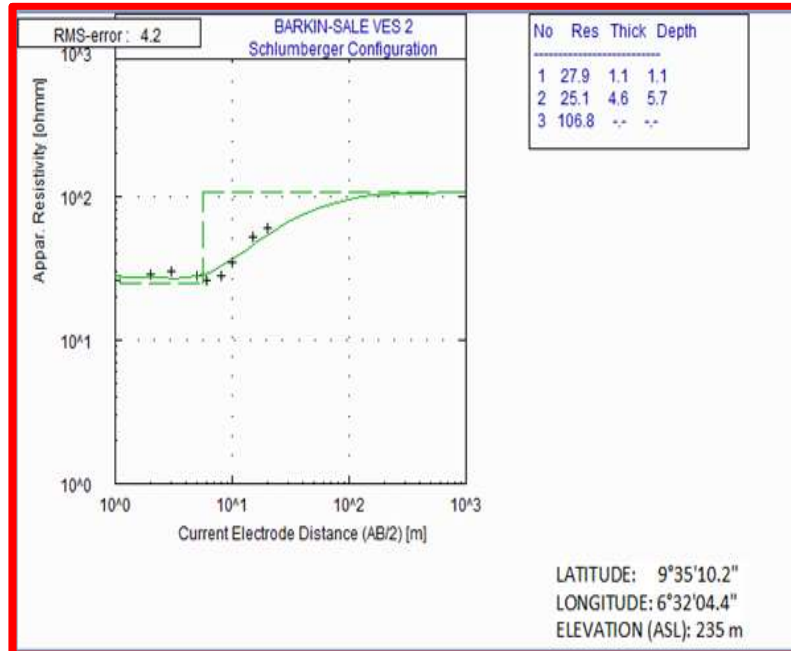
- Nigerian Standard for Drinking Water Quality (NSDWQ). (2007). Nigerian Standard for Drinking Water Quality. Nigerian Industrial Standard, NIS: 554, 1-14.
- Obaje, N. G. (2009). Geology and Mineral Resources of Nigeria. *Lecture Notes Earth Science*, (pp. 120-221). Berlin, Springer.
- Oladapo, M. I., Mohammed, M.Z., Adeoye, O. O. & Adetola, B. A. (2004). Geoelectrical Investigation of the Ondo State Housing Corporation Estate, Ijapo Akure, Southwestern Nigeria. *Journal of Mining and Geology*, 40(1), 41 - 48.
- Olayinka, A. I., (1992). Geophysical siting of boreholes in crystalline basement areas of Africa. *Journal of African Earth Sciences*, 14, 197-207.
- Olayinka, A. I., & Olayiwola, M. A. (2001). An Integrated Uses of Geoelectrical Imaging and Hydrogeochemical Methods in Delineating Limits of Polluted Surface and Groundwater at a Landfill Site in Ibadan Area, Southwestern Nigeria. *Journal of Mining and Geology*, 37(1), 53 - 68.
- Olayinka, A. I., & Yaramanci, U. (2002). Use of Block Inversion in the 2-D Interpretation of Apparent Resistivity Data and its Comparison with Smooth Inversion. *Journal of Mining and Geology*, 45, 63-81.
- Omale, M., Udensi, E. E., Okosun, E. A. & Daniyan, M. A. (2016). Assessment of Leachate Contamination of Groundwater at Some Waste Disposal Sites in Minna, North-Central Nigeria. Unpublished PhD Thesis, Federal University of technology, Minna.
- Osazuwa, I. B. & Abdullahi, N. K. (2008). 2-D Electrical Resistivity and Induced Polarisation Investigation at an Open Solid Waste Dumpsite: Case Study from Kaduna, North Central Nigeria. *Journal of Environmental Hydrology*, 16(29), 1-11.
- Owoeye, I. O., & Okojie, O. H. (2013). Environmental Audit of a Refuse Dump Site in the Niger Delta Region of Nigeria. *Journal of Public Health and Epidemiology*, 5(2), 59-65.
- Oyawoye, M. O., (1972). The Basement Complex of Nigeria. In T. F. J. Dessauvague and A.J. Whiteman, (Eds.), *African Geology* (pp.66–102). Ibadan, University Press.
- Oyedele, K. F., (2009). Total Dissolved Solids (TDS) mapping in groundwater using geophysical methods. *New York Science Journal*. 2 (3)
- Oyediran, I. A., & Adeyemi, G. O. (2011). Geotechnical Investigations of a Site in Ajibode, Southwestern Nigeria for Landfill. *Ozean Journal of Applied Sciences*, 4(3), 265-279.
- Oyediran, I. A., & Iroegbuchu, C.D. (2013). Geotechnical Characteristic of Some Southwestern Nigerian Clays as Barrier Soils. *Ife Journal of Science*, 15 (1), 17-30.
- Pascual, B., Gold-Bouchot, G., Ceja-Moreno, V. & del Ri'o-garci'a, M. (2004). Heavy Metal and Hydrocarbons in Sediments from Three Lakes from San Miguel, Chiapas,

- Mexico. *Bulletin of Environmental Contamination and Toxicology*, 73, 762–769. doi:10.1007/s00128-004-0491-0.
- Porsani, L., Filho, W. M., Ellis, V. R., Shimlis, J. D. & Moura, H. P. (2004). The Use of GRR & VES in Delineating a Contamination Plume in a Landfill Site. A Case Study in SE Brazil. *Journal of Applied Geophysics*, 55, 199–209.
- Qasim, S. R. & Chiang, W. (2017). *Sanitary Landfill Leachates – Generation, Control and Treatment*. Balin, Taylor and Francis Group.
- Rahaman, M. A., & Lancelot, J. R. (1984). Continental Crust Evolution in SW Nigeria: Constraints from U/Pb Dating of Pre-Pan-African Gneisses. In Rapport d'activite 1980–1984 – Documents et Travaux du Centre Geologique et Geophysique de Montpellier.
- Rahaman, M. A. & Ocan, O. (1978). Relationships in the Precambrian Migmatite-gneisses of Nigeria. *Nigerian Journal of Mining and Geology*, 15, 23–32.
- Rahaman, M. A. (1976). Review of the Basement Geology of South-Western Nigeria. In: C.A. Kogbe, (Ed.), *Geology of Nigeria*, (pp. 41–58). Lagos, Elizabethan Publishers.
- Rahaman, M. A. (1988). Recent Advances in the Study of the Basement Complex of Nigeria. In Geological Survey of Nigeria (Ed), *Precambrian Geology of Nigeria*, (pp.11–43). Lagos, Elizabethan Publishers.
- Rao, V. V., Raju, J. S., Prakasa, B. S. & Rao, P. K. (2004). Bedrock Investigation by Seismic Refraction Method – A Case Study. *Journal of Geophysics*, 8(3), 223-228.
- Reinhard, K. (2006). *Groundwater Geophysics*. Berlin Heidelberg, Springer-Verlag Press.
- Rosqvist, H., Dahlin, T., Foune, A., Rohrs, L., Bengtsson, A. & Larsson, M. (2003). Mapping of Leachate Plumes in Two Landfill Sites in South Africa Using Geo-electric Imaging Techniques. *Proceedings Ninth International Waste Management & landfill symposium*. Calgary, Italy, Sardina.
- Rowe, R. K. (2011). Systems Engineering: The Design and Operation of Municipal Solid Waste Landfills to Minimize Contamination of Groundwater. *Geosynthetics International*, 18, (6), 391–404. doi.org/10.1680/gein.2011.18.6.391.
- Sekabira, K., Oryem-Origa, H., Basamba, T. A., Mutumba, G. & Kakudidi, E. (2010). Assessment of Heavy Metal Pollution in the Urban Stream Sediments and its Tributaries. *International Journal of Environmental Science and Technology*, 7(3), 435-446.
- Soupios, P. M., Georgakopoulos, P., Papadopoulos, N., Saltas, V., Andreadakis, A., Vallianatos, F. & Makris, J. P. (2007). Use of Engineering Geophysics to Investigate a Site for a Building Foundation. *Journal of Geophysics and Engineering* 4, 94-103

- Tijani, M. N., Onibalusi, S .O. & Olatunji, A. S. (2002). Hydrochemical and Environmental Impact Assessment of Orita Aperin Waste Dumptsite, Ibadan Southwestern Nigeria. *Water Resource- Journal of Nigeria Association of Hydrogeologist*, 13, 78-85.
- Turner, D. C. (1983) Upper Proterozoic Schist Belt in the Nigerian Sector of Pan African Province of West Africa. In: Kogbe, C. A., Ed., *Geology of Nigeria*, 2nd Revised Edition, Rock-view Limited, Jos, Nigeria.
- United Nation Environmental Programme (UNEP). (2002). *Water Security and Ecosystem Services: The Critical Connection*. A Contribution to the United Nations World Water Assessment Programme. Nairobi: UNEP. Available at http://www.unep.org/themes/freshwater/pdf/the_critical_connection.pdf.
- Van der Valpen, B. P. A. & Sporry, R. J. (1992). Resist- A Computer Program to Process Resistivity Sounding Data on PC- Compatibles. *Computer and Geosciences*, 19, 691-703.
- World Health Organization (2010). *Guidelines for drinking water quality*, 4th ed. Geneva, World health organization incorporating first addendum). World Health Organization Press, Switzerland.
- World Health Organization (1979). Promoting Environmental Health in the Years 1978-1983. *WHO Chronicle*; 33: 169-173.
- World Health Organization (2006). Guidelines for Drinking-water Quality (3rd ed., (http://www.who.int/water_sanitation_health/publications/2011/dwq_guidelines/en/).
- vanization (2008). *Advocacy, Communication and Social Mobilization for TB Control: A Guide to Developing Knowledge, Attitude and Practice Surveys*. Geneva: WHO Press.
- Wright, J. B. (1985) *Geology and Mineral Resources of West Africa*. London: George Allen & Unwin.
- Zakaria, S. N. F., & Aziz, H. A. (2018). Characteristic of Leachate at Alor Pongsu Landfill Site, Perak, Malaysia, a Comparative Study. IOP Conference Series. *Earth and Environmental Science*, 140, Conference 1.

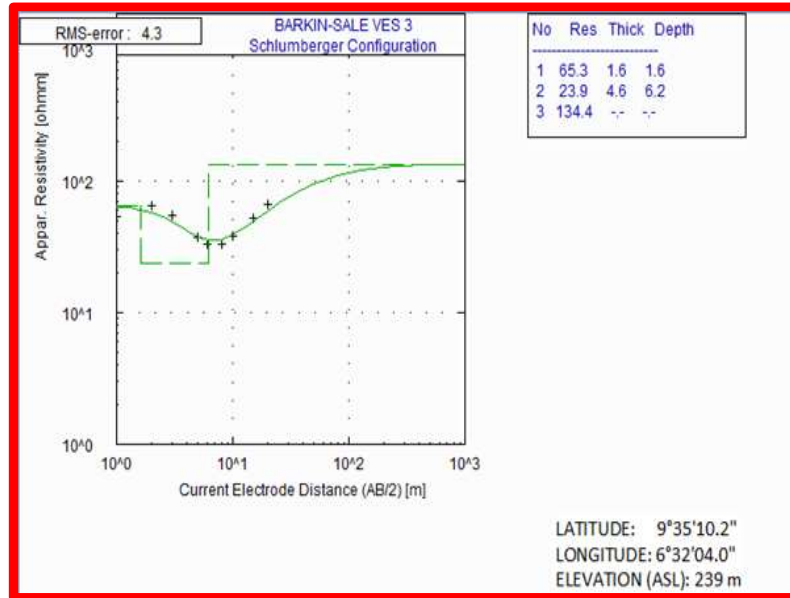
Appendix A

Distance	Resistivity	No
1.00	26.0000	1
2.00	29.0000	2
3.00	30.0000	3
5.00	28.0000	4
6.00	26.0000	5
8.00	28.0000	6
10.00	35.0000	7
15.00	52.0000	8
20.00	60.0000	9



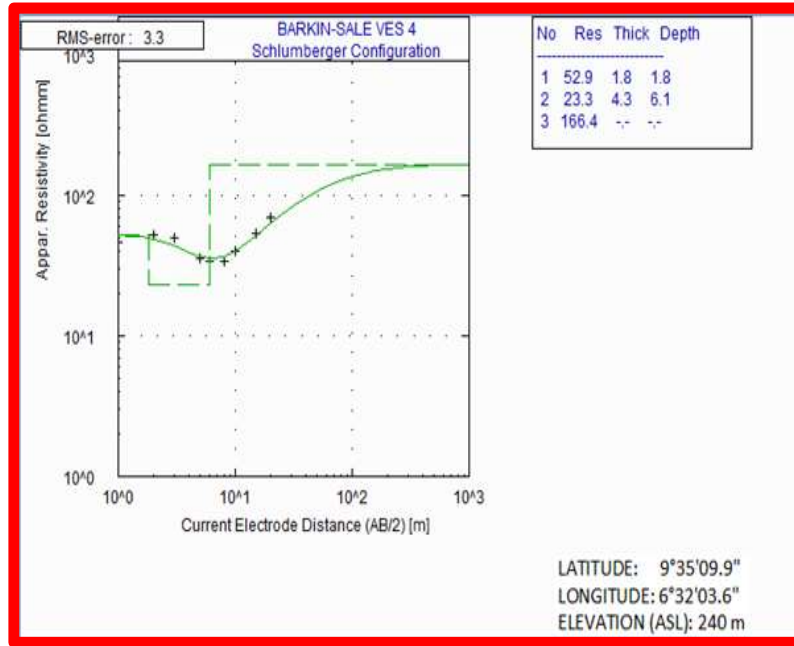
A1. Sounding Curve for VES 2

Distance	Resistivity	No
1.00	54.0000	1
2.00	65.0000	2
3.00	55.0000	3
5.00	37.0000	4
6.00	33.0000	5
8.00	33.0000	6
10.00	38.0000	7
15.00	52.0000	8
20.00	67.0000	9



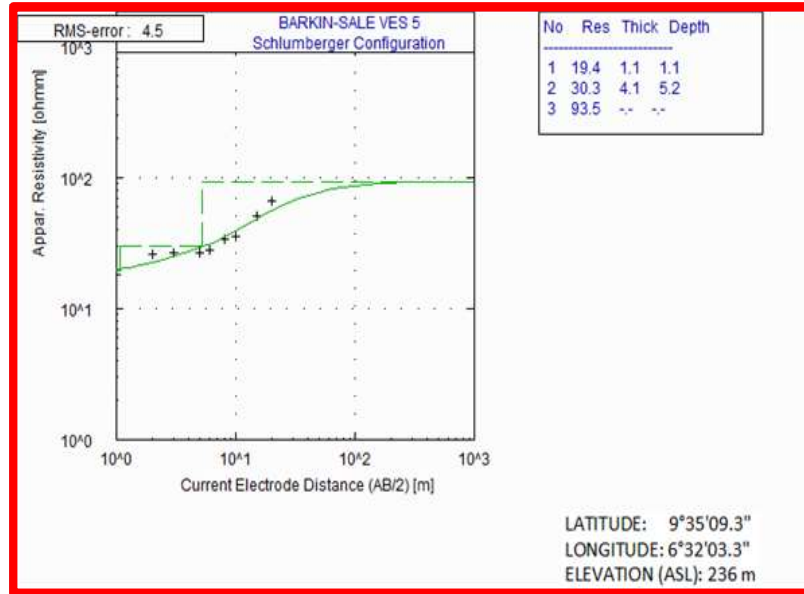
A2. Sounding Curve for VES 3

Distance	Resistivity	No
1.00	46.0000	1
2.00	52.0000	2
3.00	50.0000	3
5.00	36.0000	4
6.00	34.0000	5
8.00	34.0000	6
10.00	40.0000	7
15.00	53.0000	8
20.00	69.0000	9



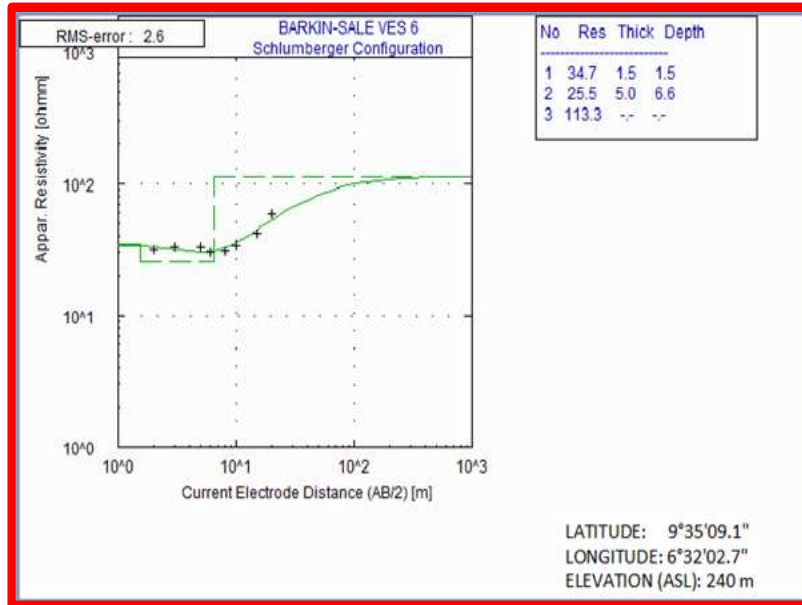
A3. Sounding Curve for VES 4

Distance	Resistivity	No
1.00	18.0000	1
2.00	26.0000	2
3.00	27.0000	3
5.00	27.0000	4
6.00	28.0000	5
8.00	34.0000	6
10.00	36.0000	7
15.00	51.0000	8
20.00	66.0000	9



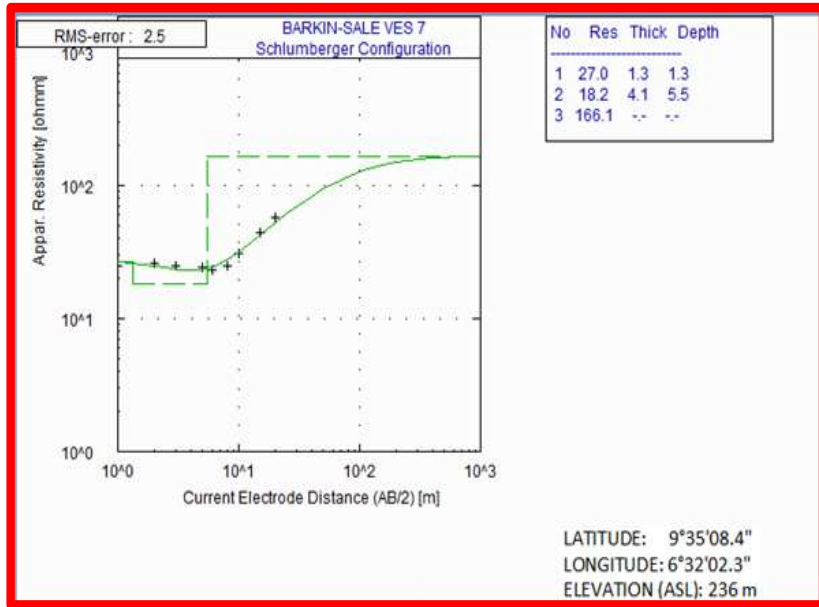
A4. Sounding Curve for VES 5

Distance	Resistivity	No
1.00	34.0000	1
2.00	32.0000	2
3.00	33.0000	3
5.00	33.0000	4
6.00	30.0000	5
8.00	31.0000	6
10.00	34.0000	7
15.00	42.0000	8
20.00	59.0000	9



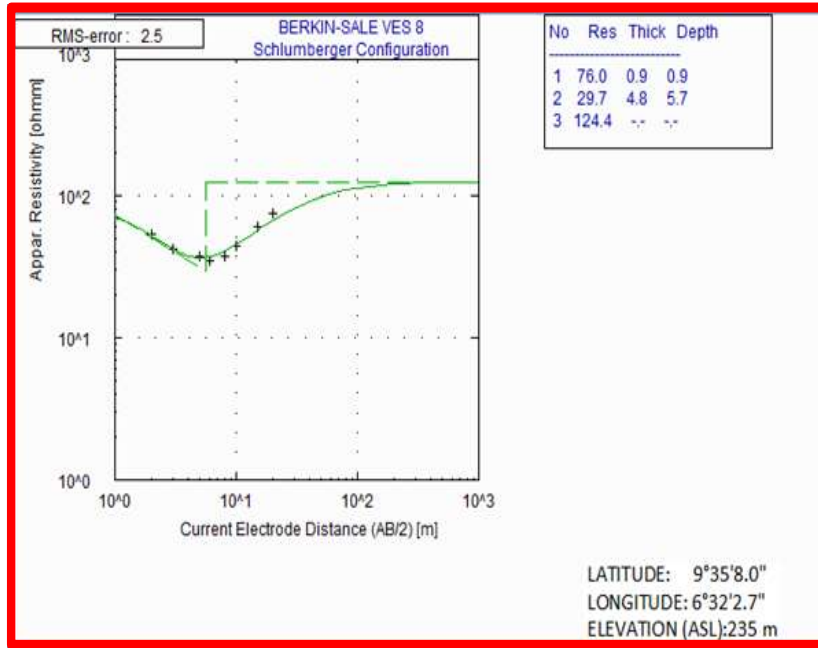
A5. Sounding Curve for VES 6

Distance	Resistivity	No
1.00	25.0000	1
2.00	26.0000	2
3.00	25.0000	3
5.00	24.0000	4
6.00	23.0000	5
8.00	25.0000	6
10.00	31.0000	7
15.00	44.0000	8
20.00	58.0000	9



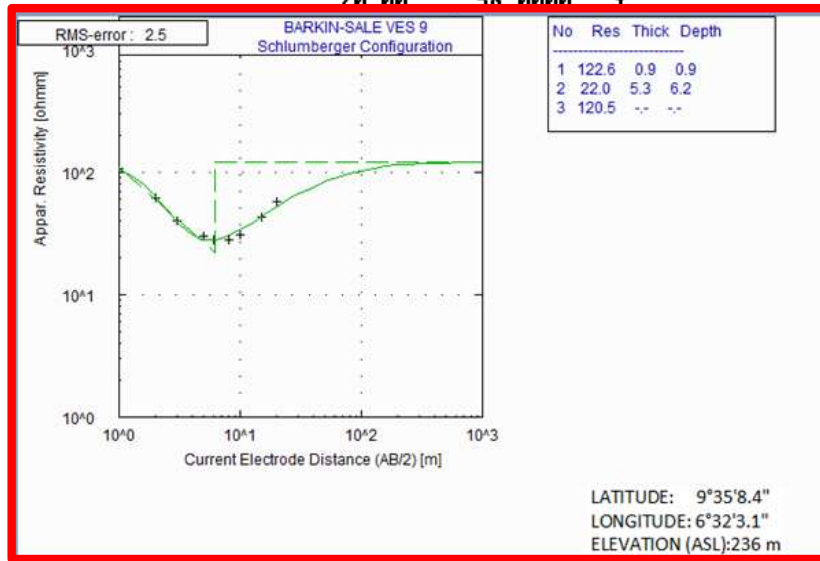
A6. Sounding Curve for VES 7

Distance	Resistivity	No
1.00	70.0000	1
2.00	53.0000	2
3.00	42.0000	3
5.00	37.0000	4
6.00	35.0000	5
8.00	37.0000	6
10.00	44.0000	7
15.00	60.0000	8
20.00	75.0000	9



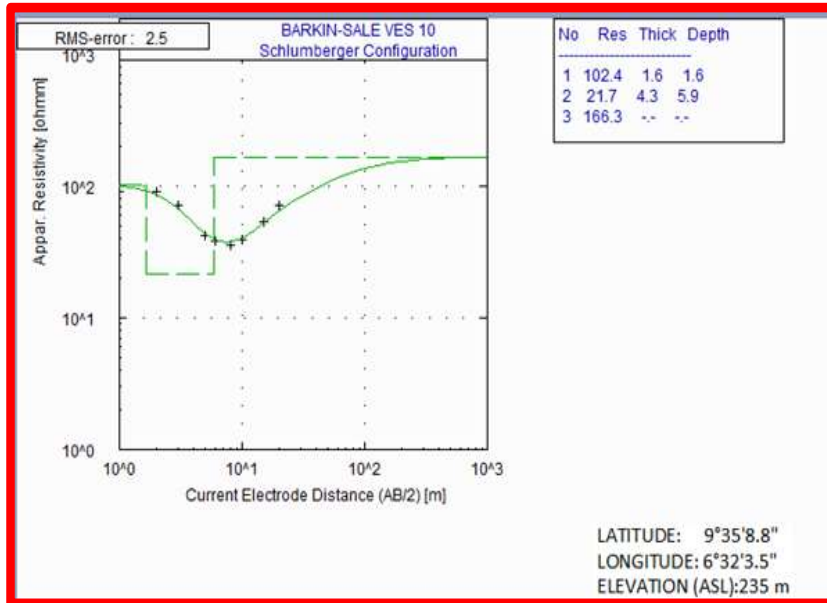
A7. Sounding Curve for VES 8

Distance	Resistivity	No
1.00	107.0000	1
2.00	62.0000	2
3.00	40.0000	3
5.00	30.0000	4
6.00	28.0000	5
8.00	28.0000	6
10.00	31.0000	7
15.00	43.0000	8
20.00	58.0000	9



A8. Sounding Curve for VES 9

Distance	Resistivity	No
1.00	91.0000	1
2.00	91.0000	2
3.00	72.0000	3
5.00	42.0000	4
6.00	38.0000	5
8.00	36.0000	6
10.00	39.0000	7
15.00	53.0000	8
20.00	71.0000	9



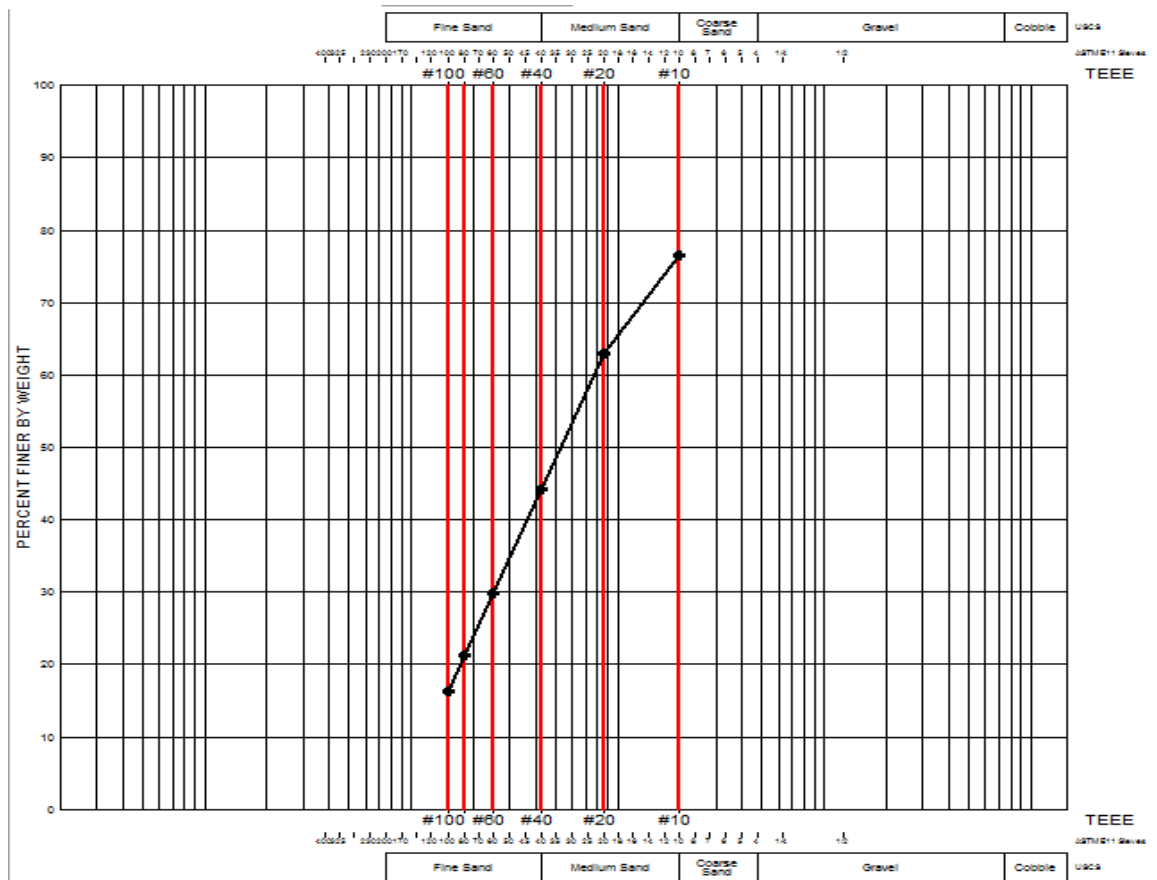
A9. Sounding Curve for VES 10

Appendix B

Table B1. Grain Size Distribution Parameters for Sample L1 at 0.5 m

Initial Dry Mass	230.52
Total Final Mass	229.63
Mass Lost	0.89 (0.4%)

Screen Name	Screen Size (mm)	Mass Retained	% Retained	Cumulative % Retained	% Finer
#10	2.00	54.23	23.5	23.5	76.5
#20	0.85	30.98	13.4	37.0	63.0
#40	0.42	43.52	18.9	55.8	44.2
#60	0.25	32.86	14.3	70.1	29.9
#80	0.18	20.01	8.7	78.8	21.2
#100	0.15	11.42	5.0	83.7	16.3

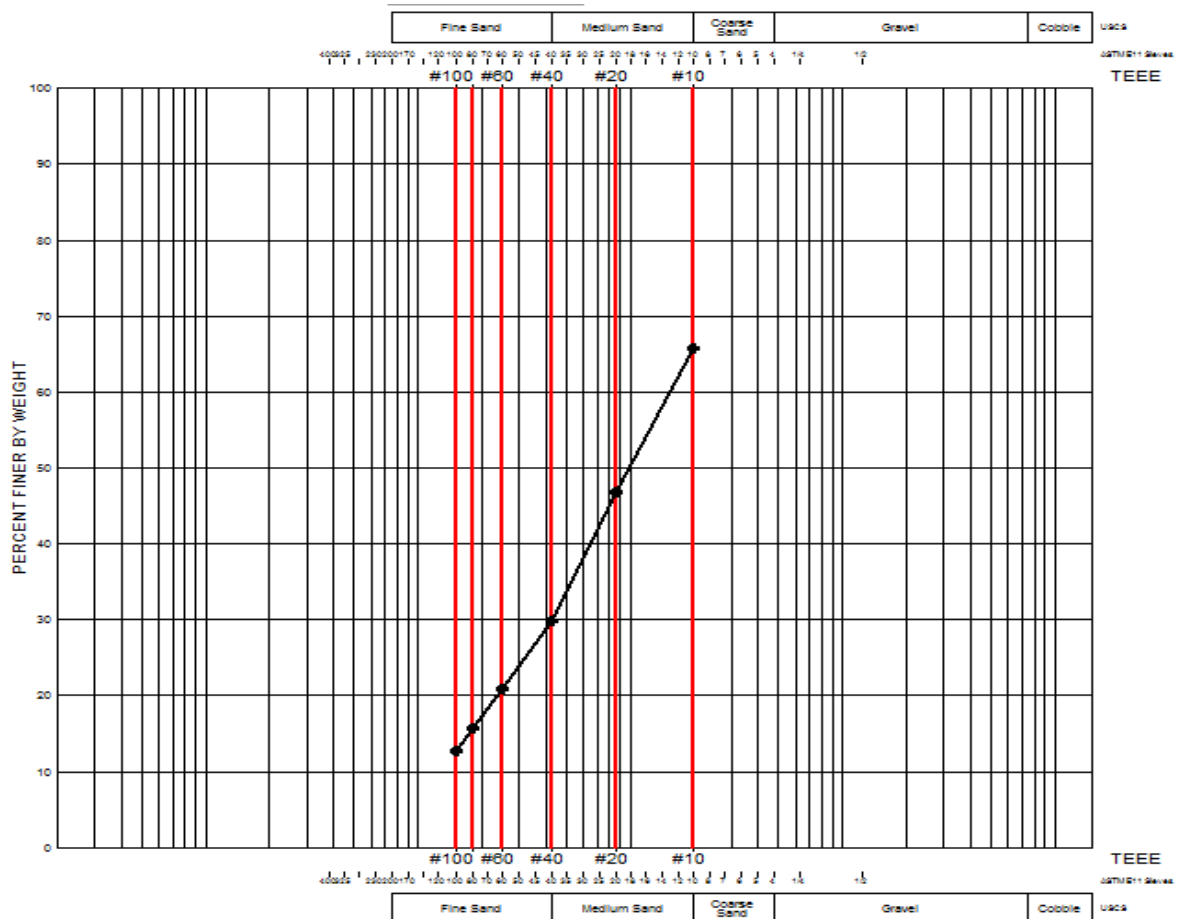


B1. Grading Curve for Sample L 1 at 0.5 m

Table B2. Grain Size Distribution Parameters for Sample L1 at 1.0 m

Initial Dry Mass 271.88
 Total Final Mass 271.78
 Mass Lost 0.1 (0.0%)

Screen Name	Screen Size (mm)	Mass Retained	% Retained	Cumulative % Retained	% Finer
#10	2.00	93.10	34.2	34.2	65.8
#20	0.85	51.48	18.9	53.2	46.8
#40	0.42	46.06	16.9	70.1	29.9
#60	0.25	24.51	9.0	79.1	20.9
#80	0.18	13.78	5.1	84.2	15.8
#100	0.15	8.58	3.2	87.4	12.6

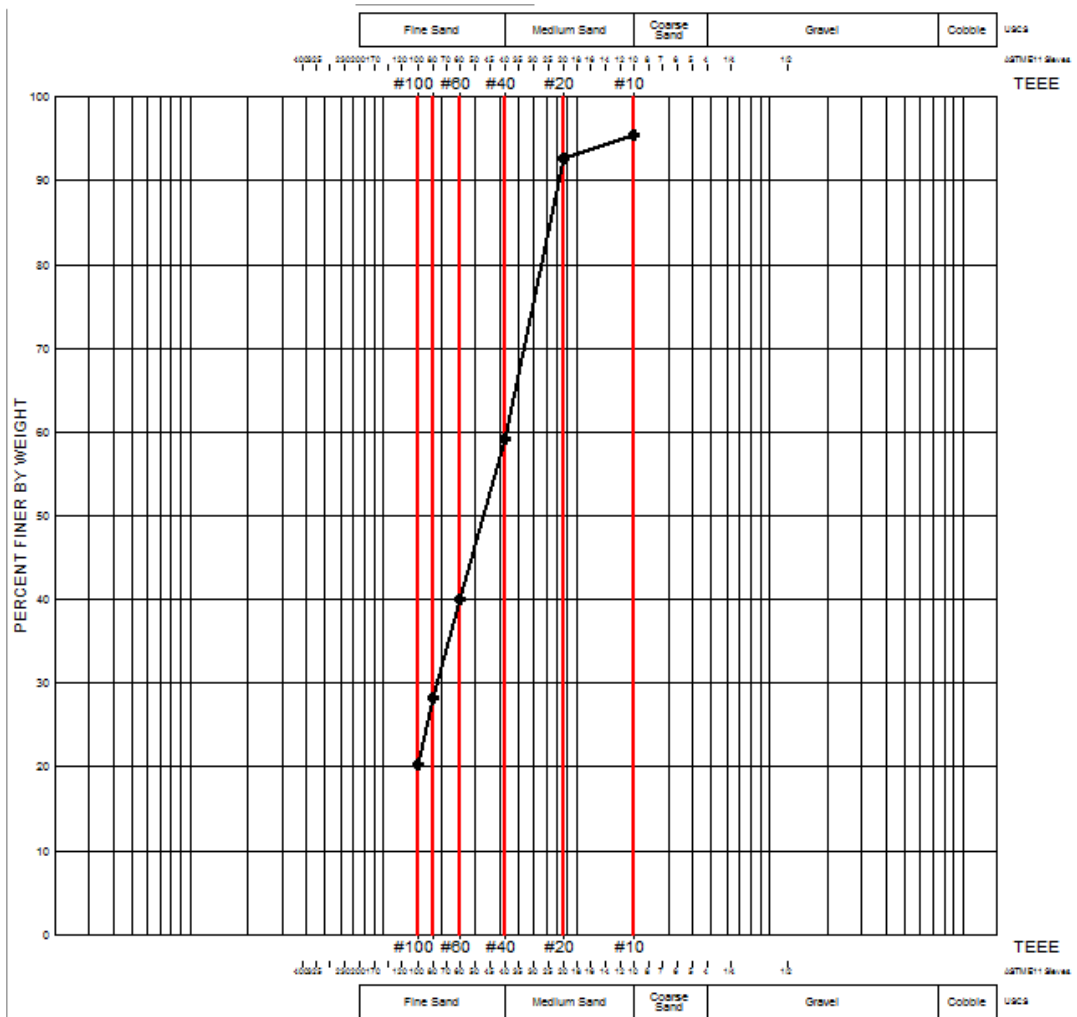


B2. Grading Curve for Sample L 1 at 1.0 m

Table B3. Grain Size Distribution Parameters for Sample L1 at 1.5 m

Initial Dry Mass 258.83
 Total Final Mass 254.19
 Mass Lost 4.64 (1.8%)

Screen Name	Screen Size (mm)	Mass Retained	% Retained	Cumulative % Retained	% Finer
#10	2.00	11.63	4.5	4.5	95.5
#20	0.85	7.15	2.8	7.3	92.7
#40	0.42	86.71	33.5	40.8	59.2
#60	0.25	49.83	19.3	60.0	40.0
#80	0.18	30.46	11.8	71.8	28.2
#100	0.15	20.36	7.9	79.6	20.4

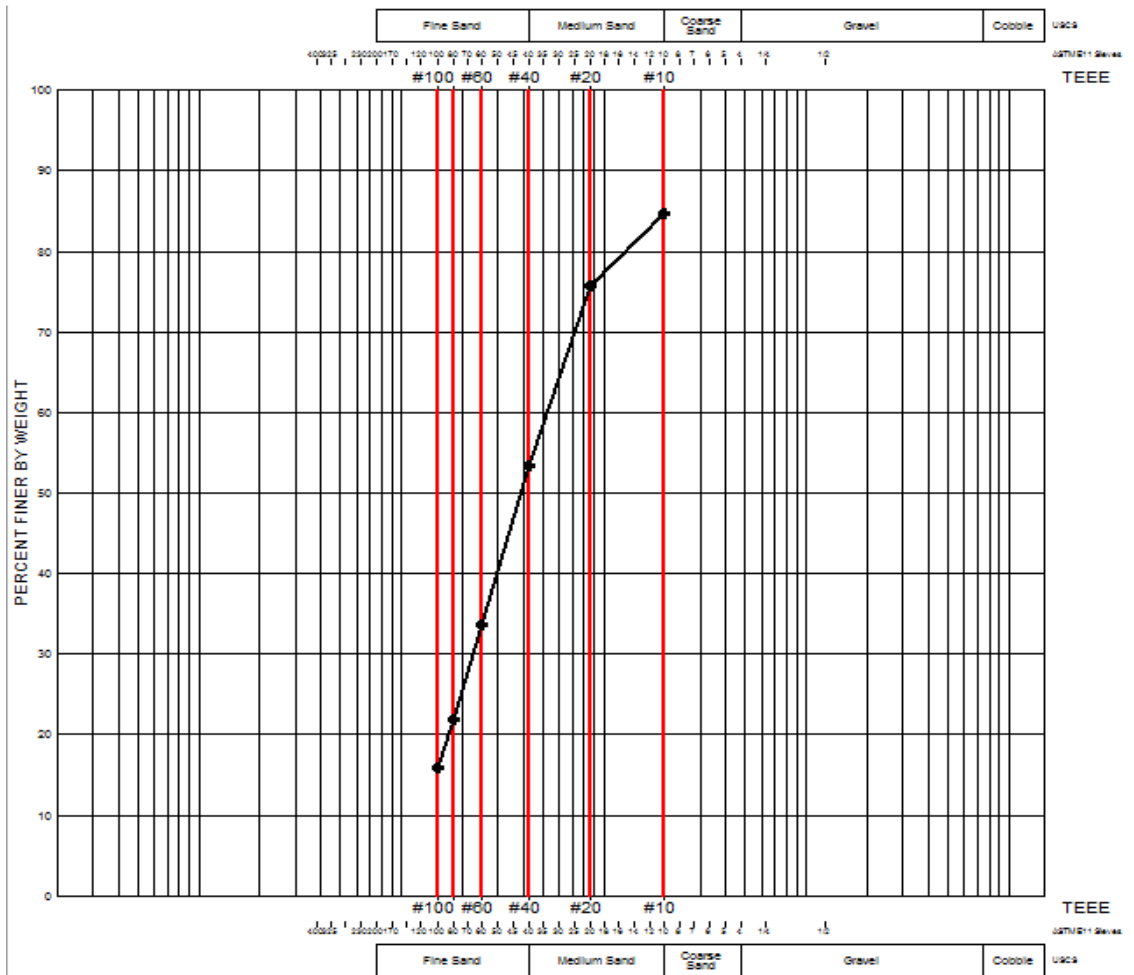


B3. Grading Curve for Sample L 1 at 1.5 m

Table B4. Grain Size Distribution Parameters for Sample L2 at 0.0 m

Initial Dry Mass 278.15
 Total Final Mass 278.08
 Mass Lost 0.07 (0.0%)

Screen Name	Screen Size (mm)	Mass Retained	% Retained	Cumulative % Retained	% Finer
#10	2.00	42.56	15.3	15.3	84.7
#20	0.85	24.76	8.9	24.2	75.8
#40	0.42	62.22	22.4	46.6	53.4
#60	0.25	54.83	19.7	66.3	33.7
#80	0.18	32.72	11.8	78.0	22.0
#100	0.15	16.95	6.1	84.1	15.9

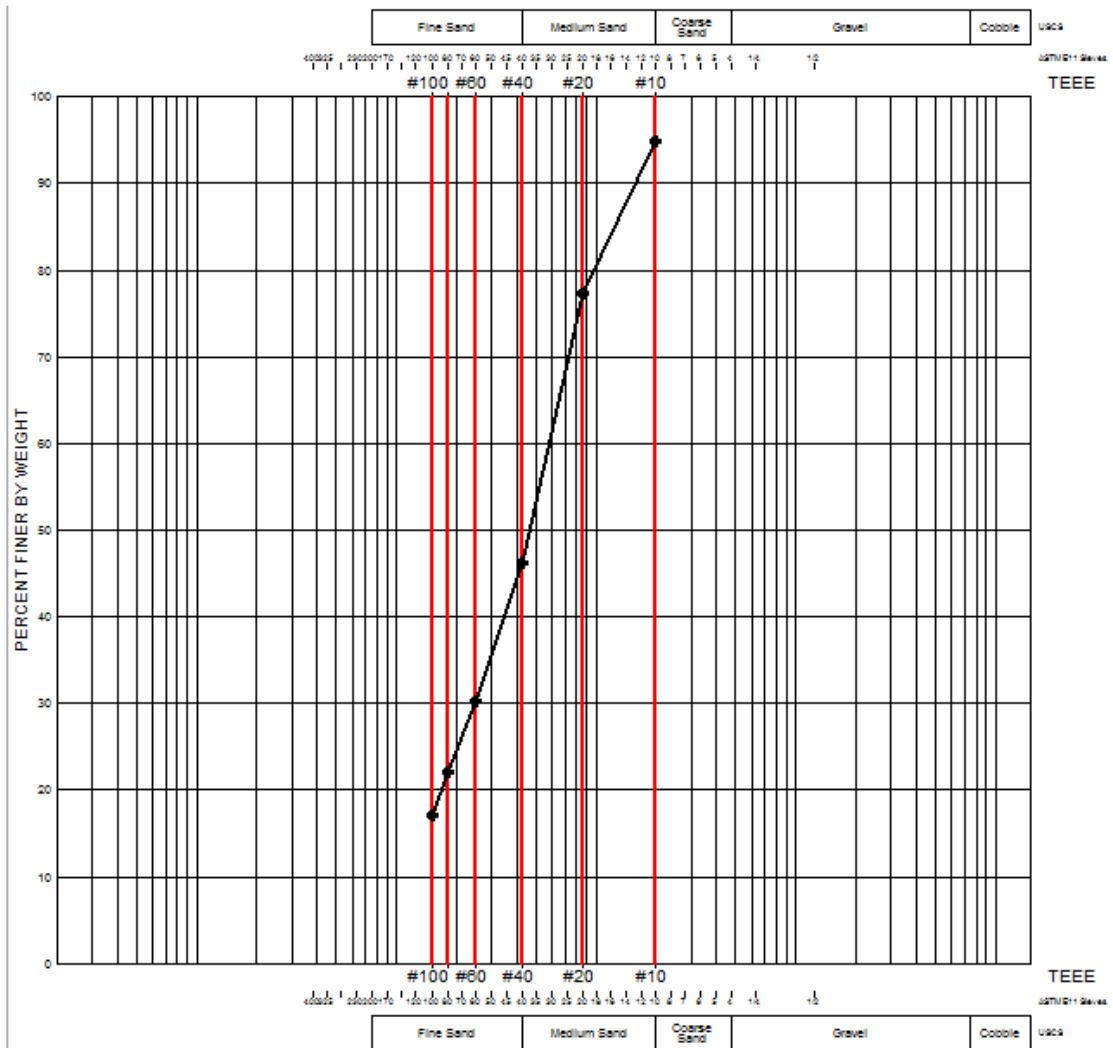


B4. Grading Curve for Sample L2 at 0.0 m

Table B5. Grain Size Distribution Parameters for Sample L2 at 0.5 m

Initial Dry Mass	256.93
Total Final Mass	256.28
Mass Lost	0.65 (0.3%)

Screen Name	Screen Size (mm)	Mass Retained	% Retained	Cumulative % Retained	% Finer
#10	2.00	13.28	5.2	5.2	94.8
#20	0.85	44.83	17.4	22.6	77.4
#40	0.42	80.09	31.2	53.8	46.2
#60	0.25	40.82	15.9	69.7	30.3
#80	0.18	21.33	8.3	78.0	22.0
#100	0.15	12.71	4.9	82.9	17.1

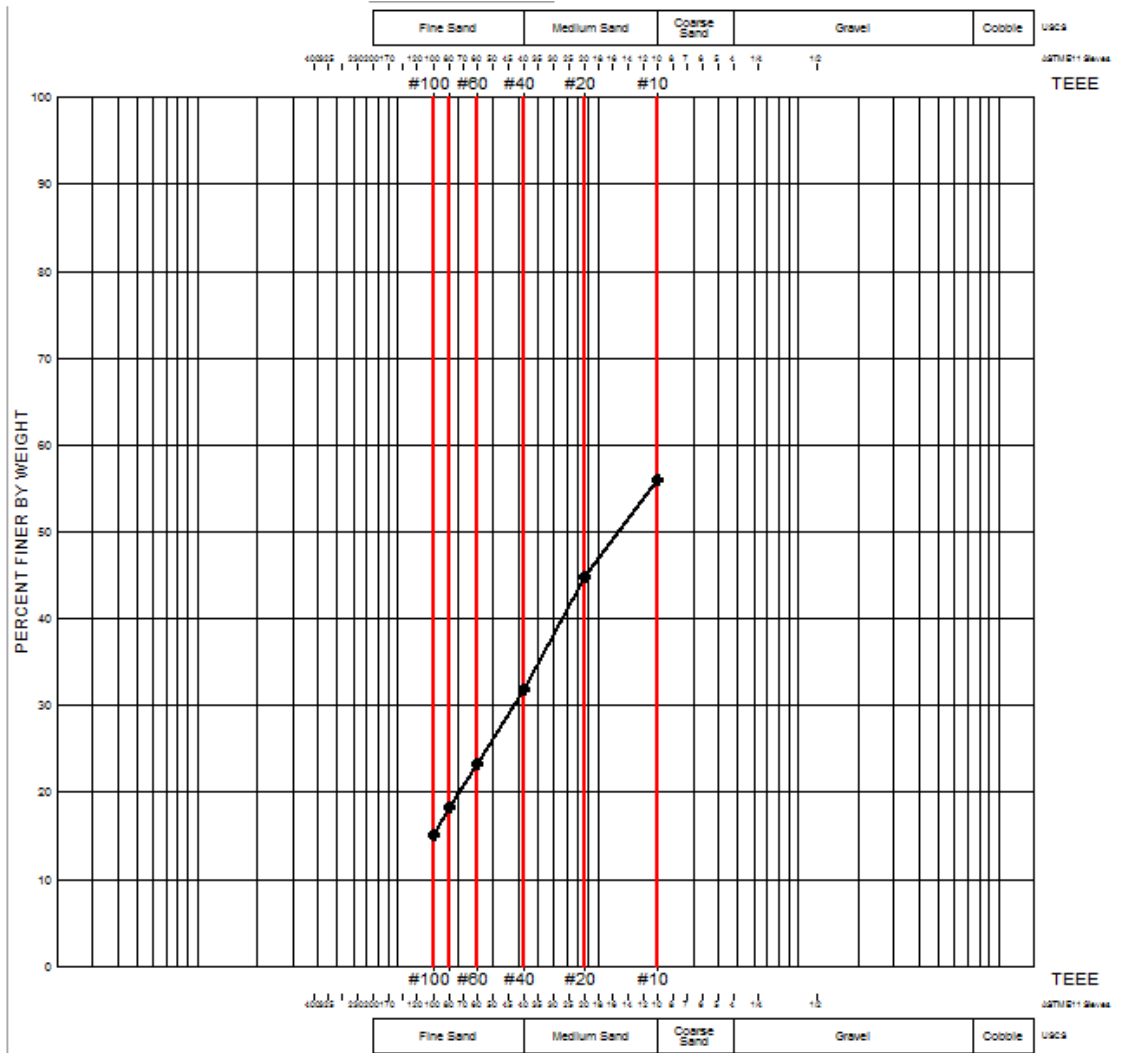


B5. Grading Curve for Sample L2 at 0.5 m

Table B6. Grain Size Distribution Parameters for Sample L2 at 1.0 m

Initial Dry Mass 268.92
 Total Final Mass 268.77
 Mass Lost 0.15 (0.1%)

Screen Name	Screen Size (mm)	Mass Retained	% Retained	Cumulative % Retained	% Finer
#10	2.00	118.60	44.1	44.1	55.9
#20	0.85	29.63	11.0	55.1	44.9
#40	0.42	34.99	13.0	68.1	31.9
#60	0.25	22.90	8.5	76.6	23.4
#80	0.18	13.46	5.0	81.7	18.3
#100	0.15	8.57	3.2	84.8	15.2

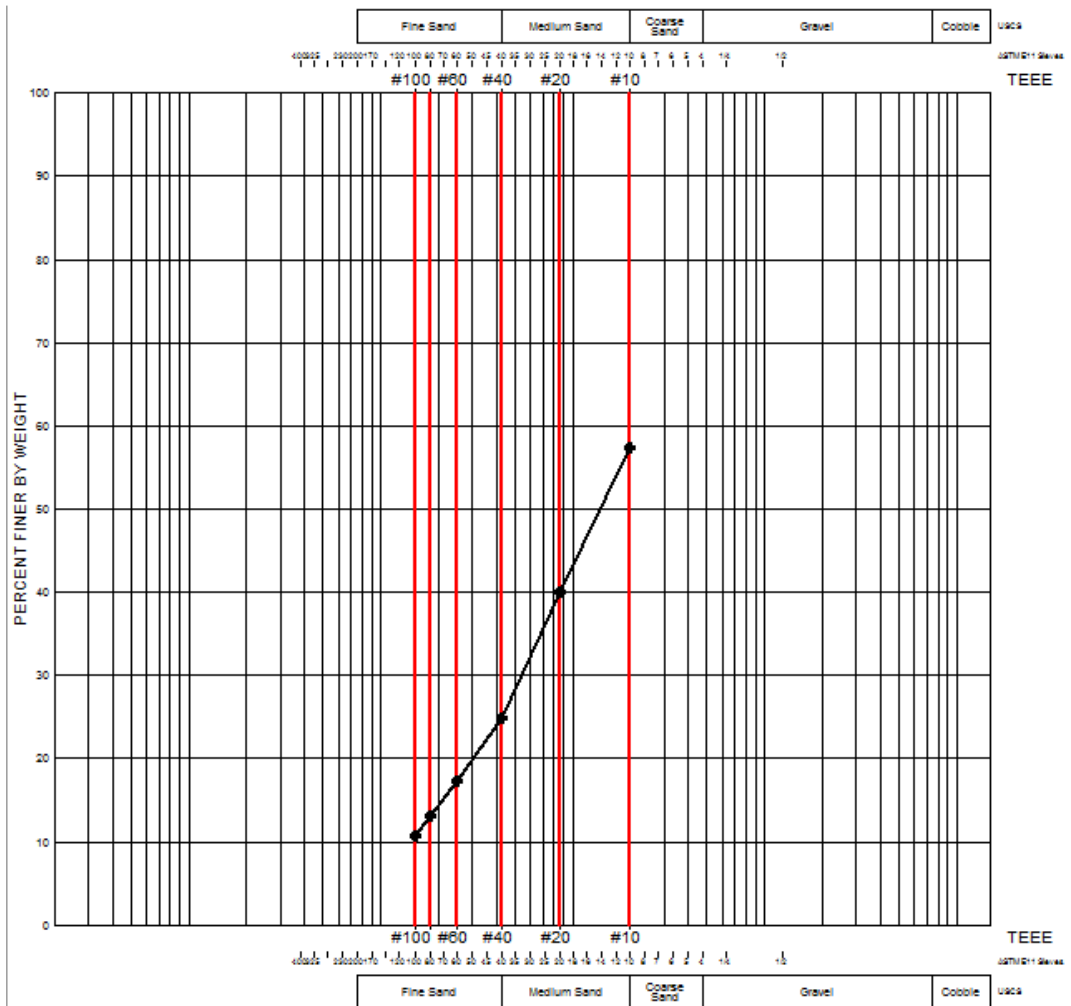


B6. Grading Curve for Sample L2 at 1.0 m

Table B7. Grain Size Distribution Parameters for Sample L2 at 1.5 m

Initial Dry Mass 265.4
 Total Final Mass 265.37
 Mass Lost 0.03 (0.0%)

Screen Name	Screen Size (mm)	Mass Retained	% Retained	Cumulative % Retained	% Finer
#10	2.00	112.96	42.6	42.6	57.4
#20	0.85	46.20	17.4	60.0	40.0
#40	0.42	40.23	15.2	75.1	24.9
#60	0.25	20.08	7.6	82.7	17.3
#80	0.18	11.28	4.3	86.9	13.1
#100	0.15	6.35	2.4	89.3	10.7

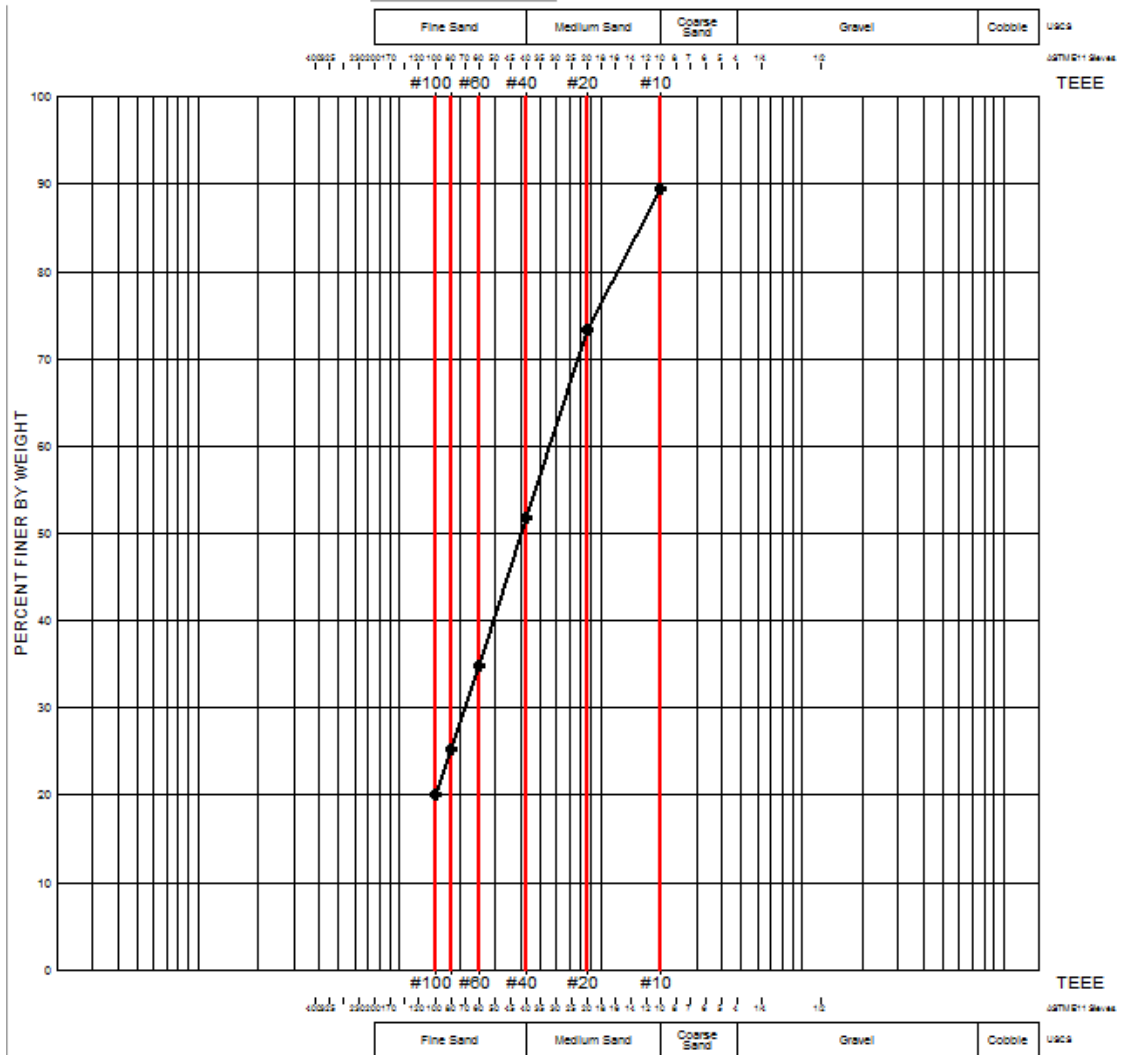


B7. Grading Curve for Sample L2 at 1.5 m

Table B8. Grain Size Distribution Parameters for Sample L3 at 0.0 m

Initial Dry Mass	248.46
Total Final Mass	248.37
Mass Lost	0.09 (0.0%)

Screen Name	Screen Size (mm)	Mass Retained	% Retained	Cumulative % Retained	% Finer
#10	2.00	25.95	10.4	10.4	89.6
#20	0.85	40.48	16.3	26.7	73.3
#40	0.42	53.38	21.5	48.2	51.8
#60	0.25	41.94	16.9	65.1	34.9
#80	0.18	23.78	9.6	74.7	25.3
#100	0.15	13.20	5.3	80.0	20.0

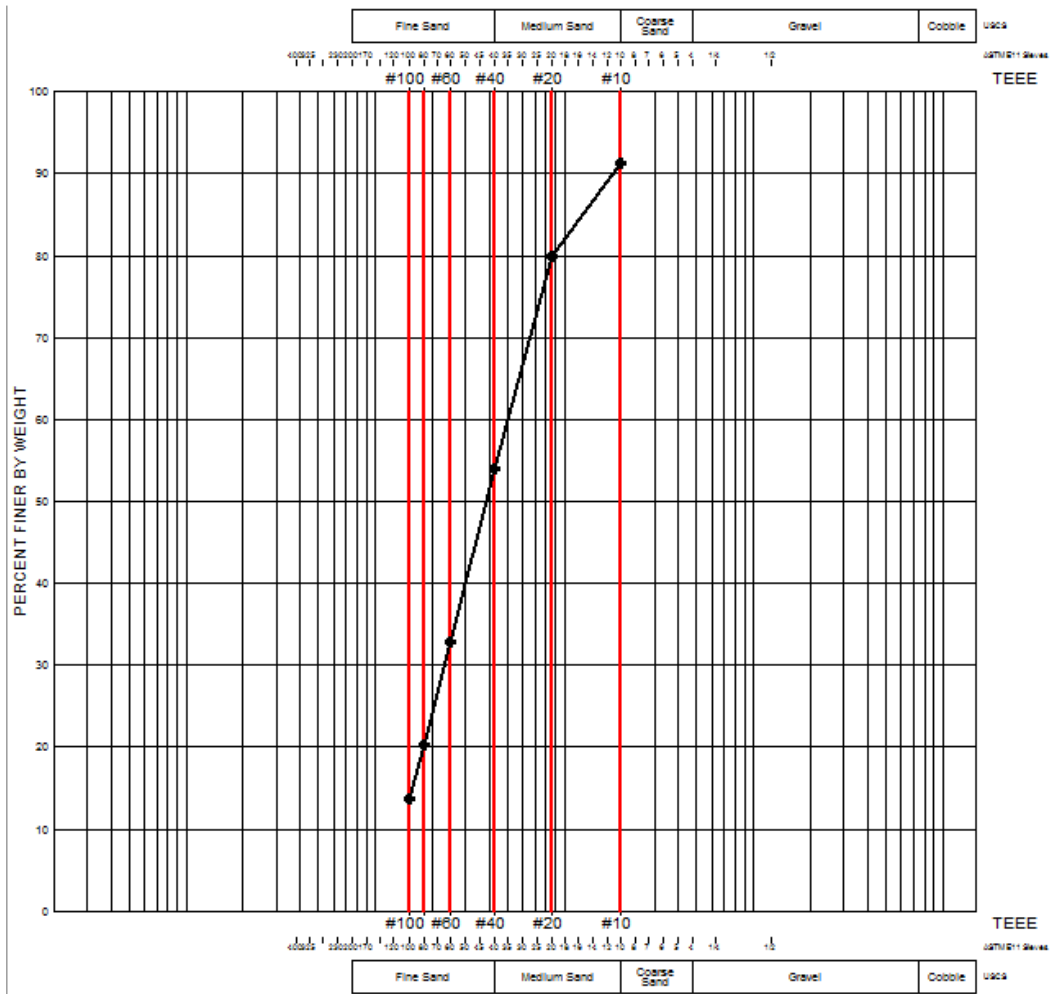


B8. Grading Curve for Sample L3 at 0.0 m

Table B9. Grain Size Distribution Parameters for Sample L3 at 0.5 m

Initial Dry Mass 245.37
 Total Final Mass 241.22
 Mass Lost 4.15 (1.7%)

Screen Name	Screen Size (mm)	Mass Retained	% Retained	Cumulative % Retained	% Finer
#10	2.00	21.20	8.6	8.6	91.4
#20	0.85	28.16	11.5	20.1	79.9
#40	0.42	63.72	26.0	46.1	53.9
#60	0.25	51.63	21.0	67.1	32.9
#80	0.18	30.87	12.6	79.7	20.3
#100	0.15	16.06	6.5	86.3	13.7

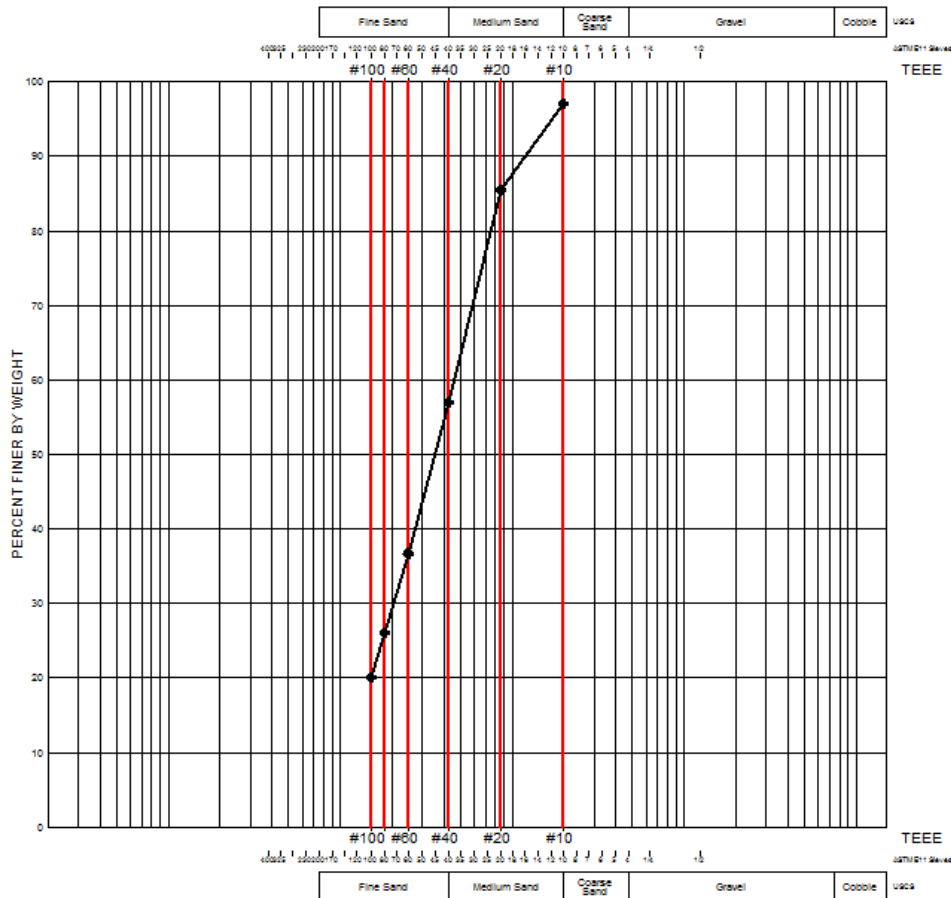


B9. Grading Curve for Sample L3 at 0.5 m

Table B10. Grain Size Distribution Parameters for Sample L3 at 1.0 m

Initial Dry Mass	271.04
Total Final Mass	270.76
Mass Lost	0.28 (0.1%)

Screen Name	Screen Size (mm)	Mass Retained	% Retained	Cumulative % Retained	% Finer
#10	2.00	7.96	2.9	2.9	97.1
#20	0.85	31.36	11.6	14.5	85.5
#40	0.42	77.48	28.6	43.1	56.9
#60	0.25	54.65	20.2	63.3	36.7
#80	0.18	28.65	10.6	73.8	26.2
#100	0.15	16.70	6.2	80.0	20.0

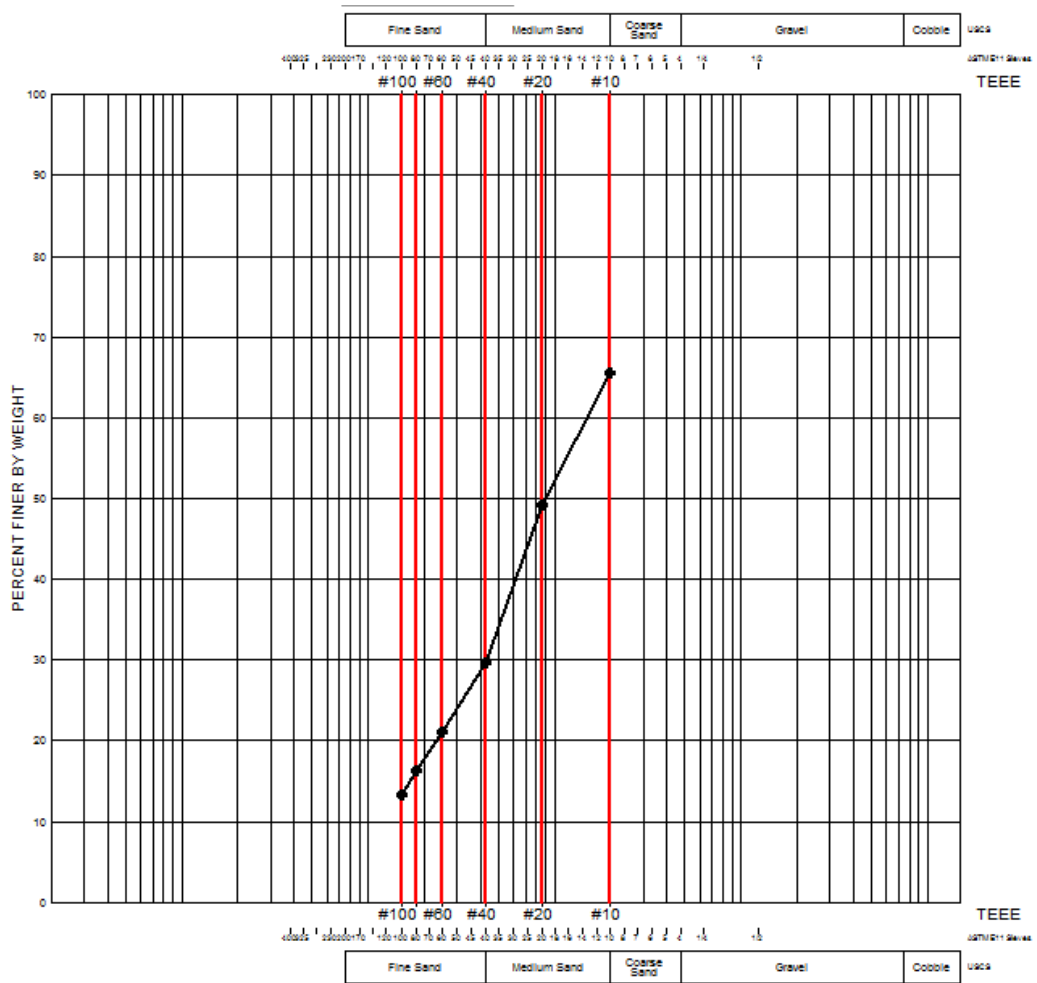


B10. Grading Curve for Sample L3 at 1.0 m

Table B11. Grain Size Distribution Parameters for Sample L3 at 1.5 m

Initial Dry Mass 270.38
 Total Final Mass 268.81
 Mass Lost 1.57 (0.6%)

Screen Name	Screen Size (mm)	Mass Retained	% Retained	Cumulative % Retained	% Finer
#10	2.00	93.17	34.5	34.5	65.5
#20	0.85	44.42	16.4	50.9	49.1
#40	0.42	52.81	19.5	70.4	29.6
#60	0.25	22.78	8.4	78.8	21.2
#80	0.18	13.17	4.9	83.7	16.3
#100	0.15	8.05	3.0	86.7	13.3



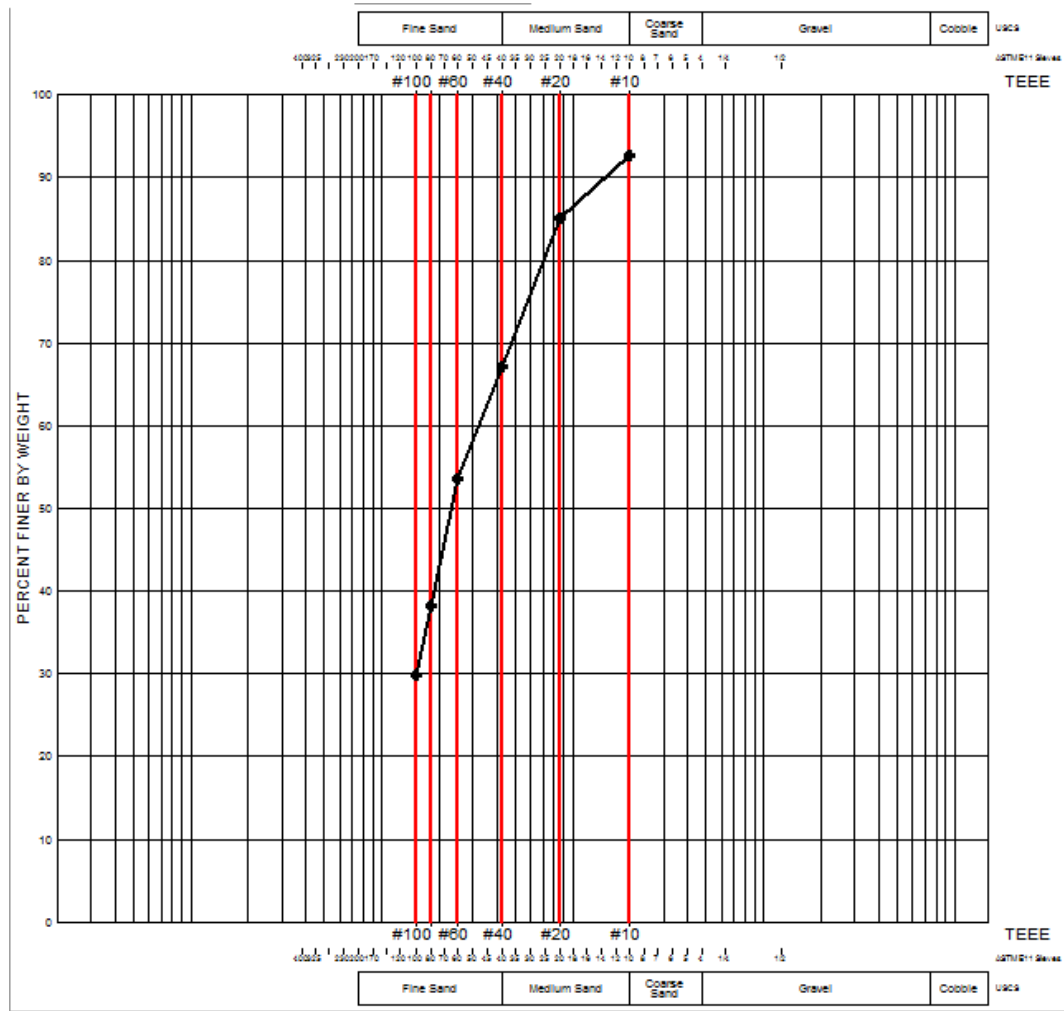
B11. Grading Curve for Sample L3 at 1.5 m

Table B12. Grain Size Distribution Parameters for Sample L4 at 0.0 m

Initial Dry Mass 223.54

Total Final Mass 221.68
 Mass Lost 1.86 (0.8%)

Screen Name	Screen Size (mm)	Mass Retained	% Retained	Cumulative % Retained	% Finer
#10	2.00	16.28	7.3	7.3	92.7
#20	0.85	16.97	7.6	14.9	85.1
#40	0.42	40.24	18.0	32.9	67.1
#60	0.25	30.10	13.5	46.3	53.7
#80	0.18	34.37	15.4	61.7	38.3
#100	0.15	18.73	8.4	70.1	29.9



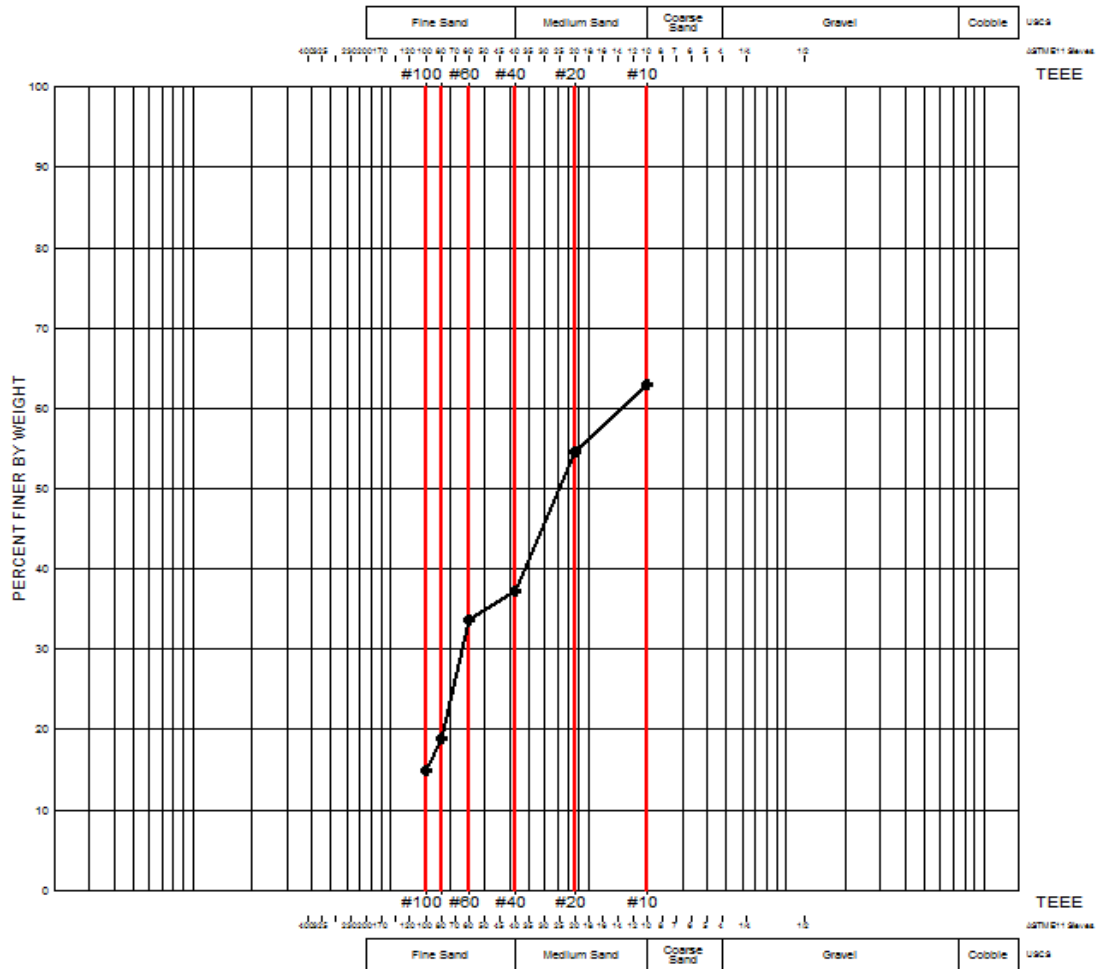
B12. Grading Curve for Sample L4 at 0.0 m

Table B13. Grain Size Distribution Parameters for Sample L4 at 0.5 m

Initial Dry Mass 275.37
 Total Final Mass 275.15

Mass Lost 0.22 (0.1%)

Screen Name	Screen Size (mm)	Mass Retained	% Retained	Cumulative % Retained	% Finer
#10	2.00	101.81	37.0	37.0	63.0
#20	0.85	23.45	8.5	45.5	54.5
#40	0.42	47.71	17.3	62.8	37.2
#60	0.25	9.97	3.6	66.4	33.6
#80	0.18	40.12	14.6	81.0	19.0
#100	0.15	11.04	4.0	85.0	15.0

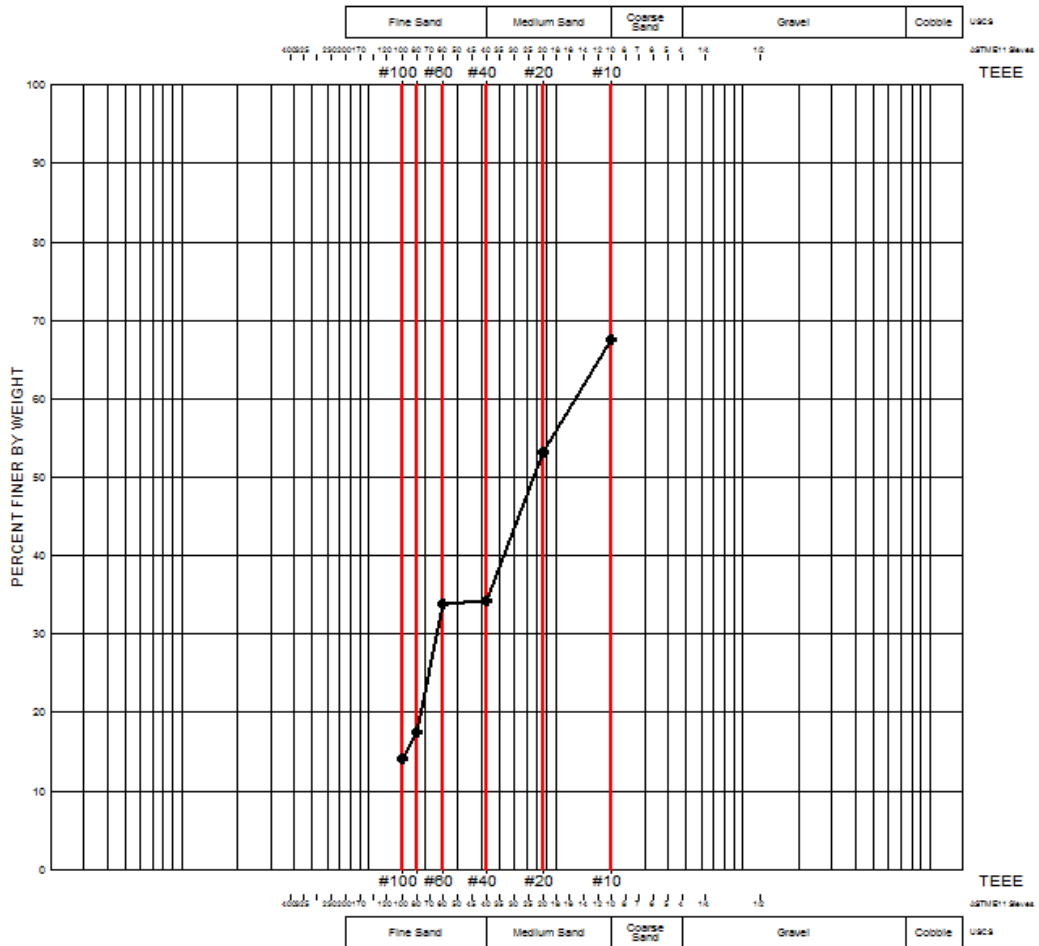


B13. Grading Curve for Sample L4 at 0.5 m

Table B14. Grain Size Distribution Parameters for Sample L4 at 1.0 m

Initial Dry Mass	274.52
Total Final Mass	274.42
Mass Lost	0.1 (0.0%)

Screen Name	Screen Size (mm)	Mass Retained	% Retained	Cumulative % Retained	% Finer
#10	2.00	89.34	32.5	32.5	67.5
#20	0.85	38.93	14.2	46.7	53.3
#40	0.42	52.38	19.1	65.8	34.2
#60	0.25	1.07	0.4	66.2	33.8
#80	0.18	44.67	16.3	82.5	17.5
#100	0.15	9.64	3.5	86.0	14.0



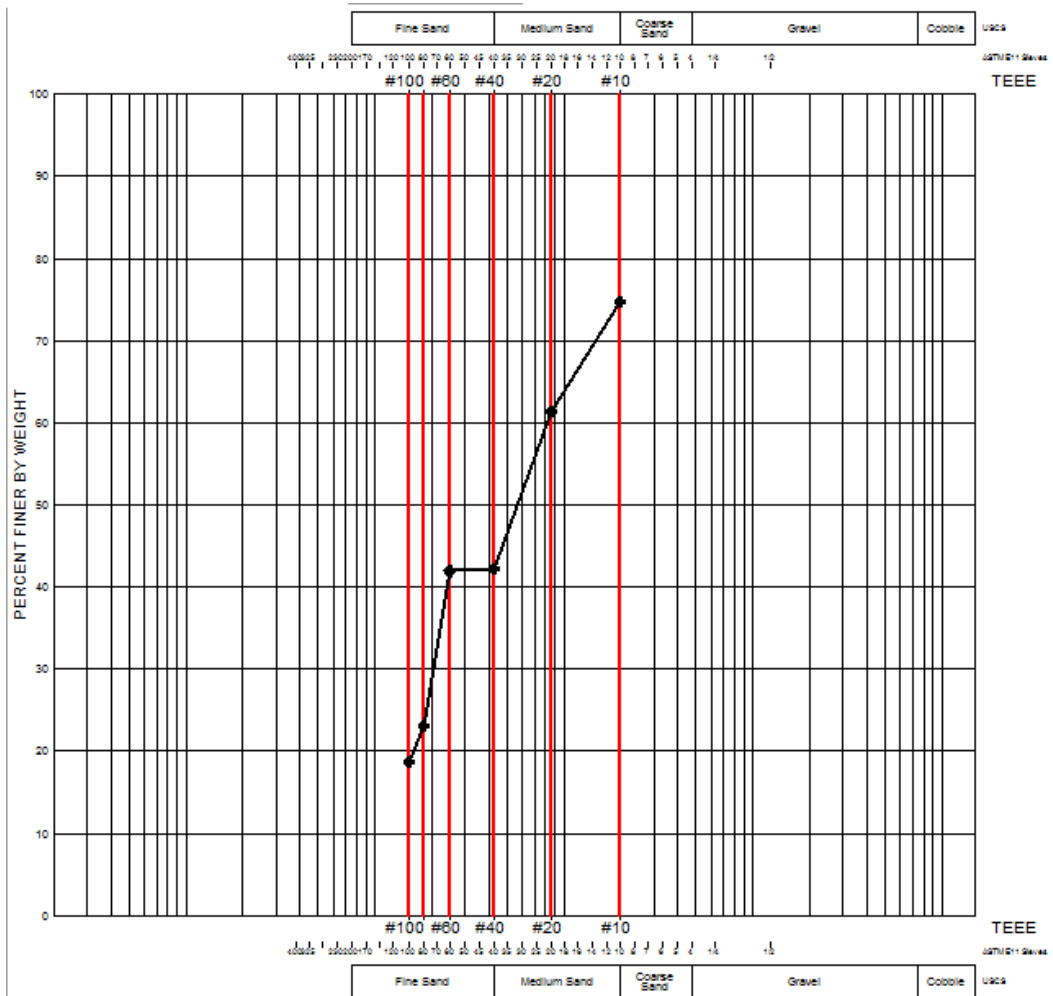
B14. Grading Curve for Sample L4 at 1.0 m

Table B15. Grain Size Distribution Parameters for Sample L4 at 1.5 m

Initial Dry Mass	245.5
Total Final Mass	245.46
Mass Lost	0.04 (0.0%)

Screen	Screen	Mass	Cumulative
--------	--------	------	------------

Name	Size (mm)	Retained	% Retained	% Retained	% Finer
#10	2.00	62.26	25.4	25.4	74.6
#20	0.85	32.48	13.2	38.6	61.4
#40	0.42	47.23	19.2	57.8	42.2
#60	0.25	0.60	0.2	58.1	41.9
#80	0.18	46.25	18.8	76.9	23.1
#100	0.15	10.88	4.4	81.3	18.7



B15. Grading Curve for Sample L4 at 1.5 m